Higher-order calculations in manifestly Lorentz-invariant baryon chiral perturbation theory

Dissertation
zur Erlangung des Grades
„Doktor der Naturwissenschaften"

am Fachbereich Physik, Mathematik und Informatik
der Johannes Gutenberg-Universität
in Mainz

Matthias R. Schindler
geboren in Mainz

Mainz, 26. März 2007

Datum der mündlichen Prüfung: 24.07.2007

Abstract

This thesis is concerned with calculations in manifestly Lorentz-invariant baryon chiral perturbation theory beyond order $D = 4$. We investigate two different methods. The first approach consists of the inclusion of additional particles besides pions and nucleons as explicit degrees of freedom. This results in the resummation of an infinite number of higher-order terms which contribute to higher-order low-energy constants in the standard formulation. In this thesis the nucleon axial, induced pseudoscalar, and pion-nucleon form factors are investigated. They are first calculated in the standard approach up to order $D = 4$. Next, the inclusion of the axial-vector meson $a_1(1260)$ is considered. We find three diagrams with an axial-vector meson which are relevant to the form factors. Due to the applied renormalization scheme, however, the contributions of the two loop diagrams vanish and only a tree diagram contributes explicitly. The appearing coupling constant is fitted to experimental data of the axial form factor. The inclusion of the axial-vector meson results in an improved description of the axial form factor for higher values of momentum transfer. The contributions to the induced pseudoscalar form factor, however, are negligible for the considered momentum transfer, and the axial-vector meson does not contribute to the pion-nucleon form factor. The second method consists in the explicit calculation of higher-order diagrams. This thesis describes the applied renormalization scheme and shows that all symmetries and the power counting are preserved. As an application we determine the nucleon mass up to order $D = 6$ which includes the evaluation of two-loop diagrams. This is the first complete calculation in manifestly Lorentz-invariant baryon chiral perturbation theory at the two-loop level. The numerical contributions of the terms of order $D = 5$ and $D = 6$ are estimated, and we investigate their pion-mass dependence. Furthermore, the higher-order terms of the nucleon σ term are determined with the help of the Feynman-Hellmann theorem.

Zusammenfassung

Die vorliegende Dissertation befasst sich mit Rechnungen in manifest Lorentz-invarianter baryonischer chiraler Störungstheorie, die über die chirale Ordnung $D = 4$ hinausgehen. Hierbei werden zwei unterschiedliche Ansätze untersucht. Die erste Methode besteht darin, neben Pionen und Nukleonen zusätzliche Freiheitsgrade explizit zu berücksichtigen. Dadurch wird eine unendliche Anzahl an Termen, die in der herkömmlichen Formulierung zu den Niederenergiekonstanten höherer Ordnungen beitragen, aufsummiert. In der vorliegenden Arbeit werden der axiale, der induziert pseudoskalare und der Pion-Nukleon-Formfaktor untersucht. Diese werden zunächst auf herkömmliche Weise bis zur Ordnung $D = 4$ berechnet. Anschließend wird der Einbau des Axialvektormesons $a_1(1260)$ betrachtet. Man findet drei Diagramme mit einem Axialvektormeson, welche für die Formfaktoren relevant sind. Auf Grund des verwendeten Renormierungsschemas verschwinden jedoch die Beiträge der zwei Schleifendiagramme und nur ein Baumdiagramm trägt explizit bei. Die auftretende Kopplungskonstante wird an experimentelle Daten des axialen Formfaktors angepasst. Durch die Berücksichtigung des Axialvektormesons wird die Beschreibung des axialen Formfaktors für höhere Werte des Impulsübertrags verbessert. Die Beiträge des Axialvektormesondiagramms zum induziert pseudoskalaren Formfaktor sind hingegen bei den betrachteten Impulsüberträgen vernachlässigbar, und das Axialvektormeson trägt nicht zum Pion-Nukleon-Formfaktor bei. Die zweite Methode besteht in einer expliziten Berechnung der Diagramme höherer Ordnung. Die vorliegende Dissertation beschreibt das verwendete Renormierungsschema und zeigt, dass alle Symmetrien und das Zählschema erhalten werden. Als Anwendung wird die Nukleonmasse bis zur Ordnung $D = 6$ berechnet, was auch die Berechnung von Zweischleifendiagrammen beinhaltet. Hierbei handelt es sich um die erste vollständige Rechnung in manifest Lorentz-invarianter baryonischer chiraler Störungstheorie auf dem Zweischleifenniveau. Die numerischen Beiträge der Terme der Ordnungen $D = 5$ und $D = 6$ werden abgeschätzt und ihre Pionmassenabhängigkeit untersucht. Mittels des Feynman-Hellmann-Theorems werden zudem die Terme höherer Ordnung des σ-Terms bestimmt.

Contents

Chapter 1

Introduction

Quantum chromodynamics (QCD) [GW 73a, Wei 73, FGL 73] has been established as the field theory describing the strong interactions. It is an SU(3) gauge theory formulated in terms of quark and gluon fields. In the Standard Model of particle physics, quarks form one kind of fundamental constituents of matter, with leptons being the other kind. There exist 6 different kinds of quarks, called flavors, which differ in their electric charges and masses. These flavors are called up (u), down (d), strange (s), charmed (c), bottom (b), and top (t). While the electric charge only takes two values, $2/3$ for the u, c, and t quarks and $-1/3$ for the d, s, and b quarks, respectively, the masses range from a few MeV for the u and d quarks to about 172 GeV for the t quark [Yao+ 06]. In addition, each flavor carries a so-called "color" charge, which can take three values. The strong interaction between quarks is mediated through the exchange of massless gluons, the gauge bosons of QCD which themselves carry color charge and interact with each other through three- and four-gluon vertices.

QCD exhibits two especially remarkable features. While quarks are the constituents of matter, no isolated quark has been observed. Only color-neutral combinations of quarks and gluons, called hadrons, seem to appear in nature. This is known as confinement [GW 73b], and the derivation of confinement from QCD remains an open question of high interest. One possible explanation is related to the second phenomenon, called asymptotic freedom [GW 73a, GW 73b, Pol 73]. It was shown that the running of the strong coupling constant is such that it decreases for increasing energies, or equivalently for shorter length scales. However, for lower energies, i.e. larger distances, the coupling between quarks increases, providing a possible mechanism for confinement. The increase of the strong coupling constant for low energies poses a significant problem for QCD calculations in this regime. For large values of the coupling constant a perturbative treatment of the theory in powers of the coupling constant is no longer applicable. So far no analytical method is known to solve QCD at low energies.

One of the tools for the non-perturbative treatment of QCD is given by lattice QCD [Wil 74] (for a review see, e.g., [Rot 05]). Here, space-time is discretized onto a finite lattice, which in turn transforms path integrals into finite dimensional integrals that are accessible by numerical calculations. While lattice calculations have made and continue to make great progress, an analytical method for calculations in the energy region below 1 GeV remains desirable. One possible tool is the use of an effective field theory (EFT) (see, e.g., [Pol 92, Geo 93, Kap 95, Man 96, Pic 98, Kap 05]). In general, effective field theories are low-energy approximations to more fundamental theories. According to a "folk theorem" by Weinberg [Wei 97], Lorentz-invariant quantum theories that satisfy the cluster decomposition principle will, at sufficiently low energies, have the form of a quantum field theory. This means that, instead of having to solve the underlying theory, low-energy physics can be described with a set of variables that is suited for the particular energy region of interest by writing down the "most general possible Lagrangian consistent with the symmetries of the theory" [Wei 97]. The effective field theory can then be used to calculate physical quantities in terms of an expansion in q/Λ, where q stands for momenta or masses that are smaller than some scale Λ. An effective field theory obviously has a limited range of applicability as the expansion in q/Λ becomes useless for sufficiently large values of q. In addition, EFTs give an appropriate description up to *finite* accuracy, as in actual calculations only a finite number of terms in the expansion in q/Λ is considered.

The general prescription for EFTs requires the most general Lagrangian consistent with the symmetries of the underlying theory. With no further restrictions the Lagrangian contains an infinite number of terms. Each term in the Lagrangian is accompanied by a coefficient, called low-energy coupling constant (LEC). Since one does not want to include any additional assumptions beyond invariance under the symmetries, the quantum nature of the theory and cluster decomposition, the LECs are free parameters from the EFT viewpoint. If the underlying theory is known, these constants can in principle be calculated. There are cases where the fundamental theory is unknown or the connection to the effective theory cannot be established directly. In these cases the coefficients in the EFT Lagrangian can be obtained by comparison with experimental data. The values of the LECs are independent of physical processes, therefore once their values have been determined they can be used in all other calculations. The general prescription for the construction of an EFT leads to two immediate concerns. The infinite number of terms in the Lagrangian of an EFT might suggest that the theory lacks predictive power. This is not the case, since calculations are perturbative in q/Λ, and one works to a finite order. Only a finite number of LECs contributes up to a certain order, and once these have been determined, either by matching to the underlying theory or by comparison with a set of experiments, all further results can be predicted. The second issue is related to renormalization. The LECs accompany operators with arbitrarily high mass dimensions. An infinite number of the LECs in an EFT will therefore have negative mass dimensions. This means that EFTs are non-renormalizable in the traditional sense, i.e. there is no *finite* set of parameters that can be fixed to render calculations finite up to infinite order. However, since one always works to finite order and the Lagrangian contains all terms allowed by the symmetries, infinities appearing up to any finite order can be absorbed by the LECs up to that order. EFTs are said to be renormalizable in a "modern sense" [Wei 97].

The method of EFTs can be applied to QCD at low energies. Instead of using quarks and gluons as dynamical degrees of freedom, one formulates an EFT called chiral perturbation theory [Wei 79, GL 84, GL 85]. Chiral perturbation theory (ChPT) is described in terms of the degrees of freedom relevant to low-energy strong processes which, in its SU(2) formulation, are pions and nucleons. Physical quantities are then calculated as expansions in terms of small parameters such as the pion mass and small momenta. The Lagrangian of ChPT contains an infinite number of terms, from which an infinite number of Feynman diagrams contributing to any physical process can be derived. In the mesonic sector the choice which of these diagrams is relevant for a calculation up to a given accuracy can be made with a scheme called "Weinberg's power counting" [Wei 79]. It assigns a chiral order D to each diagram, and diagrams with higher D are suppressed relative to those with lower D. However, the extension to processes including a nucleon [GSS 88] originally turned out to be problematic, as expressions renormalized with the methods known from the mesonic sector did not obey the proposed power counting. These problems can, however, be overcome by the application of a suitable renormalization scheme, which restores the power counting.

ChPT relies on a perturbative expansion in terms of small parameters for which the question of convergence arises. Assuming the parameters of the expansion to be of natural size one would expect contributions at order $D+1$ to be suppressed by a factor q/Λ compared to contributions at order D. For q of the order of the pion mass and $\Lambda \approx 1\,\mathrm{GeV}$, which is the expected size of Λ for ChPT, this corresponds to a correction of about 20%. In the mesonic sector this rough estimate seems accurate, the situation is less clear for the baryonic sector though. While for example the chiral expansion of the nucleon mass shows a good convergence behavior, the nucleon axial coupling g_A receives large contributions from higher-order terms [KM 99]. Further examples include the electromagnetic form factors of the nucleon (see, e.g., [KM 01]), which only describe the data for very low values of momentum transfer. For some of these quantities higher-order contributions clearly play an important role.

The convergence properties of baryon chiral perturbation theory (BChPT) are also of great importance for lattice QCD. While the physical value of the pion mass is fixed, lattice calculations treat the pion mass as an adjustable parameter. Due to numerical costs, present lattice calculations still require pion masses larger than the physical one, and results obtained on the lattice have to be extrapolated to the physical point. ChPT as an expansion in the pion mass is the appropriate tool to perform such extrapolations, which again poses the question for which values of small parameters the ChPT expansion gives reliable predictions.

In quantum electrodynamics (QED) the inclusion of higher-order terms has proven to be successful in increasing the accuracy of theoretical predictions. The electron anomalous magnetic moment a_e has been calculated up to four-loop order, resulting in an impressive agreement between experiment and theory of $a_e(exp) - a_e(th) = 12.4(4.3)(8.5) \times 10^{-12}$ [KN 06]. This is possible since QED is renormalizable in the traditional sense. Only a fixed number of constants, in the case of QED the charge e of the electron and its mass m_e, have to be determined and contribute in calculations of arbitrary order in the loop expansion. Since ChPT as an effective field theory is non-renormalizable in the standard sense, an infinite number of counterterms occurs. Even though the number of terms is finite up to a given accuracy, it increases with the order of the calculation. Performing higher-order calculations therefore results in the inclusion of a number of previously undetermined LECs. Higher-order calculations can only result in increased accuracy once a sufficient number of physical quantities has been calculated and the LECs have been extracted from comparison with experimental data.

In this thesis we discuss two methods of calculating higher-order contributions in baryonic ChPT. The first approach consists of including additional particles in the theory. In ChPT calculations the contributions from resonances like vector and axial-vector mesons are included in the LECs of the Lagrangian. Symbolically, the resonance propagator is expanded,

$$\frac{1}{q^2 - M_R^2} = -\frac{1}{M_R^2}\left[1 + \frac{q^2}{M_R^2} + \left(\frac{q^2}{M_R^2}\right)^2 + \left(\frac{q^2}{M_R^2}\right)^3 + \mathcal{O}(q^8)\right], \tag{1.1}$$

and the contributions stemming from these expressions at each order are absorbed in the LECs of the ChPT Lagrangian at that order. By considering resonances as explicit degrees of freedom, one does not have to expand the propagator and can take into account all terms on the right-hand side of Eq. (1.1). The inclusion of additional degrees of freedom therefore allows for a convenient resummation of higher-order terms. There is an additional aspect why the inclusion of additional particles is of interest. The mass of the lowest-lying particle not included as an explicit degree of freedom provides an upper bound on the energy domain in which an effective field theory can be applied. By including additional degrees of freedom explicitly one therefore hopes to increase the range of applicability of the EFT. One of the prerequisites, however, is the existence of a consistent power counting. The lightest resonances not included in the standard ChPT Lagrangian are the ρ mesons, which can decay into two pions. Due to the mass of the ρ these pions have momenta that can no longer be considered small and so far no consistent power counting exists for vector mesons that are real particles. This problem does not occur though if the resonances only appear as internal particles in Feynman diagrams at low energies. An application where the method of including additional particles has proven to be successful is the calculation of the nucleon electromagnetic form factors. The ChPT results up to fourth order for the electromagnetic form factors only agree with experimental data for small values of momentum transfer (see, e.g., Refs. [Ber+ 92, Fea+ 97, KM 01, FGS 04]). It is known that the low-lying vector mesons, such as the ρ, ω, and ϕ, play an important role in the description of the nucleon form factors and it was shown in Refs. [KM 01, SGS 05] that the inclusion of these vector mesons into the effective theory results in an improved description of the data. Although the inclusion of vector mesons seems to resum the important higher-order terms, it does not include *all* of these terms. Therefore the method has to be viewed as a phenomenological extension of ChPT. However, it is based on a consistent power counting and allows for the systematic determination of which diagrams to consider in a calculation. It should be noted that in a strict chiral expansion the results with and without additional degrees of freedom do not differ up to a given order once the LECs have been adjusted accordingly.

The question arises why one does not simply perform a straightforward calculation of higher-order terms for each physical quantity. This approach is applied in the mesonic sector of ChPT where calculations are now performed up to sixth order in the chiral expansion (see, e.g., [Bij 07] for a recent review), and for the SU(2) case good agreement with experimental results is found. The extension to BChPT is more difficult. The renormalization in the mesonic sector is performed using a version of the minimal subtraction scheme (see, e.g., [Col 84]), which is also extensively used in other areas of particle physics. However, as mentioned above, this method does not result in a proper power counting in BChPT. The framework of heavy baryon ChPT (HBChPT) [JM 91, Ber+ 92], in which an expansion in inverse powers of the nucleon mass is performed in the Lagrangian, was the first solution to this problem. While HBChPT has been applied successfully to a variety of physical processes (for a review see [BKM 95]) it produces the wrong analytical structure for some Green functions in certain kinematical regimes [BKM 96]. In addition, the expansion in $1/m$ creates a large number of terms in the effective Lagrangian. Several manifestly Lorentz-invariant renormalization schemes [ET 98, BL 99, GJ 99, GJW 03, Goi+ 01, Fuc+ 03a] have been developed which give a proper power counting while also respecting the analytic structure in the whole low-energy domain. The most commonly used of these is the infrared (IR) regularization of Ref. [BL 99], which is also employed in this thesis. All these renormalization schemes have in common that there is a relation between the chiral order and the loop expansion. For example, for both HBChPT and IR regularization a calculation up to chiral order $D = 4$ includes the evaluation of one-loop diagrams, while chiral orders $D = 5$ and $D = 6$ also require two-loop diagrams. In the framework of HBChPT a calculation of the nucleon mass at order $D = 5$ exists [MB 99], and the leading nonanalytic contributions to the nucleon axial-vector coupling constant g_A have been determined using renormalization group techniques in Ref. [BM 06]. However, to the best of our knowledge no complete calculation beyond $D = 4$ has been performed in a manifestly Lorentz-invariant renormalization scheme. In the framework of the extended-on-mass-shell scheme [Fuc+ 03a] a two-loop calculation for a toy-model Lagrangian showed the applicability of this method in higher-order calculations [SGS 04b]. In its original formulation the IR regularization can be applied to one-loop diagrams, and a generalization of this method to allow for the treatment of multi-loop diagrams was proposed in Ref. [LP 02]. There also exists a reformulation of the IR regularization [SGS 04a] that allows for the application to multi-loop diagrams [SGS 04b]. In this thesis we show the details of how the renormalization of two-loop diagrams can be performed while preserving all relevant symmetries and present the details of the first complete two-loop calculation in infrared regularization.

This thesis is organized as follows. In Chapter 2 we discuss the QCD Lagrangian and its symmetries, which are relevant for the construction of the ChPT Lagrangian. Power counting is described and we present the Lagrangians relevant to the following calculations. One renormalization scheme which results in a consistent power counting for the baryonic sector of ChPT, the infrared regularization of Becher and Leutwyler [BL 99], is introduced in Chapter 3. We also present an alternative formulation of this scheme which can also be applied to diagrams containing additional degrees of freedom and to multi-loop diagrams. The axial, induced pseudoscalar, and pion-nucleon form factors are calculated in Chapter 4. After presenting the results of a calculation in the standard formulation of ChPT, we show how an axial-vector meson can be included to resum important higher-order contributions. The results of this work have been published in Ref. [Sch+ 07]. Chapter 5 discusses details of the infrared renormalization of two-loop diagrams. It is shown how the renormalization is performed such that all relevant symmetries as well as the power counting are preserved, and we then introduce a simplified method applicable to the calculation of the nucleon mass. The details of such a calculation up to and including order $D = 6$ are presented in Chapter 6. As a result we obtain the chiral expansion of the nucleon mass up to sixth order, and estimates for the numerical contributions of the higher-order terms are given. These results can also be found in Ref. [Sch+ 06]. We analyze the pion mass dependence of a specific term and estimate the contribution to the σ term. A summary and conclusions can be found in Chapter 7, while the appendices contain theoretical details such as the definition and explicit expressions of integrals and a discussion of the method of dimensional counting analysis.

Chapter 2

QCD and chiral perturbation theory

Quantum chromodynamics (QCD) [GW 73a, Wei 73, FGL 73] describes the strong interactions between quarks by the exchange of massless gauge bosons, the gluons. It is a non-Abelian gauge theory with SU(3) as the underlying gauge group. The present chapter discusses the Lagrangian of QCD and its symmetries, which play a crucial role in the construction of the corresponding effective field theory, chiral perturbation theory. The Lagrangians of the mesonic and baryonic sectors of baryon ChPT relevant for this work are presented.

2.1 Quantum chromodynamics

Denoting the quark fields by q_f, where the subscript f stands for one of the six flavors up (u), down (d), strange (s), charm (c), bottom (b) or top (t), and the gluon fields by $\mathcal{A}_{\mu,a}$, the QCD Lagrangian is given by [MP 78, Alt 82]

$$\mathcal{L}_{QCD} = \sum_f \bar{q}_f \left(i\not{D} - m_f\right) q_f - \frac{1}{4}\,\mathcal{G}_{\mu\nu,\,a}\mathcal{G}_a^{\mu\nu}. \tag{2.1}$$

Quarks carry the so-called color charge, which takes the three values red (r), green (g) and blue (b). The quark fields are color triplets,

$$q_f = \begin{pmatrix} q_{f,r} \\ q_{f,g} \\ q_{f,b} \end{pmatrix}, \tag{2.2}$$

and $D_\mu\, q_f$ denotes the covariant derivative on the quark fields,

$$D_\mu q_f = \partial_\mu q_f - ig\sum_{a=1}^{8}\frac{\lambda_a}{2}\,\mathcal{A}_{\mu,\,a} q_f\,, \tag{2.3}$$

with λ_a the Gell-Mann matrices. The gluon field is also contained in the field strength tensor $\mathcal{G}_{\mu\nu,\,a}$,

$$\mathcal{G}_{\mu\nu,a} = \partial_\mu\mathcal{A}_{\nu,\,a} - \partial_\nu\mathcal{A}_{\mu,\,a} + g f_{abc}\,\mathcal{A}_{\mu,\,b}\,\mathcal{A}_{\nu,\,c} \tag{2.4}$$

where f_{abc} are the structure functions of SU(3) and g is the coupling constant of the strong interactions. The parameters m_f in the Lagrangian of Eq. (2.1) are referred to as quark masses and their values span a wide range, from $1.5 - 3$ MeV for the u quark and $3 - 7$ MeV for the d quark, up to about 172 GeV for the t quark [Yao+ 06].[1] The Lagrangian of Eq. (2.1) is invariant under parity transformations (P), charge conjugation (C) and time reversal (T). Gauge invariance would also allow a term in the Lagrangian that violates P and CP symmetry, the so-called θ-term,

$$\mathcal{L}_\theta = \frac{g^2\bar{\theta}}{64\pi^2}\,\epsilon^{\mu\nu\rho\sigma}\sum_{a=1}^{8}\mathcal{G}^a_{\mu\nu}\mathcal{G}^a_{\rho\sigma}\,. \tag{2.5}$$

Since the experimental situation seems to indicate a very small value for the parameter $\bar{\theta}$ [Bak 06] and no P- or CP-violating processes are considered in this work, we neglect this term and only consider the P- and CP-invariant Lagrangian of Eq. (2.1).

Using the compact notation

$$q = (q_u, q_d, q_s, q_c, q_b, q_t)^T$$

and introducing the projection operators

$$P_R = \frac{1}{2}(1+\gamma_5), \quad P_L = \frac{1}{2}(1-\gamma_5)\,, \tag{2.6}$$

which project the quark fields q onto their chiral components q_R and q_L, respectively, the QCD Lagrangian can be written as

$$\mathcal{L}_{QCD} = (\bar{q}_R\, i\not{D} q_R + \bar{q}_L\, i\not{D} q_L - \bar{q}_R\,\mathcal{M} q_L - \bar{q}_L\,\mathcal{M} q_R) - \frac{1}{4}\,\mathcal{G}_{\mu\nu,\,a}\mathcal{G}^{\mu\nu}_a\,. \tag{2.7}$$

Here, $\mathcal{M}$ denotes the quark mass matrix,

$$\mathcal{M} = \begin{pmatrix} m_u & 0 & 0 & \\ 0 & m_d & 0 & \cdots \\ 0 & 0 & m_s & \\ & \vdots & & \ddots \end{pmatrix}.$$

One sees that in the derivative term right-handed (left-handed) fields exclusively couple to right-handed (left-handed) fields, while the mass term introduces couplings between right- and left-handed fields. Setting the quark mass parameters equal to zero, the coupling between right- and left-handed fields vanishes,

$$\mathcal{L}^0_{QCD} = \sum_f (\bar{q}_{f,\,R}\, i\not{D} q_{f,\,R} + \bar{q}_{f,\,L}\, i\not{D} q_{f,\,L}) - \frac{1}{4}\,\mathcal{G}_{\mu\nu,\,a}\mathcal{G}^{\mu\nu}_a\,. \tag{2.8}$$

The Lagrangian $\mathcal{L}^0_{QCD}$ is invariant under independent global U(N_f) transformations for q_L and q_R,

$$\begin{aligned} q_L &\mapsto U_L q_L\,, \\ q_R &\mapsto U_R q_R\,, \end{aligned} \tag{2.9}$$

[1] Since quarks do not appear as asymptotic physical states, the definition of their masses is ambiguous (see the note on quark masses in [Yao+ 06]).

in other words the massless QCD Lagrangian has a $\mathrm{U}(N_f)_L \times \mathrm{U}(N_f)_R$ symmetry. The group $\mathrm{U}(N_f)_L \times \mathrm{U}(N_f)_R$ is locally isomorphic to $\mathrm{SU}(N_f)_L \times \mathrm{SU}(N_f)_R \times \mathrm{U}(1)_V \times \mathrm{U}(1)_A$, where $\mathrm{U}(1)_V$ ($\mathrm{U}(1)_A$) refers to a multiplication of the right- and left handed fields with an equal (opposite) phase.[2] The symmetry considerations above hold on the classical level. Due to an anomaly [AB 69, Adl 69, Bar 69, BJ 69] the axial $\mathrm{U}(1)_A$ symmetry is not preserved upon quantization, and only a $\mathrm{SU}(N_f)_L \times \mathrm{SU}(N_f)_R \times \mathrm{U}(1)_V$ symmetry remains. The $\mathrm{U}(1)_V$ invariance is related to baryon number conservation, and the $\mathrm{SU}(N_f)_L \times \mathrm{SU}(N_f)_R$ symmetry is referred to as chiral symmetry.[3]

Non-zero quark masses explicitly break chiral symmetry, as they couple left-handed to right-handed quarks. In the simplest quark model picture the proton is thought to consist of two u quarks and one d quark. However, comparing the proton mass $m_p = 938$ MeV to the sum of quark masses one sees that $m_p \gg 2m_u + m_d$. The bulk of the proton mass does not seem to stem from the quark masses. As a starting point one can assume the u and d quarks to be massless and think of the chiral symmetry breaking due to their finite masses as a perturbation. For the case of massless u and d quarks the QCD Lagrangian has a $\mathrm{SU}(2)_L \times \mathrm{SU}(2)_R$ symmetry, and this symmetry of the Lagrangian should manifest itself in the spectrum of hadrons which (in quark model language) contain only u and d quarks. Arranging the generators of $\mathrm{SU}(2)_L \times \mathrm{SU}(2)_R$ into linear combinations with positive and negative parity, $Q_V^a = Q_R^a + Q_L^a$ and $Q_A^a = Q_R^a - Q_L^a$ ($a = 1, 2, 3$), one thus expects degenerate SU(2) multiplets of opposite parity. The observed spectrum, however, does not show the expected symmetry pattern. Instead the low-energy hadrons containing u and d quarks can be arranged in SU(2) multiplets, with all members of a certain multiplet having the same behavior under parity transformations, but degenerate multiplets of opposite parity are not observed. It was shown that for massless u and d quarks $\mathrm{SU}(2)_V$ is not broken [VW 84]. The absence of parity doubling then suggests that the axial symmetry, related to the generators Q_A^a, is spontaneously broken.

2.2 Spontaneous symmetry breaking

A symmetry is said to be spontaneously broken if the ground state of a theory is not invariant under the full symmetry group of the Hamiltonian. In a quantum field theory this is the case when the Hamiltonian allows for several (up to infinitely many) degenerate ground states. The choice of one of those ground states as the physical one breaks the symmetry.[4] Spontaneous breaking does not have to occur for the complete symmetry group, it can leave the ground state invariant under a subgroup. If the considered symmetry is a continuous symmetry and n_G denotes the number of

[2] To be precise, the group $\mathrm{U}(N) \times \mathrm{U}(N)$ is isomorphic to $\mathrm{U}(1) \times \mathrm{SU}(N)/Z_N \times \mathrm{U}(1) \times \mathrm{SU}(N)/Z_N$, where Z_N is the center of $\mathrm{SU}(N)$.

[3] In the literature the term chiral symmetry is sometimes also used for a $\mathrm{U}(N_f)_L \times \mathrm{U}(N_f)_R$ symmetry.

[4] Note that in quantum mechanics the existence of several degenerate ground states does not result in spontaneous symmetry breaking, since the physical ground state can be a linear superposition of ground states.

generators of the symmetry group G, while n_H stands for the number of generators of the residual symmetry subgroup H, Goldstone's theorem [Gol 61, GSW 62] predicts the existence of $n_G - n_H$ massless spin-0 bosons, called Goldstone bosons. In the case where the underlying symmetry group G is not exact, but only approximate, the appearing spinless particles have a non-vanishing, but small mass and are called pseudo-Goldstone bosons.

Let us apply the above considerations to the QCD Lagrangian with small values of the u and d quarks. The Lagrangian is approximately invariant under $G = \mathrm{SU}(2)_L \times \mathrm{SU}(2)_R$ with $n_G = 6$. The symmetry is assumed to be broken to a $H = \mathrm{SU}(2)_V$ symmetry with $n_H = 3$. One therefore expects the existence of $n_G - n_H = 6 - 3 = 3$ light spinless particles. In the hadron spectrum the pions have spin 0 and are much lighter than other hadrons containing only u and d quarks, like the ρ mesons for example, which leads to the identification of the pions as the pseudo-Goldstone bosons of spontaneously broken chiral symmetry.

2.3 Ward identities and local symmetry

The global $\mathrm{SU}(2)_L \times \mathrm{SU}(2)_R$ symmetry for massless u and d quarks provides constraints on the Green functions of QCD. In particular, it also imposes relations among different Green functions, known as Ward-Fradkin-Takahashi identities (Ward identities for short) [War 50, Fra 55, Tak 57]. The QCD Green functions for the vector, axial vector, scalar and pseudoscalar currents can be derived from a generating functional when a coupling of the quarks to external fields is considered,

$$\mathcal{L} = \mathcal{L}^0_{QCD} + \mathcal{L}_{ext} = \mathcal{L}^0_{QCD} + \bar{q}\gamma_\mu(v^\mu + \frac{1}{3}v^\mu_{(s)} + \gamma_5 a^\mu)q - \bar{q}(s - i\gamma_5 p)q. \tag{2.10}$$

The external fields are hermitian and color-neutral matrices acting in flavor space. Note that the QCD Lagrangian is obtained by setting $s = \mathcal{M}$ and $v^\mu = v^\mu_{(s)} = a^\mu = p = 0$. Since in the following we will be interested in Green functions of currents of the u and d quarks, we restrict the discussion to these two flavors. The external fields are then given by 2×2 matrices,

$$v^\mu = \sum_{i=1}^{3} \frac{\tau_i}{2} v_i^\mu, \quad v^\mu_{(s)} = \frac{\tau_0}{2} v_0^\mu, \quad a^\mu = \sum_{i=1}^{3} \frac{\tau_i}{2} a_i^\mu, \quad s = \sum_{i=0}^{3} \tau_i s_i, \quad p = \sum_{i=0}^{3} \tau_i p_i, \tag{2.11}$$

where τ_0 is the two-dimensional unit matrix and τ_i $(i = 1, 2, 3)$ are the Pauli matrices. The generating functional takes the form

$$\exp(iZ[v, a, s, p]) = \langle 0| T \exp\left[i \int d^4x \mathcal{L}_{ext}(x) \right] |0\rangle, \tag{2.12}$$

and by functional differentiation with respect to the external fields the Green functions can be obtained. The resulting Green functions obey the Ward identities stemming from the *global* $\mathrm{SU}(2)_L \times \mathrm{SU}(2)_R$ symmetry of the massless QCD Lagrangian. These Ward identities imply that the generating functional is invariant under the same *local* transformation of the external fields as occur if one requires the Lagrangian of Eq. (2.10) to be invariant under *local* $\mathrm{SU}(2)_L \times \mathrm{SU}(2)_R$ transformations,

$$\begin{aligned}
(v^\mu + a^\mu) &\mapsto V_R(v^\mu + a^\mu)V_R^\dagger + iV_R\partial^\mu V_R^\dagger, \\
(v^\mu - a^\mu) &\mapsto V_L(v^\mu - a^\mu)V_L^\dagger + iV_L\partial^\mu V_L^\dagger, \\
(s + ip) &\mapsto V_R(s + ip)V_L^\dagger, \\
(s - ip) &\mapsto V_L(s - ip)V_R^\dagger,
\end{aligned} \tag{2.13}$$

where $(V_L, V_R) \in \mathrm{SU}(2)_L \times \mathrm{SU}(2)_R$. The invariance of the generating functional under local transformations of the external fields allows to obtain all Ward identities by functional derivatives of a master equation (see, e.g., Appendix A of Ref. [Sch 03]). While at the level of QCD the invariance of the generating functional under local transformations collects the Ward identities in a very compact form, the local version of the symmetry plays a crucial role for the corresponding effective field theory. As shown in Ref. [Leu 94] the effective Lagrangian reproducing the Green functions obtained from the generating functional of Eq. (2.12) can be brought into a form that is invariant under *local* $\mathrm{SU}(2)_L \times \mathrm{SU}(2)_R$ transformations, which provides important constraints for the construction of the Lagrangian. In addition, local invariance also allows for the coupling of the effective degrees of freedom to external gauge fields such as the electromagnetic field.

2.4 Chiral perturbation theory

Having established the symmetries of the QCD Lagrangian, one can proceed to construct the corresponding effective field theory for low-energy hadronic processes, called chiral perturbation theory (ChPT) [Wei 79, GL 84, GL 85]. For an extensive introduction to ChPT see, e.g., Ref. [Sch 03]. One of the advantages of an EFT is that the degrees of freedom can be chosen to be those relevant to the energy region of interest. For strong interaction processes far below 1 GeV these are hadrons instead of the more fundamental quarks and gluons. Considering only the u and d quarks to be light, one expects the hadron spectrum to show an SU(2) multiplet pattern. The lowest-lying SU(2) multiplet is the triplet of pions, which as explained above are considered the Goldstone bosons of spontaneous chiral symmetry breaking. In its mesonic sector ChPT describes the interaction among pions as well as of pions with external fields. One needs to write down the most general Lagrangian in terms of the pion fields that is consistent with the symmetries of QCD as discussed above, and in particular is invariant under *local* $\mathrm{SU}(2)_L \times \mathrm{SU}(2)_R$ transformations. Physical quantities are then calculated as expansions in q/Λ, where q stands for small momenta or the pion mass and Λ is expected to be approximately 1 GeV, the scale of spontaneous chiral symmetry breaking. As an extension the interaction of pions with baryons can be considered. The lowest-lying baryon multiplet is the nucleon doublet of proton and neutron. The interaction of nucleons with pions and external fields can also be described by ChPT, provided that the appearing nucleon three momenta are much smaller than 1 GeV [GSS 88].

2.4.1 Power counting

The ChPT Lagrangian contains an infinite number of terms, which can be ordered according to the number of derivatives acting on pion fields and powers of pion masses,

$$\mathcal{L} = \mathcal{L}_1 + \mathcal{L}_2 + \mathcal{L}_3 + \cdots . \tag{2.14}$$

As will be explained below, the mesonic Lagrangian only contains terms of even power, while in the baryonic sector also odd numbers of derivatives appear. Since an infinite number of Feynman diagrams derived from this Lagrangian contributes to any physical process, a scheme is required to determine the relative importance of each diagram, which in turn allows to identify those diagrams necessary for a calculation to a certain accuracy. For the mesonic sector this is achieved by Weinberg's power counting [Wei 79]. Consider the behavior of the invariant amplitude $\mathcal{M}(p, m_q)$ under linear rescaling of the external pion momenta, $p_i \mapsto tp_i$, and quadratic rescaling of quark masses, $m_q \mapsto t^2 m_q$,

$$\mathcal{M}(p_i, m_q) \mapsto \mathcal{M}(tp_i, t^2 m_q) = t^D \mathcal{M}(p_i, m_q). \tag{2.15}$$

Here, D is the so-called chiral dimension and is given by

$$D = 2 + \sum_{n=0}^{\infty} 2(n-1) N_{2n} + 2N_L, \tag{2.16}$$

where N_{2n} is the number of vertices from $\mathcal{L}_{2n}$ and N_L stands for the number of loop integrations. For small values of t diagrams with low D dominate and diagrams with D larger than a certain value can be neglected in calculations to a given accuracy. Using the relation

$$N_V = N_I - N_L + 1,$$

where N_V is the total number of vertices and N_I denotes the number of internal pion lines, one can write D as

$$D = 4N_L - 2N_I + \sum_{n=0}^{\infty} 2n N_{2n}. \tag{2.17}$$

One therefore assigns the following chiral orders to the individual parts of Feynman diagrams: Loop integration in 4 dimensions counts as order $D = 4$, a pion propagator as $D = -2$ and a vertex from $\mathcal{L}_{2n}$ as $D = 2n$.

When extended to the nucleonic sector, the same power counting rules can be chosen with the addition that a nucleon propagator counts as $D = -1$ and vertices from the jth-order nucleonic Lagrangian count as order $D = j$ [Wei 91, Eck 95].

2.4.2 Mesonic Lagrangian

Following the general description of Ref. [CWZ 69, Cal+ 69], the Goldstone boson fields are collected in the unimodular unitary 2×2 matrix U,

$$U(x) = \exp\left(\frac{i\Phi(x)}{F}\right), \quad \Phi(x) = \sum_{i=1}^{3} \tau_i \Phi_i = \begin{pmatrix} \pi^0 & \sqrt{2}\pi^+ \\ \sqrt{2}\pi^- & -\pi^0 \end{pmatrix}, \tag{2.18}$$

the covariant derivative of which is defined as

$$D_\mu U = \partial_\mu U - i r_\mu U + i U l_\mu \,,$$

with

$$r_\mu = v_\mu + a_\mu, \quad l_\mu = v_\mu - a_\mu, \quad \chi = 2B(s + ip)\,.$$

The quantities v_μ, a_μ, s, and p stand for external vector, axial-vector, scalar, and pseudoscalar sources, respectively, and B is related to the quark condensate $\langle \bar{q}q \rangle_0$ in the chiral limit. To construct a chirally invariant Lagrangian the transformation properties of the different building blocks under the group $\mathrm{SU}(2)_L \times \mathrm{SU}(2)_R$ need to be known. The Goldstone boson fields transform as

$$U(x) \mapsto V_R U(x) V_L^\dagger, \tag{2.19}$$

where $(V_L, V_R) \in \mathrm{SU}(2)_L \times \mathrm{SU}(2)_R$, while the transformation behavior of the external fields is given by

$$\begin{aligned} r^\mu &\mapsto V_R r^\mu V_R^\dagger + i V_R \partial^\mu V_R^\dagger\,, \\ l^\mu &\mapsto V_L l^\mu V_L^\dagger + i V_L \partial^\mu V_L^\dagger\,, \\ \chi &\mapsto V_R \chi V_L^\dagger\,, \\ \chi^\dagger &\mapsto V_L \chi^\dagger V_R^\dagger\,. \end{aligned} \tag{2.20}$$

For the construction of higher-order terms it is useful to define the field strength tensors of the external fields,

$$\begin{aligned} f_{\mu\nu}^R &= \partial_\mu r_\nu - \partial_\nu r_\mu - i[r_\mu, r_\nu]\,, \\ f_{\mu\nu}^L &= \partial_\mu l_\nu - \partial_\nu l_\mu - i[l_\mu, l_\nu]\,, \end{aligned} \tag{2.21}$$

which transform under $\mathrm{SU}(2)_L \times \mathrm{SU}(2)_R$ as

$$\begin{aligned} f_{\mu\nu}^R &\mapsto V_R f_{\mu\nu}^R V_R^\dagger\,, \\ f_{\mu\nu}^L &\mapsto V_L f_{\mu\nu}^L V_L^\dagger\,. \end{aligned} \tag{2.22}$$

The chiral orders of these building blocks are given by

$$U = \mathcal{O}(q^0), \quad D_\mu U = \mathcal{O}(q^1), \quad f_{\mu\nu}^{R/L} = \mathcal{O}(q^2), \quad \chi = \mathcal{O}(q^2)\,. \tag{2.23}$$

Together with the transformation behavior under charge conjugation C and parity P, which are listed in Table 2.1, one can proceed to construct the most general Lagrangian invariant under these symmetries at any given order. Due to Lorentz invariance the mesonic Lagrangian only contains even powers,

$$\mathcal{L}_\pi = \mathcal{L}_2 + \mathcal{L}_4 + \cdots\,. \tag{2.24}$$

The lowest-order Lagrangian $\mathcal{L}_2$ reads [GL 84]

$$\mathcal{L}_2 = \frac{F^2}{4}\,\mathrm{Tr}\left[D_\mu U (D^\mu U)^\dagger\right] + \frac{F^2}{4}\,\mathrm{Tr}\left[\chi U^\dagger + U \chi^\dagger\right]\,. \tag{2.25}$$

	U	$D_\mu U$	χ	$D_\mu \chi$	r_μ	l_μ	$f^R_{\mu\nu}$	$f^L_{\mu\nu}$
C	U^T	$(D_\mu U)^T$	χ^T	$(D_\mu \chi)^T$	$-l^T_\mu$	$-r^T_\mu$	$-(f^L_{\mu\nu})^T$	$-(f^R_{\mu\nu})^T$
P	$U^\dagger$	$(D^\mu U)^\dagger$	$\chi^\dagger$	$(D^\mu \chi)^\dagger$	l^μ	r^μ	$f^{L,\mu\nu}$	$f^{R,\mu\nu}$

Table 2.1: Transformation behavior under C, P.

Two low-energy coupling constants (LECs) appear in the lowest-order Lagrangian, F and B. As mentioned above, B is related to the quark condensate in the chiral limit, and one finds that the constant F is the pion decay constant in the chiral limit, $F_\pi = F + \mathcal{O}(\hat{m})$, with $\hat{m} = (m_u + m_d)/2$. Furthermore, the leading-order expression for the pion mass squared in terms of the average light quark mass is given by $M^2 = 2B\hat{m}$ [GL 84]. For the following calculations only two terms from the Lagrangian $\mathcal{L}_4$ are needed. We will employ the notation of Ref. [GSS 88] in which the relevant terms of the Lagrangian read

$$\mathcal{L}_4 = \cdots + \frac{l_3 + l_4}{16} \left[\mathrm{Tr}(\chi U^\dagger + U\chi^\dagger)\right]^2 + \frac{l_4}{8} \left[D_\mu U (D^\mu U)^\dagger\right] \mathrm{Tr}(\chi U^\dagger + U\chi^\dagger) + \cdots \,. \quad (2.26)$$

2.4.3 Baryonic Lagrangian

In order to construct the most general Lagrangian for processes including nucleons, the nucleon degrees of freedom are contained in the isospinor

$$\Psi = \begin{pmatrix} p \\ n \end{pmatrix} . \quad (2.27)$$

The transformation behavior of Ψ under the chiral group $\mathrm{SU}(2)_L \times \mathrm{SU}(2)_R$ is given in terms of the compensator $K(V_L, V_R, U)$,

$$\begin{aligned} \Psi &\mapsto K(V_L, V_R, U)\Psi \,, \\ \bar{\Psi} &\mapsto \bar{\Psi} K^{-1}(V_L, V_R, U) \,. \end{aligned} \quad (2.28)$$

$K(V_L, V_R, U)$ is a function of the group elements (V_L, V_R) of $\mathrm{SU}(2)_L \times \mathrm{SU}(2)_R$ as well as the Goldstone boson fields. Its explicit form is given by

$$K(V_L, V_R, U) = u'^{-1} V_R u = \sqrt{V_R U V_L^\dagger}^{\,-1} V_R \sqrt{U} \quad (2.29)$$

where the notation $u = \sqrt{U}$ has been used for the Goldstone boson fields and $u' = \sqrt{V_R U V_L^\dagger}$ is related to the transformed Goldstone boson fields. With the definition of the so-called connection [Eck 95],

$$\Gamma_\mu = \frac{1}{2} \left[u^\dagger (\partial_\mu - i r_\mu) u + u (\partial_\mu - i l_\mu) u^\dagger\right] , \quad (2.30)$$

the covariant derivative of the nucleon is given by

$$D_\mu \Psi = \left(\partial_\mu + \Gamma_\mu - i v^{(s)}_\mu\right) \Psi \,. \quad (2.31)$$

Here, $v_\mu^{(s)}$ stands for the external isoscalar vector field and the covariant derivative transforms in the same way under $\mathrm{SU}(2)_L \times \mathrm{SU}(2)_R$ transformations as the isospinor Ψ,

$$D_\mu \Psi \mapsto K(V_L, V_R, U) D_\mu \Psi\,. \tag{2.32}$$

In order to construct a Lagrangian that is invariant under $\mathrm{SU}(2)_L \times \mathrm{SU}(2)_R$ it is convenient to define new building blocks which contain the Goldstone bosons as well as external fields and which have specific transformation properties in terms of the compensator $K(V_L, V_R, U)$. These building blocks are given by

$$\begin{aligned}
u_\mu &= i\left[u^\dagger(\partial_\mu - i r_\mu)u - u(\partial_\mu - i l_\mu)u^\dagger\right], \\
\chi_\pm &= u^\dagger \chi u^\dagger \pm u \chi^\dagger u, \\
f_{\mu\nu}^\pm &= u f_{\mu\nu}^L u^\dagger \pm u^\dagger f_{\mu\nu}^R u, \\
v_{\mu\nu}^{(s)} &= \partial_\mu v_\nu^{(s)} - \partial_\nu v_\mu^{(s)},
\end{aligned} \tag{2.33}$$

which transform as

$$\begin{aligned}
X &\mapsto K(V_L, V_R, U) X K^{-1}(V_L, V_R, U), \quad X = u_\mu, \chi_\pm, f_{\mu\nu}^\pm, \\
v_{\mu\nu}^{(s)} &\mapsto v_{\mu\nu}^{(s)}
\end{aligned} \tag{2.34}$$

under chiral transformations. Furthermore the covariant derivatives of the building blocks are given by

$$D_\mu X = \partial_\mu X + [\Gamma_\mu, X]\,, \tag{2.35}$$

which transform in the same way as the building blocks. With these definitions one can construct a Lagrangian containing terms of the form $\bar\Psi \mathcal{O} \Psi$, where $\mathcal{O}$ is an operator composed from the building blocks of Eq. (2.33) and their covariant derivatives.

The lowest-order Lagrangian reads [GSS 88]

$$\mathcal{L}_{\pi N}^{(1)} = \bar\Psi \left[i \not{D} - m + \frac{\mathsf{g}_A}{2} \gamma^\mu \gamma_5 u_\mu \right] \Psi, \tag{2.36}$$

where m is the nucleon mass in the chiral limit and g_A is the nucleon axial-vector coupling constant, also in the chiral limit. The complete Lagrangians of orders $\mathcal{O}(q^2)$, $\mathcal{O}(q^3)$, and $\mathcal{O}(q^4)$ are given in [EM 96, Fet+ 00]. We only show those terms explicitly which are required for our calculations. The Lagrangian at order $\mathcal{O}(q^2)$ contains seven terms, of which we need

$$\begin{aligned}
\mathcal{L}_{\pi N}^{(2)} &= c_1 \mathrm{Tr}(\chi_+) \bar\Psi \Psi - \frac{c_2}{4m^2}\left[\bar\Psi \mathrm{Tr}(u_\mu u_\nu) D^\mu D^\nu \Psi + \mathrm{h.c.}\right] + \frac{c_3}{2} \bar\Psi \mathrm{Tr}(u_\mu u^\mu) \Psi \\
&\quad + \bar\Psi \left[i \frac{c_4}{4} [u_\mu u_\nu] + \frac{c_6}{2} f_{\mu\nu}^+ \right] \sigma^{\mu\nu} \Psi + \cdots\,,
\end{aligned} \tag{2.37}$$

where *h.c.* stands for the hermitian conjugate. Out of the 23 terms at order $\mathcal{O}(q^3)$ the following are relevant for our purposes,

$$\mathcal{L}_{\pi N}^{(3)} = \frac{d_{16}}{2} \bar\Psi \mathrm{Tr}(\chi_+) \gamma^\mu \gamma_5 u_\mu \Psi + i \frac{d_{18}}{2} \bar\Psi \gamma^\mu \gamma_5 [D_\mu, \chi_-] \Psi + \frac{d_{22}}{2} \bar\Psi \gamma^\mu \gamma_5 [D^\nu, F_{\mu\nu}^-] \Psi + \cdots\,. \tag{2.38}$$

The Lagrangian at order $\mathcal{O}(q^4)$ reads

$$\begin{aligned}
\mathcal{L}_{\pi N}^{(4)} \;=\;& \cdots + e_{14}\bar{\Psi}\mathrm{Tr}(h_{\mu\nu}h^{\mu\nu})\Psi - \frac{e_{15}}{4m^2}\bar{\Psi}\mathrm{Tr}(h_{\lambda\mu}h^{\lambda}{}_{\nu})D^{\mu\nu}\Psi + h.c. \\
&+\frac{e_{16}}{48m^4}\bar{\Psi}\mathrm{Tr}(h_{\lambda\mu}h_{\lambda\rho})D^{\lambda\mu\nu\rho}\Psi + h.c. + e_{19}\bar{\Psi}\mathrm{Tr}(\chi_+)\mathrm{Tr}(u_\mu u^\mu)\Psi \\
&-\frac{e_{20}}{4m^2}\bar{\Psi}\mathrm{Tr}(\chi_+)\mathrm{Tr}(u_\mu u_\nu)D^{\mu\nu}\Psi + h.c. - i\frac{e_{35}}{4m^2}\bar{\Psi}\mathrm{Tr}(\chi_- h_{\mu\nu})D^{\mu\nu}\Psi + h.c. \\
&+ie_{36}\bar{\Psi}\mathrm{Tr}(u_\mu)D^\mu\chi_-\Psi + e_{38}\bar{\Psi}\mathrm{Tr}(\chi_+)^2\Psi + \frac{e_{115}}{4}\bar{\Psi}\mathrm{Tr}(\chi_+^2 - \chi_-^2)\Psi \\
&-\frac{e_{116}}{4}\bar{\Psi}\left[\mathrm{Tr}(\chi_-^2) - \mathrm{Tr}(\chi_-)^2 + \mathrm{Tr}(\chi_+^2) - \mathrm{Tr}(\chi_+)^2\right]\Psi + \cdots\,,
\end{aligned} \tag{2.39}$$

where $h.c.$ again stands for the hermitian conjugate and always refers to the structure immediately in front of it. The notation

$$h_{\mu\nu} = D_\mu u_\nu + D_\nu u_\mu, \quad D_{\mu\nu}\Psi = (D_\mu D_\nu + D_\nu D_\mu)\Psi \tag{2.40}$$

has been introduced for the symmetrized combinations of the covariant derivative.

The Lagrangians of order $\mathcal{O}(q^5)$ and $\mathcal{O}(q^6)$ have not been constructed yet. However, in a calculation of the nucleon mass to order $\mathcal{O}(q^6)$ they will only contribute to tree-level diagrams. Since an expression proportional to M^5, where M denotes the pion mass, is nonanalytic in the quark masses it cannot appear in the Lagrangian. Therefore only terms from the Lagrangian at order $\mathcal{O}(q^6)$ are needed. There are several relevant terms in the Lagrangian of that order and the contribution to the nucleon mass involves a linear combination of LECs, which we denote by $\hat{g}_1$. The relevant part of the Lagrangian can then be written as

$$\mathcal{L}_{\pi N}^{(6)} \;\sim\; \hat{g}_1 M^6\bar{\Psi}\Psi + \cdots\,. \tag{2.41}$$

Chapter 3

Infrared regularization

When chiral perturbation theory was first extended to include processes with one nucleon [GSS 88], problems with the power counting appeared. Consider the diagram of Fig. 3.1, which corresponds to a nucleon self-energy contribution. According to the power counting specified in Chapter 2, the result should be of order

$$D = n + 2 \cdot 1 - 1 - 2 = n - 1 \stackrel{n\to 4}{\longrightarrow} 3. \tag{3.1}$$

In the mesonic sector diagrams are evaluated using dimensional regularization [HV 72] in combination with the modified minimal subtraction scheme of ChPT ($\widetilde{\mathrm{MS}}$) [Fuc+ 03a].

When the same methods are applied to the diagram of Fig. 3.1, however, the lowest-order term in the result has chiral order

$$D = 2, \tag{3.2}$$

lower than suggested by Eq. (3.1). It was already realized in Ref. [GSS 88] that the failure of the power counting rules is related to the regularization and renormalization procedure. The first solution to this power counting problem was given by heavy-baryon ChPT (HBChPT) [JM 91, Ber+ 92], in which an expansion in inverse powers of the nucleon mass is performed in the Lagrangian. The price of this method, besides an increase in the number of terms in the Lagrangian, is that manifest Lorentz invariance is lost. Subsequently several manifestly Lorentz-invariant renormalization schemes have been developed that also result in a proper power counting [ET 98, BL 99, GJ 99, GJW 03, Goi+ 01, Fuc+ 03a]. The most commonly used scheme is the infrared (IR) regularization of Becher and Leutwyler [BL 99], which is also applied in this work.

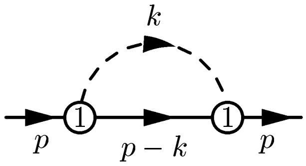

Figure 3.1: Nucleon self-energy contribution.

3.1 Infrared regularization of Becher and Leutwyler

The method of infrared regularization [BL 99] is based on dimensional regularization and the analytic properties of loop integrals. It is applicable to one-loop integrals in the one-nucleon sector of ChPT. Consider the general integral

$$H_{\pi\cdots N\cdots}(q_1,\ldots,p_1,\ldots) = i\int \frac{d^nk}{(2\pi)^n}\,\frac{1}{a_1\cdots a_m\; b_1\cdots b_l}, \tag{3.3}$$

where $a_i=(k+q_i)^2-M^2+i0^+$ and $b_j=(k+p_j)^2-m^2+i0^+$ denote inverse pion and nucleon propagators, respectively, and n is the number of space-time dimensions. One combines the pion propagators using

$$\frac{1}{a_1\cdots a_m} = \left(\frac{\partial}{\partial M^2}\right)^{(m-1)} \int_0^1 dx_1\cdots\int_0^1 dx_{m-1}\frac{X}{A}\,, \tag{3.4}$$

with the numerator given by

$$X = \left\{\begin{array}{ll} 1 & \text{for } m=2, \\ x_2(x_3)^2\cdots(x_{m-1})^{m-2} & \text{for } m>2, \end{array}\right. \tag{3.5}$$

and the recursive relation for the denominator

$$\begin{array}{rcl} A &=& A_m, \\ A_1 &=& a_1, \\ A_{p+1} &=& x_pA_p+(1-x_p)a_{p+1} \qquad (p=1,\ldots,m-1). \end{array} \tag{3.6}$$

The denominator A can be written as

$$A=(k+\bar{q})^2-\bar{A}+i0^+, \tag{3.7}$$

where $\bar{q}$ is a linear combination of the external momenta q_i and $\bar{A}$ is a constant.

Similarly we combine the nucleon propagators

$$\frac{1}{b_1\cdots b_l} = \left(\frac{\partial}{\partial m^2}\right)^{(l-1)} \int_0^1 dy_1\cdots\int_0^1 dy_{l-1}\frac{Y}{B}\,, \tag{3.8}$$

where the numerator reads

$$Y = \left\{\begin{array}{ll} 1 & \text{for } l=2, \\ y_2(y_3)^2\cdots(y_{l-1})^{l-2} & \text{for } l>2, \end{array}\right. \tag{3.9}$$

and the recursive relation for the denominator B is given by

$$\begin{array}{rcl} B &=& B_l, \\ B_1 &=& b_1, \\ B_{p+1} &=& y_pB_p+(1-y_p)b_{p+1} \qquad (p=1,\ldots,l-1). \end{array} \tag{3.10}$$

Again the result for the denominator is quadratic in k,

$$B=(k+\bar{p})^2-\bar{B}+i0^+, \tag{3.11}$$

where $\bar{p}$ is a linear combination of the external momenta p_i. The two resulting denominators can be combined using the identity

$$\frac{1}{AB} = \int_0^1 \frac{dz}{[(1-z)A + zB]^2}, \tag{3.12}$$

resulting in

$$\begin{aligned} &H_{\pi\cdots N\cdots}(q_1,\ldots,p_1,\ldots) \\ &= i\left(\frac{\partial}{\partial M^2}\right)^{(m-1)}\left(\frac{\partial}{\partial m^2}\right)^{(l-1)} \int_0^1 dz \int_0^1 dx_i \int_0^1 dy_j \; XY \int \frac{d^nk}{(2\pi)^n} \frac{1}{[(1-z)A+zB]^2}, \end{aligned} \tag{3.13}$$

where

$$\int_0^1 dx_i = \int_0^1 dx_1 \cdots \int_0^1 dx_{m-1}\,, \quad \int_0^1 dy_j = \int_0^1 dy_1 \cdots \int_0^1 dy_{l-1}\,.$$

After evaluating the derivatives and performing the integration over k one obtains

$$\begin{aligned} &H_{\pi\cdots N\cdots}(q_1,\ldots,p_1,\ldots) \\ &= \frac{(-1)^{1-l-m}}{(4\pi)^{n/2}}\Gamma(l+m-n/2)\int_0^1 dz\, z^{l-1}(1-z)^{m-1}\int_0^1 dx_i \int_0^1 dy_j\, XY[f(z)]^{(n/2)-l-m}, \end{aligned} \tag{3.14}$$

with

$$f(z) = \bar{p}^2 z^2 - \left(\bar{p}^2 - \bar{B}\right) z + \bar{A}(1-z) - \left(\bar{q}^2 - 2\bar{p}\cdot\bar{q}\right) z(1-z) - i0^+\,.$$

The infrared regularization consists of rewriting the z integration as

$$\int_0^1 dz \cdots = \int_0^\infty dz \cdots - \int_1^\infty dz \cdots\,. \tag{3.15}$$

The first term on the right-hand side of Eq. (3.15) is called the infrared singular part I, while the second term is referred to as the infrared regular part R,

$$H_{\pi\cdots N\cdots} = I_{\pi\cdots N\cdots} + R_{\pi\cdots N\cdots}\,, \tag{3.16}$$

or for short

$$H = I + R\,. \tag{3.17}$$

The advantage of splitting the original integral into two parts is that the infrared singular part I satisfies the power counting, while R contains terms that violate the power counting. In addition, the infrared singular and infrared regular parts differ in their analytic properties. For noninteger n the expansion of I in small quantities results in only noninteger powers of these variables, while R only contains analytic contributions. As mentioned in Chapter 2, symmetries introduce relations among various Green functions of the theory, called Ward identities. Expressions containing the integrals H satisfy the Ward identities,[1] since they are derived from an invariant Lagrangian and dimensional regularization does not violate the symmetries. Since I only contains nonanalytic terms, while R consists of analytic contributions only, each part has to satisfy the Ward identities separately in order for the sum $H = I + R$ not to violate any symmetry.

3.2 Reformulation of infrared regularization

In its original formulation by Becher and Leutwyler, infrared regularization[2] is applicable to one-loop integrals containing pion and nucleon propagators in the one-nucleon sector of ChPT. It is possible to formulate IR renormalization in a way that it can also be applied to multi-loop diagrams and diagrams containing additional degrees of freedom, such as vector or axial-vector mesons [SGS 04a].

In the original formulation the integration over the parameter z in the infrared regular part R is given by

$$-\int_1^\infty dz\, z^{l-1}(1-z)^{m-1}[f(z)]^{(n/2)-l-m}. \tag{3.18}$$

The chiral expansion for R can be performed before evaluating the z integration [BL 99]. The infrared regular part is then given as a sum of terms containing integrals over z of the type

$$R_i = -\int_1^\infty dz\, z^{n+i}. \tag{3.19}$$

These integrals are calculated by analytic continuation from the domain of n in which they converge,

$$R_i = -\left.\frac{z^{n+i+1}}{n+i+1}\right|_1^\infty = \frac{1}{n+i+1}\,. \tag{3.20}$$

One can reproduce the result of Eq. (3.20) without having to split the integral over z into two parts. Instead one performs the chiral expansion of the integrand in the *original* integral H of Eq. (3.14) and interchanges summation and integration. Since the result only contains terms analytic in small parameters, but H in most cases also contains nonanalytic terms, this does *not* reproduce the chiral expansion of H. The resulting series contains the same coefficients as the expansion of R, except that the integrals R_i are replaced by integrals of the type

$$J_i = \int_0^1 dz\, z^{n+i}. \tag{3.21}$$

[1] In the following we use the phrase that integrals satisfy the Ward identities, by which we mean that expressions containing these integrals satisfy the Ward identities.

[2] Since the infrared regularization actually also describes a renormalization procedure, the term infrared renormalization is used in the following.

Again performing an analytic continuation the integrals J_i are given by

$$J_i = \left.\frac{z^{n+i+1}}{n+i+1}\right|_0^1 = \frac{1}{n+i+1}. \tag{3.22}$$

Comparing Eqs. (3.20) and (3.22) one sees that the two results agree. The infrared regular part of the integral H can therefore be obtained by reducing H to an integral over Schwinger or Feynman parameters, expanding the resulting expression in small quantities and interchanging summation and integration.

As an example consider the integral

$$H_{\pi N}(0,-p) = i \int \frac{d^n k}{(2\pi)^n} \frac{1}{[k^2 - M^2 + i0^+][(k-p)^2 - m^2 + i0^+]}. \tag{3.23}$$

To apply the reformulated version of IR renormalization we combine the two propagators using Eq. (3.12), and perform the integration over the loop momentum k, resulting in

$$H_{\pi N}(0,-p) = -\frac{1}{(4\pi)^{n/2}}\, \Gamma(2-n/2) \int_0^1 dz \;\; [C(z)]^{(n/2)-2}, \tag{3.24}$$

where $C(z) = m^2 z^2 - (p^2 - m^2)(1-z)z + M^2(1-z) - i0^+$. We now expand $[C(z)]^{(n/2)-2}$ in $p^2 - m^2$ and M^2 and interchange summation and integration. The chiral expansion of the infrared regular part R is then given by

$$R = -\frac{m^{n-4}\Gamma(2-n/2)}{(4\pi)^{n/2}(n-3)} \left[1 - \frac{p^2-m^2}{2m^2} + \frac{(n-6)\left(p^2-m^2\right)^2}{4m^4(n-5)} + \frac{(n-3)M^2}{2m^2(n-5)} + \cdots\right]. \tag{3.25}$$

which coincides with the expansion of R given in Ref. [BL 99].

In the original formulation the extension of infrared renormalization beyond one-loop diagrams of the one-nucleon sector of BChPT is not straightforward, as it is not obvious which of the Schwinger or Feynman parameter integrals needs to be divided into two distinct parts. Such a problem does not occur in the new formulation which can be applied to multi-loop diagrams [SGS 04b] and diagrams containing additional degrees of freedom [SGS 05].

In both formulations R and I contain additional divergences not present in the original integral H. These divergences, R^{add}/ϵ and I^{add}/ϵ, respectively, with $\epsilon = \frac{n-4}{2}$, are generated by the splitting of the z integration in the original formulation, or equivalently by the interchange of summation and integration in the reformulated version. Since these additional divergences do not appear in H, they have to cancel in the sum of $I + R = H$. This means that

$$\frac{R^{add}}{\epsilon} = -\frac{I^{add}}{\epsilon}. \tag{3.26}$$

3.3 Renormalization

The ϵ expansion of H is given by

$$\begin{aligned} H &= \frac{H^{UV}}{\epsilon} + H^0 + \mathcal{O}(\epsilon) \\ &= \frac{H^{UV}}{\epsilon} + \frac{I^{add}}{\epsilon} + \frac{R^{add}}{\epsilon} + \tilde{I} + \bar{R}, \end{aligned} \tag{3.27}$$

where H^{UV}/ϵ denotes the ultraviolet divergence of H, H^0 refers to the terms proportional to ϵ^0, and we have explicitly shown the additional divergences in the second line. The renormalized expression H^r of the integral H is defined as its finite infrared singular term,

$$H^r = \tilde{I}, \tag{3.28}$$

which satisfies the power counting since all terms violating it are contained in R. One of the fundamental properties used in the construction of the effective Lagrangian is the invariance under symmetries of the underlying theory. It is therefore of utmost importance that these symmetries are not violated at any step in the calculations. We now show that the definition of the renormalized integral H^r of Eq. (3.28) satisfies this requirement. The original integral H is obtained from a chirally symmetric Lagrangian using dimensional regularization, which preserves all symmetries. Therefore expressions containing H satisfy the Ward identities; and in particular their ϵ expansions satisfy the Ward identities order by order. As explained above, R satisfies the Ward identities separately from I. This also means that the Ward identities are satisfied order by order in the ϵ expansion of R and I, respectively. Therefore the identification of the renormalized integral H^r as $H^r = \tilde{I}$ does not violate any symmetry constraints. Since the sum of additional divergences cancels, the subtraction term to arrive at Eq. (3.28) is given by

$$\tilde{R} = \frac{H^{UV}}{\epsilon} + \bar{R}. \tag{3.29}$$

With Eq. (3.26) and the definition of Eq. (3.29) we can write

$$H = \tilde{I} + \tilde{R}. \tag{3.30}$$

Chapter 4

Axial, induced pseudoscalar, and pion-nucleon form factors

The electroweak form factors are sets of functions that are used to parameterize the structure of the nucleon as seen by the electromagnetic and the weak probes. While a wealth of data and theoretical predictions exist for the electromagnetic form factors (see, e.g., [Gao 03, FW 03, HWJ 04] and references therein), the nucleon form factors of the isovector axial-vector current, the axial form factor $G_A(q^2)$ and, in particular, the induced pseudoscalar form factor $G_P(q^2)$, are not as well-known (see, e.g., [BEM 02, GF 04] for a review). However, there are ongoing efforts to increase our understanding of these form factors. Chiral perturbation theory as the low-energy effective theory of the Standard Model allows for model-independent calculations of these form factors, and calculations in HBChPT can be found in Refs. [BKM 92, Ber+ 94, Fea+ 97, Ber+ 98]. In this chapter the axial, the induced pseudoscalar, and the pion nucleon form factors of the nucleon are calculated in manifestly Lorentz-invariant ChPT up to and including order $\mathcal{O}(q^4)$ using infrared renormalization. In addition the a_1 meson is included as an explicit degree of freedom, which resums certain higher-order contributions and results in an improved description of the experimental data of the axial form factor.

4.1 Definition and properties of the form factors

The axial and induced pseudoscalar form factors are defined via the matrix element of the isovector axial-vector current. In QCD the three components of this current are defined as

$$A^{\mu,a}(x) \equiv \bar{q}(x)\gamma^\mu\gamma_5\frac{\tau^a}{2}q(x), \quad q = \begin{pmatrix} u \\ d \end{pmatrix}, \quad a = 1, 2, 3. \tag{4.1}$$

The operators $A^{\mu,a}(x)$ are hermitian,

$$A^{\mu,a\dagger}(x) = A^{\mu,a}(x), \tag{4.2}$$

and obey the following equal-time commutation relations with the vector charges:

$$[Q_V^a(t), A^{\mu,b}(t,\vec{x})] = i\epsilon^{abc}A^{\mu,c}(t,\vec{x}). \tag{4.3}$$

Under parity the operators $A^{\mu,a}(x)$ transform as

$$A^{\mu,a}(x) \stackrel{\mathcal{P}}{\mapsto} -A^{a}_{\mu}(\tilde{x}), \quad \tilde{x}^{\mu} = x_{\mu}, \tag{4.4}$$

while their behavior under charge conjugation is given by

$$\begin{aligned} A^{\mu,a}(x) &\stackrel{\mathcal{C}}{\mapsto} A^{\mu,a}(x), \quad a = 1, 3, \\ A^{\mu,2}(x) &\stackrel{\mathcal{C}}{\mapsto} -A^{\mu,2}(x). \end{aligned} \tag{4.5}$$

The isovector axial-vector operators also obey the partially conserved axial-vector current (PCAC) relation,

$$\partial_{\mu} A^{\mu,a} = i\bar{q}\gamma_5\{\frac{\tau^a}{2}, \mathcal{M}\}q, \tag{4.6}$$

where $\mathcal{M} = \mathrm{diag}(m_u, m_d)$ is the quark mass matrix.

Assuming isospin symmetry, $m_u = m_d = \hat{m}$, the most general parametrization of the isovector axial-vector current evaluated between one-nucleon states in terms of axial-vector covariants is given by

$$\langle N(p')|A^{\mu,a}(0)|N(p)\rangle = \bar{u}(p') \left[\gamma^{\mu}\gamma_5 G_A(q^2) + \frac{q^{\mu}}{2m_N}\gamma_5 G_P(q^2)\right] \frac{\tau^a}{2} u(p), \tag{4.7}$$

where $q_{\mu} = p'_{\mu} - p_{\mu}$ is the momentum transfer and m_N denotes the nucleon mass. $G_A(q^2)$ is called the axial form factor and $G_P(q^2)$ is the induced pseudoscalar form factor. From the Hermiticity of Eq. (4.2) we find that G_A and G_P are real for space-like momenta ($q^2 \leq 0$). In the case of perfect isospin symmetry the strong interactions are invariant under $\mathcal{G}$ conjugation, which is a combination of charge conjugation $\mathcal{C}$ and a rotation by π about the 2 axis in isospin space (charge symmetry operation),

$$\mathcal{G} = \mathcal{C} \exp(i\pi Q^2_V). \tag{4.8}$$

The presence of a third, so-called second-class structure [Wei 58] of the type $i\sigma^{\mu\nu}q_{\nu}$ $\gamma_5 G_T(q^2)$ in the charged transition would indicate a violation of $\mathcal{G}$ conjugation. As there seems to be no clear empirical evidence for such a contribution [Wil 00, Min+ 02] $G_T(q^2)$ is not considered in the following.

Compared to the electromagnetic form factors the axial form factor $G_A(q^2)$ is not as well known. The value of G_A at zero momentum transfer is defined as the axial-vector coupling constant g_A and is quite precisely determined from neutron beta decay. The q^2 dependence of the axial form factor can be obtained either through neutrino scattering or pion electroproduction (see [BEM 02] and references therein). The induced pseudoscalar form factor $G_P(q^2)$ is even less known than $G_A(q^2)$. It has been investigated in ordinary and radiative muon capture as well as pion electroproduction. Analogous to the axial-vector coupling constant g_A, the induced pseudoscalar coupling constant is defined through $g_P = \frac{m_{\mu}}{2m_N} G_P(q^2 = -0.88 m_{\mu}^2)$, where $q^2 = -0.88\, m_{\mu}^2$ corresponds to muon capture kinematics and the additional factor $\frac{m_{\mu}}{2m_N}$ stems from a different convention used in muon capture. For a comprehensive review on the experimental and theoretical situation concerning $G_P(q^2)$

see for example Ref. [GF 04]. A discrepancy between the results in ordinary and radiative muon capture has recently been addressed in [Cla+ 06]. Theoretical approaches to the axial and induced pseudoscalar form factors include the early current algebra and PCAC calculations [AG 66, NS 62, SYT 67], various quark model (see, e.g., [TW 83, HE 85, Bof+ 02, Mer+ 02, MQS 02, Kho+ 04, Sil+ 05]) and lattice calculations [Liu+ 94, Liu+ 95]. For a recent discussion on extracting the axial form factor in the timelike region from $\bar{p} + n \to \pi^- + \ell^- + \ell^+$ ($\ell = e$ or μ) see Ref. [Ada+ 06].

Similar to the isovector axial-vector current the nucleon matrix element of the pseudoscalar density $P^a(x) = i\bar{q}(x)\gamma_5\tau^a q(x)$ can be parameterized as

$$\hat{m}\langle N(p')|P^a(0)|N(p)\rangle = \frac{M_\pi^2 F_\pi}{M_\pi^2 - q^2} G_{\pi N}(q^2) i\bar{u}(p')\gamma_5\tau^a u(p), \tag{4.9}$$

where M_π is the pion mass and F_π the pion decay constant. Equation (4.9) *defines* the form factor $G_{\pi N}(q^2)$ in terms of the QCD operator $\hat{m}P^a(x)$. The operator $\hat{m}P^a(x)/(M_\pi^2 F_\pi)$ serves as an interpolating pion field and thus $G_{\pi N}(q^2)$ is also referred to as the pion-nucleon form factor for this specific choice of the interpolating pion field [BKM 95]. Analogous to the axial-vector and pseudoscalar coupling constants, one defines the value of $G_{\pi N}(q^2)$ evaluated at $q^2 = M_\pi^2$ as the pion-nucleon coupling constant $g_{\pi N}$.

The PCAC relation, Eq. (4.6), relates the three form factors G_A, G_P, and $G_{\pi N}$,

$$2m_N G_A(q^2) + \frac{q^2}{2m_N} G_P(q^2) = 2\frac{M_\pi^2 F_\pi}{M_\pi^2 - q^2} G_{\pi N}(q^2), \tag{4.10}$$

and this relation serves as an important check for the calculations of the three form factors.

4.2 Results without explicit axial-vector mesons

The Lagrangians required for the calculation of the form factors are given in Chapter 2. To couple to an external axial-vector source one needs to set $a_\mu = \tau^a a_\mu^a/2$ in the corresponding expressions, while the quark masses are contained in the external scalar source s. For example, the pion covariant derivative $D_\mu U$ with a coupling to an external axial-vector field only is given by

$$D_\mu U = \partial_\mu U - i a_\mu U - i U a_\mu \,.$$

4.2.1 Axial form factor $G_A(q^2)$

The axial form factor $G_A(q^2)$ only receives contributions from the one-particle-irreducible diagrams of Fig. 4.1. The unrenormalized result reads

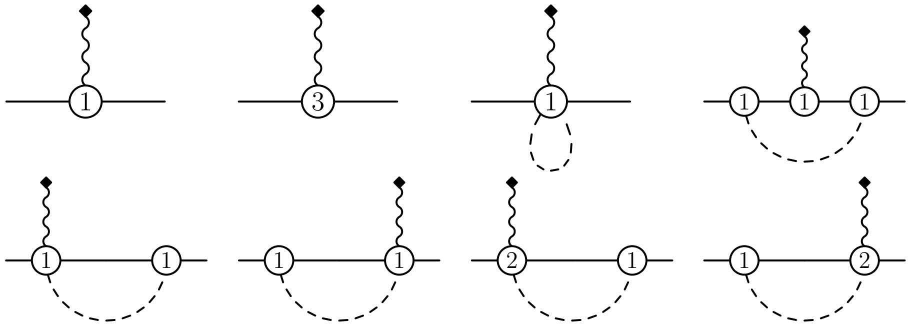

Figure 4.1: One-particle-irreducible diagrams contributing to the nucleon matrix element of the isovector axial-vector current.

$$
\begin{aligned}
G_{A0}(q^2) \;=\;& \mathsf{g}_A + 4M^2 d_{16} - d_{22}q^2 - \frac{\mathsf{g}_A}{F^2} I_\pi + 2\frac{\mathsf{g}_A}{F^2} M^2 I_{\pi N}(m_N^2) \\
&+8\frac{\mathsf{g}_A}{F^2} m_N \left\{ c_4 \left[M^2 I_{\pi N}(m_N^2) - I_{\pi N}^{(00)}(m_N^2) \right] - c_3 I_{\pi N}^{(00)}(m_N^2) \right\} \\
&-\frac{\mathsf{g}_A^3}{4F^2} \left[I_\pi - 4m_N^2 I_{\pi N}^{(p)}(m_N^2) + 4m_N^2 (n-2) I_{\pi NN}^{(00)}(q^2) \right. \\
&\left. +16 m_N^4 I_{\pi NN}^{(PP)}(q^2) + 4m_N^2 t I_{\pi NN}^{(qq)}(q^2) \right] . \qquad (4.11)
\end{aligned}
$$

The definition of the integrals can be found in App. B. To renormalize the expression for $G_A(q^2)$ we multiply Eq. (4.11) by the nucleon wave function renormalization constant Z [BL 99],

$$
Z = 1 - \frac{9\mathsf{g}_A^2 M^2}{32\pi^2 F^2} \left[\frac{1}{3} + \ln\left(\frac{M}{m}\right) \right] + \frac{9\mathsf{g}_A^2 M^3}{64\pi F^2 m} , \qquad (4.12)
$$

and replace the integrals with their infrared singular parts.

The axial-vector coupling constant g_A is defined as $g_A = G_A(q^2 = 0) = 1.2695(29)$ [Yao+ 06]. Besides experimental and theoretical efforts such as quark model calculations, g_A has been the aim of several lattice QCD studies (see, e.g., [Oht+ 03, Sas+ 03, Kha+ 05, Edw+ 06]), from which the value at the physical pion mass can be determined using a chiral extrapolation. We obtain for the quark-mass expansion of g_A

$$
g_A = \mathsf{g}_A + g_A^{(1)} M^2 + g_A^{(2)} M^2 \ln\left(\frac{M}{m}\right) + g_A^{(3)} M^3 + \mathcal{O}(M^4), \qquad (4.13)
$$

with

$$
\begin{aligned}
g_A^{(1)} &= 4d_{16} - \frac{\mathsf{g}_A^3}{16\pi^2 F^2} , \\
g_A^{(2)} &= -\frac{\mathsf{g}_A}{8\pi^2 F^2}(1 + 2\mathsf{g}_A^2) , \\
g_A^{(3)} &= \frac{\mathsf{g}_A}{8\pi F^2 m}(1 + \mathsf{g}_A^2) - \frac{\mathsf{g}_A}{6\pi F^2}(c_3 - 2c_4), \qquad (4.14)
\end{aligned}
$$

where all coefficients are understood as IR renormalized parameters. These results agree with the chiral coefficients obtained in HBChPT [KM 99, BM 06] as well as the IR calculation of Ref. [AF 07]. It is worth noting that an agreement for the algebraic expression of the analytic term $g_A^{(1)}$ cannot be expected in general. For example, when expressed in terms of the renormalized couplings of the extended on-mass-shell (EOMS) renormalization scheme of [Fuc+ 03a], the $g_A^{(1)}$ coefficient is given by [AF 07]

$$4d_{16}^{EOMS} - \frac{\mathsf{g}_A}{16\pi^2 F^2}(2+3\mathsf{g}_A^2) + \frac{c_1 \mathsf{g}_A m}{4\pi^2 F^2}(4-\mathsf{g}_A^2).$$

The difference between the two expressions is due to the fact that also the expressions for renormalized LECs differ in the various renormalization schemes. For a similar discussion regarding the chiral expansion of the nucleon mass, see [Fuc+ 03a]. It was pointed out in [KM 99] that the chiral expansion of Eq. (4.13) does not converge well, as the term proportional to M^3 gives a correction of the order of 30%. Neither g_A nor d_{16} have been reliably determined in the IR renormalization scheme, so we do not attempt to determine the size of $g_A^{(1)}$. To get an estimate for the size of $g_A^{(2)}$ and $g_A^{(3)}$ we use the three values $\mathsf{g}_A = \{1.0, 1.1, 1.2\}$. Together with the constants $c_3 = -4.2 m_N^{-1}$ and $c_4 = 2.3 m_N^{-1}$ [BL 01] we obtain

$$\begin{aligned} g_A^{(2)} M^2 \ln\left(\frac{M}{m}\right) &= \{0.17, 0.21, 0.27\}, && (4.15)\\ g_A^{(3)} M^3 &= \{0.19, 0.21, 0.23\}, && (4.16)\end{aligned}$$

which compared to the leading order term g_A gives

$$\begin{aligned} \frac{g_A^{(2)} M^2 \ln\left(\frac{M}{m}\right)}{\mathsf{g}_A} &= \{17\%, 19\%, 21\%\}, && (4.17)\\ \frac{g_A^{(3)} M^3}{\mathsf{g}_A} &= \{19\%, 19\%, 19\%\}. && (4.18)\end{aligned}$$

While the corrections found here are not as large as the ones in Ref. [KM 99], one still sees that the convergence of g_A is slow. In Ref. [BM 06] the leading nonanalytic contributions to g_A at the two-loop level have been considered, which, however, are not unusually large at the physical value of the pion mass.

The axial form factor can be written as

$$G_A(q^2) = g_A + \frac{1}{6}\, g_A \, \langle r_A^2 \rangle \, q^2 + \frac{\mathsf{g}_A^3}{4F^2} H(q^2), \tag{4.19}$$

where $\langle r_A^2 \rangle$ is the axial mean-square radius and $H(q^2)$ contains loop contributions and satisfies $H(0) = H'(0) = 0$. The LECs d_{16} and d_{22} are thus absorbed in the axial-vector coupling constant g_A and the axial mean-square radius $\langle r_A^2 \rangle$. The numerical contribution of $H(q^2)$ for the low-energy region we are interested in is negligible. This can be understood by expanding H in a Taylor series in q^2. Such an expansion generates powers of q^2/m^2 where the individual coefficients have a chiral expansion similar to Eq. (4.13) and $H(q^2)$ is at least of order $(q^2/m^2)^2$.

For the analysis of experimental data, $G_A(q^2)$ is conventionally parameterized using a dipole form as

$$G_A(q^2) = \frac{g_A}{(1 - \frac{q^2}{M_A^2})^2}, \tag{4.20}$$

where the so-called axial mass M_A is related to the axial root-mean-square radius by $\langle r_A^2 \rangle^{\frac{1}{2}} = 2\sqrt{3}/M_A$. The global average for the axial mass extracted from neutrino scattering experiments given in Ref. [Lie+ 99] is

$$M_A = (1.026 \pm 0.021)\,\mathrm{GeV}, \tag{4.21}$$

whereas a recent analysis [BBA 03] taking account of updated expressions for the vector form factors finds a slightly smaller value

$$M_A = (1.001 \pm 0.020)\,\mathrm{GeV}. \tag{4.22}$$

On the other hand, smaller values of (0.95 ± 0.03) GeV and (0.96 ± 0.03) GeV have been obtained in [KLN 06] as world averages from quasielastic scattering and (1.12 ± 0.03) GeV from single pion neutrinoproduction. Finally, the most recent result extracted from quasielastic $\nu_\mu n \to \mu^- p$ in oxygen nuclei reported by the K2K Collaboration, $M_A = (1.20 \pm 0.12)$ GeV, is considerably larger [Gra+ 06].

The extraction of the axial mean-square radius from charged pion electroproduction at threshold is motivated by current algebra results and the PCAC hypothesis (see, e.g., [Gel 64, AD 68]). The most recent result for the reaction $p(e, e'\pi^+)n$ has been obtained at MAMI at an invariant mass of $W = 1125$ MeV (corresponding to a pion center-of-mass momentum of $|\vec{q}^*| = 112$ MeV) and photon four-momentum transfers of $-k^2 = 0.117$, 0.195 and 0.273 GeV^2 [Lie+ 99]. Using an effective-Lagrangian model an axial mass of

$$\bar{M}_A = (1.077 \pm 0.039)\,\mathrm{GeV}$$

was extracted, where the bar is used to distinguish the result from the neutrino scattering value. In the meantime, the experiment has been repeated including an additional value of $-k^2 = 0.058$ GeV^2 [Bau 04] and is currently being analyzed. The global average from several pion electroproduction experiments is given by [BEM 02]

$$\bar{M}_A = (1.068 \pm 0.017)\,\mathrm{GeV}. \tag{4.23}$$

It can be seen that the values of Eqs. (4.21) and (4.22) for the neutrino scattering experiments are smaller than that of Eq. (4.23) for the pion electroproduction experiments. The discrepancy was explained in heavy baryon chiral perturbation theory [BKM 92]. It was shown that at order $\mathcal{O}(q^3)$ pion loop contributions modify the k^2 dependence of the electric dipole amplitude from which $\bar{M}_A$ is extracted. These contributions result in a change of

$$\Delta M_A = 0.056\,\mathrm{GeV}, \tag{4.24}$$

bringing the neutrino scattering and pion electroproduction results for the axial mass into agreement.

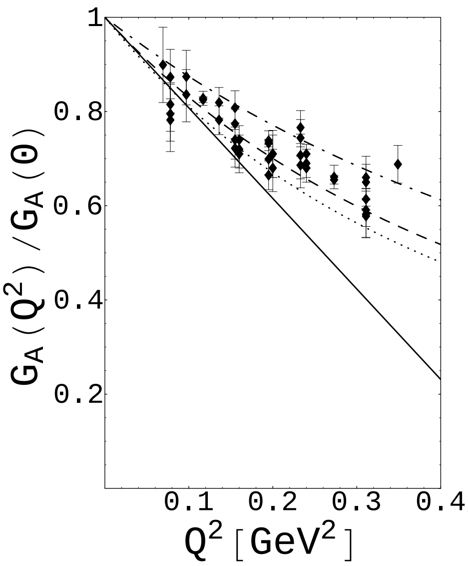

Figure 4.2: The axial form factor G_A in manifestly Lorentz-invariant ChPT at $\mathcal{O}(q^4)$. Full line: result in infrared renormalization with parameters fitted to reproduce the axial mean-square radius corresponding to the dipole parametrization with $M_A = 1.026$ GeV (dashed line). The dotted and dashed-dotted lines refer to dipole parameterizations with $M_A = 0.95$ GeV and $M_A = 1.20$ GeV, respectively. The experimental values are taken from [BEM 02].

Using the convention $Q^2 = -q^2$ the result for the axial form factor $G_A(q^2)$ in the momentum transfer region $0\,\mathrm{GeV}^2 \leq Q^2 \leq 0.4\,\mathrm{GeV}^2$ is shown in Fig. 4.2. The parameters have been determined such as to reproduce the axial mean-square radius corresponding to the dipole parametrization with $M_A = 1.026$ GeV (dashed line). The dotted and dashed-dotted lines refer to dipole parameterizations with $M_A = 0.95$ GeV and $M_A = 1.20$ GeV, respectively. As anticipated, the loop contributions from $H(q^2)$ are small and the result does not produce enough curvature to describe the data for momentum transfers $Q^2 \geq 0.1\,\mathrm{GeV}^2$. The situation is reminiscent of the electromagnetic case [KM 01, FGS 04] where ChPT at $\mathcal{O}(q^4)$ also fails to describe the form factors beyond $Q^2 \geq 0.1\,\mathrm{GeV}^2$.

4.2.2 Induced pseudoscalar form factor

The one-particle-irreducible diagrams of Fig. 4.1 also contribute to the induced pseudoscalar form factor $G_P(q^2)$,

$$G_P^{irr}(q^2) = 4m_N^2 d_{22} + 8m_N^4 \frac{g_A^3}{F^2} I_{\pi NN}^{(qq)}(q^2)\,. \tag{4.25}$$

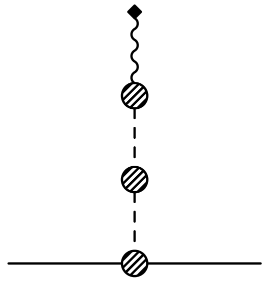

Figure 4.3: Pion pole graph of the isovector axial-vector current.

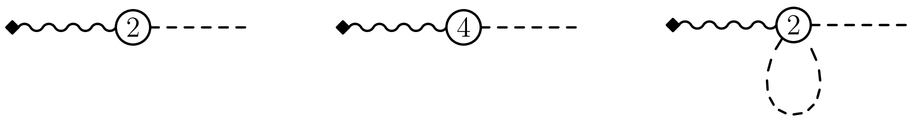

Figure 4.4: Diagrams contributing to the coupling of the isovector axial-vector current to a pion up to order $\mathcal{O}(q^4)$.

Furthermore, $G_P(q^2)$ receives contributions from the pion pole graph of Fig. 4.3. It consists of three building blocks: The coupling of the external axial source to the pion, the pion propagator, and the πN vertex, respectively. We consider each part separately.

The renormalized coupling of the external axial source to a pion up to order $\mathcal{O}(q^4)$ is given by

$$\epsilon_A \cdot q F_\pi \delta_{ij}, \tag{4.26}$$

where the diagrams in Fig. 4.4 have been taken into account and the renormalized pion decay constant reads

$$F_\pi = F\left[1 + \frac{M^2}{F^2}\, l_4^r - \frac{M^2}{8\pi^2 F^2} \ln\left(\frac{M}{m}\right) + \mathcal{O}(M^4)\right]. \tag{4.27}$$

We have used the pion wave function renormalization constant

$$Z_\pi = 1 - \frac{2M^2}{F^2}\left[l_4^r + \frac{1}{24\pi^2}\left(R - \ln\left(\frac{M}{m}\right)\right)\right], \tag{4.28}$$

with l_4^r the renormalized coupling of Eq. (2.26) and $R = \frac{2}{n-4} + \gamma_E - 1 - \ln(4\pi)$.

The renormalized pion propagator is obtained by simply replacing the lowest-order pion mass M by the expression for the physical mass M_π up to order $\mathcal{O}(q^4)$,

$$M_\pi^2 = M^2 + \Sigma(M_\pi^2) = M^2\left[1 + \frac{2M^2}{F^2}\left(l_3^r + \frac{1}{32\pi^2}\ln\left(\frac{M}{m}\right)\right)\right]. \tag{4.29}$$

The πN vertex evaluated between on-mass-shell nucleon states up to order $\mathcal{O}(q^4)$ receives contributions from the diagrams in Fig. 4.5 and the unrenormalized result

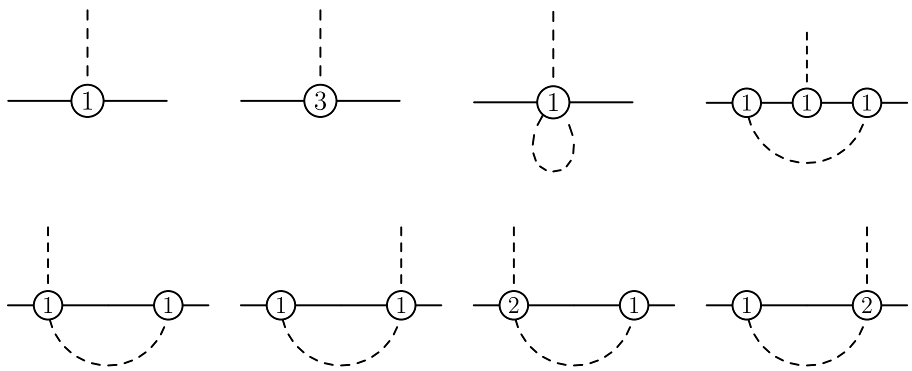

Figure 4.5: Diagrams contributing to the pion-nucleon vertex up to order $\mathcal{O}(q^4)$.

for a pion with isospin index i is given by

$$\begin{aligned}\Gamma(q^2)\gamma_5\tau_i &= \bigg(-\frac{\mathrm{g}_A}{F}m_N + 2\frac{M^2}{F}m_N(d_{18}-2d_{16}) + \frac{\mathrm{g}_A}{3F^2}m_N I_\pi - 2\frac{\mathrm{g}_A}{F^3}M^2 m_N I_{\pi N}(m_N^2) \\ &\quad -8\frac{\mathrm{g}_A}{F^2}m_N^2\left\{c_4\left[M^2 I_{\pi N}(m_N^2) - I_{\pi N}^{(00)}(m_N^2)\right] - c_3 I_{\pi N}^{(00)}(m_N^2)\right\} \\ &\quad +\frac{\mathrm{g}_A^3}{4F^3}m_N\left[I_\pi + 4mM^2 I_{NN}(q^2) + 4m_N^2 M^2 I_{\pi NN}(q^2)\right]\bigg)\gamma_5\tau_i\,. \end{aligned} \tag{4.30}$$

To find the renormalized vertex one multiplies with $Z\sqrt{Z_\pi}$ and replaces the integrals with their infrared singular parts.

However, the renormalized result should not be confused with the pion-nucleon form factor $G_{\pi N}(q^2)$ of Eq. (4.9). In general, the pion-nucleon vertex depends on the choice of the field variables in the (effective) Lagrangian. In the present case, the pion-nucleon vertex is only an auxiliary quantity, whereas the "fundamental" quantity (entering chiral Ward identities) is the matrix element of the pseudoscalar density. Only at $q^2 = M_\pi^2$, we expect the same coupling strength, since both $\hat{m}P^a(x)/(M_\pi^2 F_\pi)$ and the field Φ_i of Eq. (2.18) serve as interpolating pion fields. One can therefore determine the quark-mass expansion of the pion-nucleon coupling constant $g_{\pi N} = G_{\pi N}(M^2)$ from Eq. (4.30). After renormalization we obtain

$$g_{\pi N} = \mathrm{g}_{\pi N} + g_{\pi N}^{(1)}M^2 + g_{\pi N}^{(2)}M^2\ln\left(\frac{M}{m}\right) + g_{\pi N}^{(3)}M^3 + \mathcal{O}(M^4)\,, \tag{4.31}$$

with

$$\begin{aligned} \mathrm{g}_{\pi N} &= \frac{\mathrm{g}_A m}{F}\,, \\ g_{\pi N}^{(1)} &= -\mathrm{g}_A\frac{l_4^r m}{F^3} - 4\mathrm{g}_A\frac{c_1}{F} + \frac{2(2d_{16}-d_{18})m}{F} - \mathrm{g}_A^3\frac{m}{16\pi^2F^3}\,, \\ g_{\pi N}^{(2)} &= -\mathrm{g}_A^3\frac{m}{4\pi^2F^3}\,, \\ g_{\pi N}^{(3)} &= \mathrm{g}_A\frac{4+\mathrm{g}_A^2}{32\pi F^3} - \mathrm{g}_A\frac{(c_3-2c_4)m}{6\pi F^3}\,, \end{aligned} \tag{4.32}$$

where all coefficients are understood as IR renormalized parameters. These results agree with the chiral coefficients obtained in [BL 01]. In the chiral limit, Eq. (4.31) satisfies the Goldberger-Treiman relation $\mathsf{g}_{\pi N} = \mathsf{g}_A m/F$ [GT 58a, GT 58b, Nam 60]. The numerical violation of the Goldberger-Treiman relation as expressed in the so-called Goldberger-Treiman discrepancy [Pag 69],

$$\Delta = 1 - \frac{m_N g_A}{F_\pi g_{\pi N}}, \tag{4.33}$$

is at the percent level, $\Delta = (2.44^{+0.89}_{-0.51})$ % for $m_N = (m_p + m_n)/2 = 938.92$ MeV, $g_A = 1.2695(29)$, $F_\pi = 92.42(26)$ MeV, and $g_{\pi N} = 13.21^{+0.11}_{-0.05}$ [Sch+ 01]. Using different values for the pion-nucleon coupling constant such as $g_{\pi N} = 13.0 \pm 0.1$ [STS 93], $g_{\pi N} = 13.3 \pm 0.1$ [ELT 02], and $g_{\pi N} = 13.15 \pm 0.01$ [Arn+ 06] results in the GT discrepancies $\Delta = (0.79 \pm 0.84)$ %, $\Delta = (3.03 \pm 0.81)$ %, and $\Delta = (1.922 \pm 0.363)$ %, respectively. The chiral expansions of g_A etc. may be used to relate the parameter d_{18} to Δ [BL 01],

$$\Delta = -\frac{2 d_{18} M^2}{\mathsf{g}_A} + \mathcal{O}(M^4). \tag{4.34}$$

Note that Δ of Eq. (4.33) and Δ_{GT} of [BL 01, Sch+ 01] are related by $\Delta_{GT} = \Delta/(1-\Delta)$. In particular, the leading order of the quark-mass expansions of Δ and Δ_{GT} is the same.

The induced pseudoscalar form factor $G_P(q^2)$ is obtained by combining Eqs. (4.25), (4.27), (4.29) and the renormalized expression for Eq. (4.30). With the help of Eqs. (4.33) and (4.34) it can entirely be written in terms of known physical quantities as [BKM 94]

$$G_P(q^2) = -4 \frac{m_N F_\pi g_{\pi N}}{q^2 - M_\pi^2} - \frac{2}{3} m_N^2 g_A \langle r_A^2 \rangle + \mathcal{O}(q^2). \tag{4.35}$$

The $1/(q^2 - M_\pi^2)$ behavior of G_P is not in conflict with the book-keeping of a calculation at chiral order $\mathcal{O}(q^4)$. Since the external axial-vector field a_μ counts as $\mathcal{O}(q)$, and the definition of the matrix element contains a momentum $(p' - p)^\mu$ and the Dirac matrix γ_5, the contribution to the induced pseudoscalar form factor from a diagram with order D is of order $D - 3$. Therefore diagrams of order $\mathcal{O}(q)$ give a contribution of order $\mathcal{O}(q^{-2})$ to G_P. The terms that have been neglected in the form factor G_P are of order M^2, q^2/m^2 and higher.

Using the above values for m_N, g_A, F_π as well as $g_{\pi N} = 13.21^{+0.11}_{-0.05}$, $M_A = (1.026 \pm 0.021)$ GeV, $M = M_{\pi^+} = 139.57$ MeV and $m_\mu = 105.66$ MeV [Yao+ 06] we obtain for the induced pseudoscalar coupling

$$g_P = 8.29^{+0.24}_{-0.13} \pm 0.52, \tag{4.36}$$

which is in agreement with the heavy-baryon results 8.44 ± 0.23 [BKM 94] and 8.21 ± 0.09 [Fea+ 97], once the differences in the coupling constants used are taken in consideration. The first error given in Eq. (4.36) stems only from the empirical uncertainties in the quantities of Eq. (4.35). As an attempt to estimate the error originating in the truncation of the chiral expansion in the baryonic sector we assign a relative error of 0.5^k, where k denotes the difference between the order that has

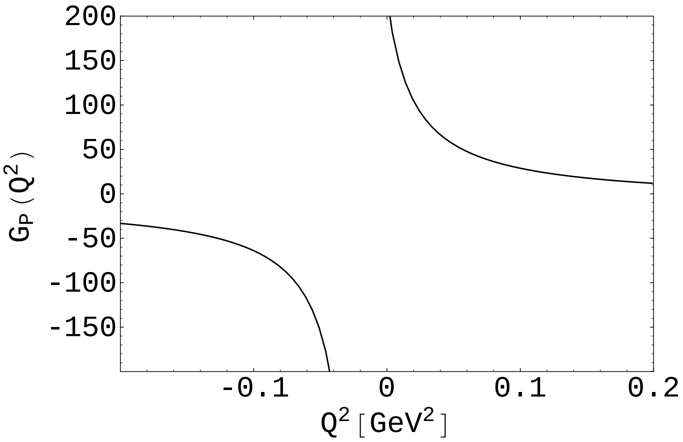

Figure 4.6: The induced pseudoscalar form factor G_P in manifestly Lorentz-invariant ChPT at $\mathcal{O}(q^4)$.

been neglected and the leading order at which a non-vanishing result appears. Such a (conservative) error is motivated by, e. g., the analysis of the individual terms of Eq. (4.13) as well as the determination of the LECs c_i at $\mathcal{O}(q^2)$ and to one-loop accuracy $\mathcal{O}(q^3)$ in the heavy-baryon framework [BKM 97]. For g_P we have thus added a truncation error of 0.52. Experimentally, g_P can be determined from ordinary and radiative muon capture (for a review see, e.g., [GF 04]). The average over the recent ordinary muon capture results is given by [GF 04]

$$g_P^{OMC} = 10.5 \pm 1.8, \tag{4.37}$$

while the radiative muon capture experiment performed at TRIUMF gives [Cla+ 06]

$$g_P^{RMC} = 10.6 \pm 1.1. \tag{4.38}$$

Both these values are larger than the result of Eq. (4.36), but still consistent at the level of 1-1.5 standard deviations. It should also be noted that value of g_P as extracted from ordinary and radiative muon capture on liquid helium depends on the ortho-para transition rate in intermediate $p\mu p$ molecules. A recent measurement of this rate yielded a significantly larger value than previously used, which results in an average value of $g_P = 5.6 \pm 4.1$ when reanalyzing earlier experiments [Cla+ 06]. Clearly, further efforts are needed to determine g_P.

Figure 4.6 shows our result for $G_P(q^2)$ in the momentum transfer region $-0.2\,\mathrm{GeV}^2 \leq Q^2 \leq 0.2\,\mathrm{GeV}^2$. One can clearly see the dominant pion pole contribution at $q^2 \approx M_\pi^2$ which is also supported by the experimental results of [Cho+ 93].

4.2.3 Pion-nucleon form factor

Using Eq. (4.10) allows one to also determine the pion-nucleon form factor $G_{\pi N}(q^2)$ in terms of the results for $G_A(q^2)$ and $G_P(q^2)$. When expressed in terms of physical quantities, it has the particularly simple form

$$G_{\pi N}(q^2) = \frac{m_N g_A}{F_\pi} + g_{\pi N}\Delta \frac{q^2}{M_\pi^2} + \mathcal{O}(q^4). \tag{4.39}$$

We have explicitly verified that the results agree with a direct calculation of $G_{\pi N}(q^2)$ in terms of a coupling to an external pseudoscalar source. There are two types of contributions, a contact term and a pion pole diagram. The contact contribution to the pion-nucleon form factor is given by

$$G_{\pi N}^{cont}(q^2) = -2m_N \frac{q^2 - M_\pi^2}{F_\pi}\, d_{18}, \tag{4.40}$$

while the pion pole diagram can be evaluated using the renormalized expressions for the pion-nucleon vertex of Eq. (4.30), the pion propagator, and the expression for the coupling of an external pseudoscalar source to a pion,

$$iM_\pi^2 F_\pi. \tag{4.41}$$

Denoting the renormalized pion-nucleon vertex by $\Gamma^r(q^2)\gamma_5\tau_i$ the pion-nucleon form factor is given by

$$G_{\pi N}(q^2) = -2m_N \frac{q^2 - M_\pi^2}{F_\pi}\, d_{18} - \Gamma^r(q^2). \tag{4.42}$$

Noting that $\Gamma^r(q^2) = -g_{\pi N} + \mathcal{O}(q^4)$, replacing d_{18} with the help of Eq. (4.34) and using Eq. (4.33) one reproduces the result of Eq. (4.39). Observe that, with our definition in terms of QCD bilinears, the pion-nucleon form factor is, in general, *not* proportional to the axial form factor. The relation $G_{\pi N}(q^2) = m_N G_A(q^2)/F_\pi$ which is sometimes used in PCAC applications implies a pion-pole dominance for $G_P(q^2)$ of the form $G_P(q^2) = 4m_N^2 G_A(q^2)/(M_\pi^2 - q^2)$. However, as can be seen from Eq. (4.39), there are deviations at $\mathcal{O}(q^2)$ from such a complete pion-pole dominance assumption.

The difference between $G_{\pi N}(q^2 = M_\pi^2)$ and $G_{\pi N}(q^2 = 0)$ is entirely given in terms of the GT discrepancy [BKM 95],

$$G_{\pi N}(M_\pi^2) - G_{\pi N}(0) = g_{\pi N}\Delta. \tag{4.43}$$

Parameterizing the form factor in terms of a monopole,

$$G_{\pi N}^{\text{mono}}(q^2) = g_{\pi N} \frac{\Lambda^2 - M_\pi^2}{\Lambda^2 - q^2}\,, \tag{4.44}$$

Eq. (4.43) translates into a mass parameter $\Lambda = 894$ MeV for $\Delta = 2.44$ %.

4.3 Inclusion of axial-vector mesons

The situation for the axial form factor $G_A(q^2)$ is similar to the electromagnetic case, where standard ChPT can only describe the form factors for small values of momentum transfer as well. It was shown that the inclusion of the ρ, ω and ϕ mesons improves the description of the experimental data [KM 01, SGS 05]. Motivated by this success we include an axial-vector meson into the theory to resum higher-order contributions.

4.3.1 Lagrangian and power counting

In order to include axial-vector mesons as explicit degrees of freedom we consider the vector-field formulation of [Eck+ 89] in which the $a_1(1260)$ meson is represented by $\mathcal{A}_\mu = \mathcal{A}_\mu^a \tau^a$. Under chiral transformations $\mathcal{A}_\mu$ transforms as

$$\mathcal{A}_\mu \overset{G}{\mapsto} K(V_L, V_R, U)\mathcal{A}_\mu K(V_L, V_R, U), \tag{4.45}$$

with the compensator $K(V_L, V_R, U)$ defined in Eq. (2.29). $\mathcal{A}_\mu$ is counted as $\mathcal{O}(q^0)$. It is convenient to define the field strength tensor

$$\mathcal{A}_{\mu\nu} = \nabla_\mu \mathcal{A}_\nu - \nabla_\nu \mathcal{A}_\mu, \tag{4.46}$$

which, due to the covariant derivative

$$\nabla_\mu \mathcal{A}_\nu = \partial_\mu \mathcal{A}_\nu + [\Gamma_\mu, \mathcal{A}_\nu], \tag{4.47}$$

is a quantity of order $\mathcal{O}(q^1)$. Under parity transformations $\mathcal{A}_\mu$ behaves as

$$\mathcal{A}_\mu(x) \overset{\mathcal{P}}{\mapsto} -\mathcal{A}^\mu(\tilde{x}), \quad \tilde{x}^\mu = x_\mu, \tag{4.48}$$

while the charge conjugation behavior is given by

$$\mathcal{A}_\mu \overset{\mathcal{C}}{\mapsto} \mathcal{A}_\mu^T. \tag{4.49}$$

Together with the properties of the chiral building blocks given in Chapter 2 the most general Lagrangian containing the axial-vector meson can be constructed. For the mesonic sector the coupling to pions and external fields starts at order $\mathcal{O}(q^3)$ and the complete list of terms can be found in [Eck+ 89]. The only term relevant for the calculation of the form factors is given by

$$\mathcal{L}_{\pi A}^{(3)} = \frac{f_A}{4}\mathrm{Tr}(\mathcal{A}_{\mu\nu} F_-^{\mu\nu}). \tag{4.50}$$

Due to Lorentz invariance and the transformation properties of the building blocks no Lagrangian at order $\mathcal{O}(q^4)$ can be constructed that satisfies all requirements.

The coupling of the axial-vector meson to the nucleon field starts at order $\mathcal{O}(q^0)$. Since we are only interested in terms that do not contain any additional fields besides the axial-vector meson and the nucleon, the corresponding Lagrangian reads

$$\mathcal{L}_{NA}^{(0)} = \frac{g_{a_1}}{2}\bar{\Psi}\gamma^\mu\gamma_5 \mathcal{A}_\mu \Psi. \tag{4.51}$$

A calculation up to order $\mathcal{O}(q^4)$ would in principle also require the Lagrangian of order $\mathcal{O}(q)$. The only term that can be constructed without violating any symmetries has the form

$$\mathcal{L}_{NA}^{(1)} \sim i\epsilon^{\mu\nu\rho\sigma}\left[\bar{\Psi}\mathcal{A}_{\mu\nu}\gamma_\rho D_\sigma \Psi - D_\sigma \bar{\Psi}\mathcal{A}_{\mu\nu}\gamma_\rho \Psi\right]. \tag{4.52}$$

However, using $\epsilon^{\mu\nu\rho\sigma}\gamma_\rho = -\frac{1}{2}\left(\gamma_5\gamma^\sigma\sigma^{\mu\nu} + \sigma^{\mu\nu}\gamma_5\gamma^\sigma\right)$ and the equation of motion for the nucleon field one can show that this term only starts to contribute at higher order. Therefore there is no coupling of the axial-vector meson to the nucleon at order $\mathcal{O}(q^1)$.

In addition to the usual power counting rules we count the axial-vector meson propagator as order $\mathcal{O}(q^0)$, vertices from $\mathcal{L}_{\pi A}^{(3)}$ as order $\mathcal{O}(q^3)$ and vertices from $\mathcal{L}_{AN}^{(0)}$ as order $\mathcal{O}(q^0)$, respectively [Fuc+ 03b].

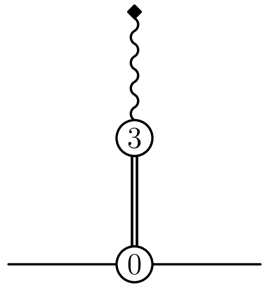

Figure 4.7: Diagram containing an axial-vector meson (double line) contributing to the form factors G_A and G_P.

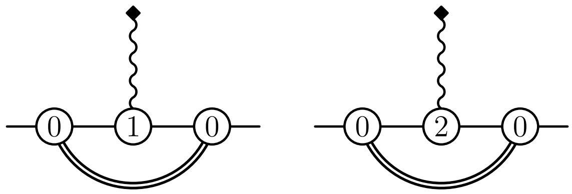

Figure 4.8: Diagrams containing an axial-vector meson (double line) that vanish in infrared renormalization.

4.3.2 Results

The contributions of the axial-vector meson to the form factors G_A and G_P up to and including order $\mathcal{O}(q^4)$ stem from the diagram in Fig. 4.7. The diagrams in Fig. 4.8 are of order $\mathcal{O}(q^3)$ and $\mathcal{O}(q^4)$, respectively, and are expected to contribute to the form factors as well. However, loop diagrams with internal axial-vector meson lines that do not contain internal pion lines vanish in the infrared renormalization employed in this work. Therefore the diagrams of Fig. 4.8 do not explicitly contribute to the form factors $G_A(q^2)$ and $G_P(q^2)$. With the Lagrangians of Eqs. (4.50) and (4.51) the axial form factor receives the contribution

$$G_A^{AVM}(q^2) = -f_A g_{a_1} \frac{q^2}{q^2 - M_{a_1}^2}\,, \tag{4.53}$$

while the result for the induced pseudoscalar form factor reads

$$G_P^{AVM}(t) = 4m_N^2 f_A g_{a_1} \frac{1}{q^2 - M_{a_1}^2}\,. \tag{4.54}$$

The Lagrangians for the axial-vector meson contain two new LECs, f_A and g_{a_1}, respectively. However, we find that they only appear through the combination $f_A g_{a_1}$, effectively leaving only one unknown LEC. Performing a fit to the data of $G_A(q^2)$ in the momentum region $0\,\mathrm{GeV}^2 \leq Q^2 \leq 0.4\,\mathrm{GeV}^2$, using $M_{a_1} = 1230\,\mathrm{MeV}$ [Yao+ 06], the product of the coupling constants is determined to be

$$f_A g_{a_1} \approx 8.70. \tag{4.55}$$

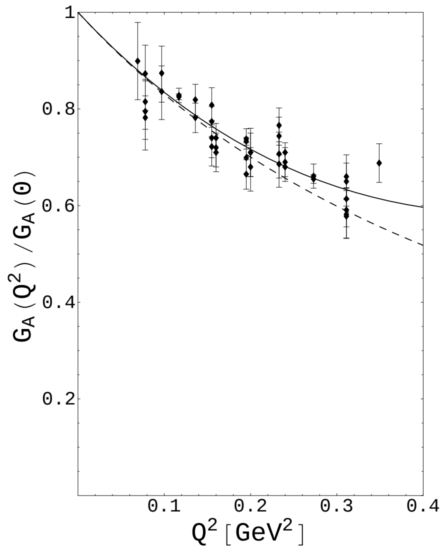

Figure 4.9: The axial form factor G_A in manifestly Lorentz-invariant ChPT at $\mathcal{O}(q^4)$ including the axial-vector meson a_1 explicitly. Full line: result in infrared renormalization, dashed line: dipole parametrization. The experimental values are taken from [BEM 02].

Figure 4.9 shows our fitted result for the axial form factor $G_A(q^2)$ at order $\mathcal{O}(q^4)$ in the momentum region $0\,\mathrm{GeV}^2 \leq Q^2 \leq 0.4\,\mathrm{GeV}^2$ with the a_1 meson included as an explicit degree of freedom. As was expected from phenomenological considerations, the description of the data has improved for momentum transfers $Q^2 \gtrsim 0.1\,\mathrm{GeV}^2$. We would like to stress again that in a strict chiral expansion up to order $\mathcal{O}(q^4)$ the results with and without axial vector mesons do not differ from each other. The improved description of the data in the case with the explicit axial-vector meson is the result of a resummation of certain higher-order terms. While the choice of which additional degree of freedom to include compared to the standard calculation is completely phenomenological, once this choice has been made there exists a systematic framework in which to calculate the corresponding contributions as well as higher-order corrections.

It can be seen from Eq. (4.53) that in our formalism the axial-vector meson does not contribute to the axial-vector coupling constant g_A. The pion-nucleon vertex also remains unchanged at the given order, while the axial mean-square radius receives a contribution. The values for the LECs d_{16} and d_{18} therefore do not change, while d_{22} can be determined from the new expression for the axial radius using the value of Eq. (4.55) for the combination of coupling constants. In Fig. 4.10 we show the result for $G_P(q^2)$ in the momentum transfer region $-0.2\,\mathrm{GeV}^2 \leq Q^2 \leq 0.2\,\mathrm{GeV}^2$. Also shown for comparison is the result without the explicit axial-vector meson. One sees that the contribution of the a_1 to $G_P(q^2)$ for these momentum transfers is rather small and that $G_P(q^2)$ is still dominated by the pion pole diagrams.

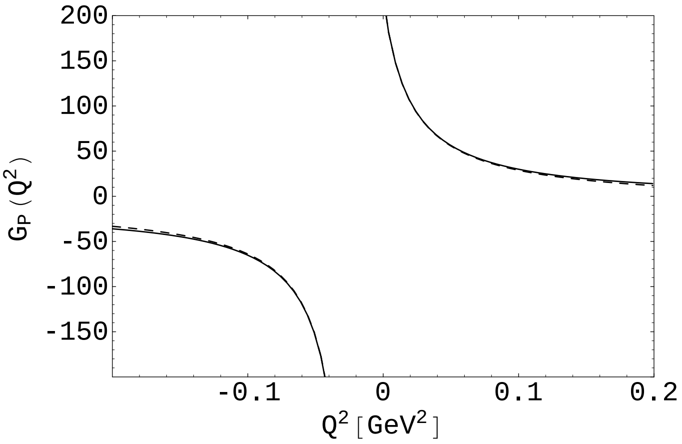

Figure 4.10: The induced pseudoscalar form factor G_P in manifestly Lorentz-invariant ChPT at $\mathcal{O}(q^4)$ including the axial-vector meson a_1 explicitly. Full line: result with axial-vector meson, dashed line: result without axial-vector meson.

The form factors G_A and G_P are related to the pion-nucleon form factor via Eq. (4.10). For the contributions of the axial-vector meson we find

$$2m_N G_A^{AVM}(q^2) + \frac{q^2}{2m_N} G_P^{AVM}(q^2) = 0\,, \tag{4.56}$$

so that the pion-nucleon form factor is not modified by the inclusion of the a_1 meson.

Chapter 5

Infrared renormalization of two-loop integrals

Chapter 3 discusses the infrared renormalization of one-loop integrals. In the following the extension to two-loop integrals contributing to the nucleon mass is described in detail. It is shown that the renormalization can be performed while preserving all relevant symmetries, in particular chiral symmetry, and that renormalized diagrams respect the same power counting rules as in the one-loop sector.

5.1 Infrared renormalization and dimensional counting

At the one-loop level an integral H is written as

$$H = I + R, \tag{5.1}$$

where I is the infrared singular part and R the infrared regular part, respectively. The chiral expansion of R can be obtained by expanding the integrand of H and interchanging summation and integration [SGS 04a].

Within the framework of dimensional regularization, the dimensional counting analysis of Ref. [GJT 94] provides a method to obtain expansions of loop integrals in small parameters. This method is described in detail in Appendix C. Here we show how the infrared regular and infrared singular parts of the integral H are related to the different terms obtained from this method. Using dimensional counting, H is written as

$$H = F_1 + F_2. \tag{5.2}$$

For F_1 we simply expand the integrand in M and interchange summation and integration. F_2 is obtained by rescaling the integration variable $k \mapsto \frac{M}{m} k$ and then expanding the integrand with subsequent interchange of summation and integration. The method of obtaining F_1 is the same as the one used to determine the expansion of the infrared-regular part R. It follows that

$$F_1 = \sum_n R_n = R, \tag{5.3}$$

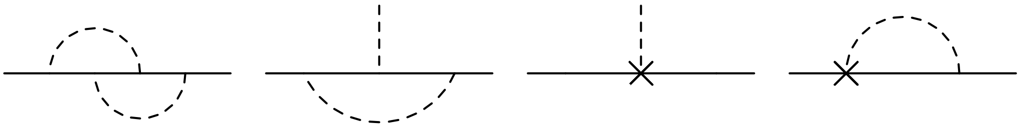

Figure 5.1: Two-loop diagram with corresponding subdiagram and counterterm diagram.

while F_2 gives the chiral expansion of the infrared singular term I,

$$F_2 = \sum_n I_n, \tag{5.4}$$

where R_n and I_n are the terms in the chiral expansion of the infrared regular and infrared singular parts, respectively. It should be noted that the expansion of I does not always converge in the entire low-energy region [BL 99]. For the integrals considered in the calculation of the nucleon mass, however, this is not the case and the expansion of I converges. The identification of F_1 and F_2 with the infrared regular and infrared singular parts, respectively, is used below to show that the renormalization process in the two-loop sector does not violate the considered symmetries.

5.2 Renormalization of two-loop integrals

We give a brief description of the general renormalization procedure for two-loop integrals before presenting details of the IR renormalization. The discussion follows Ref. [Col 84].

At the two-loop level integrals not only contain overall UV divergences, but can also contain subdivergences for the case where one integration momentum is fixed while the other one goes to infinity. As an example consider the two-loop diagram of Fig. 5.1 (a). It contains one-loop subdiagrams, shown in Fig. 5.1 (b). The renormalization of subdiagrams requires vertices as shown in Fig. 5.1 (c), which are of order $\hbar$. At order $\hbar^2$ these vertices appear in so-called counterterm diagrams as the one shown in Fig. 5.1 (d). When the sum of the original diagram and the one-loop counterterm diagrams, Fig. 5.1 (a) and twice the contribution from Fig. 5.1 (d), respectively, is considered, the remaining divergence is local and can be absorbed by counterterms. In order to renormalize a two-loop diagram one therefore has to take into account all corresponding one-loop counterterm diagrams.

We distinguish two general types of two-loop integrals. The first type can be directly written as the product of two one-loop integrals, while this decomposition is not possible for the second type.

5.3 Infrared renormalization of products of one-loop integrals

Consider the product of two one-loop integrals,

$$H = H_1 H_2. \tag{5.5}$$

H is a two-loop integral and the result of a dimensional counting analysis reads (see App. C.2)

$$H = F_1 + F_2 + F_3 + F_4, \tag{5.6}$$

where F_1, $F_2 + F_3$, and F_4 satisfy the Ward identities separately due to different analytic structures, i.e. different overall powers of M in n dimensions. Using Eq. (5.1), H can also be expressed as

$$H = I_1 I_2 + I_1 R_2 + R_1 I_2 + R_1 R_2, \tag{5.7}$$

where again $I_1 I_2$, $I_1 R_2 + R_1 I_2$, and $R_1 R_2$ satisfy the Ward identities individually.

To renormalize the integral H we need to add the contributions of (renormalized) counterterm integrals. The vertex used in the counterterm integral is determined by standard IR renormalization of a one-loop subintegral. In a one-loop calculation we do not have to consider terms proportional to ϵ for the subtraction terms, since at the end of the calculation the limit $\epsilon \to 4$ is taken. At the two-loop level, however, the subtraction terms are multiplied with terms proportional to ϵ^{-1} from the second loop integration. Therefore the choice whether or not to include the terms proportional to ϵ in one-loop subtraction terms results in different finite contributions in the two-loop integrals. In addition to the UV divergences and the terms proportional to ϵ^0 we choose the subtraction terms for one-loop integrals to contain *all* positive powers of ϵ,

$$\tilde{R} = \frac{H^{UV}}{\epsilon} + \tilde{R}^0 + \epsilon \tilde{R}^1 + \cdots . \tag{5.8}$$

This choice is crucial for the preservation of the relevant symmetries as is discussed in the following. H contains two subintegrals, H_1 and H_2. The expressions for the unrenormalized counterterm integrals then read

$$-\tilde{R}_1 H_2 - \tilde{R}_2 H_1. \tag{5.9}$$

The H_i are one-loop integrals from which we would subtract the term $\tilde{R}_i$ in a one-loop calculation, excluding the additional divergences. However, the term $\tilde{R}_j$ multiplying H_i contains terms with positive powers of ϵ, so that in the product of $\tilde{R}_j$ and R_i we get finite terms from the additional divergences in R_i. These would not be removed if we chose the subtraction term to be $\tilde{R}_j \tilde{R}_i$. Instead we define the subtraction term for the product $\tilde{R}_j H_i$ to be

$$-\tilde{R}_j R_i + \frac{H_j^{UV} R_i^{add}}{\epsilon^2} + \tilde{R}_j^0 \frac{R_i^{add}}{\epsilon}, \tag{5.10}$$

i.e. we subtract all finite terms stemming from the additional divergences in R_i but do not subtract the additional divergences themselves. This is analogous to the one-loop sector, where we do not subtract the additional divergences in the infrared regular part either (see Eqs. (3.27) and (3.29)).

We now show that this renormalization procedure for the counterterm integrals does not violate the Ward identities. We know that the subtraction terms S for one-loop integrals do not violate the Ward identities and result in a modification of the coupling constants and fields in the Lagrangian. The counterterm integrals are then calculated with the help of this new Lagrangian which means that the term

$$-S\,H \tag{5.11}$$

also respects all Ward identities. H is a one-loop integral and Eq. (5.11) can be written as

$$-S\,I - S\,R \tag{5.12}$$

where $-S\,I$ and $-S\,R$ satisfy the Ward identities separately. In particular, the Ward identities are satisfied term by term in an expansion in ϵ for $S\,I$ and $S\,R$, respectively. The expansion for $S\,I$ is given by

$$S\,I = \left(\frac{S^{div}}{\epsilon} + S^{fin}\right)\left(\frac{I^{add}}{\epsilon} + I^{fin}\right) = \frac{S^{div}\,I^{add}}{\epsilon^2} + \frac{1}{\epsilon}\left[S^{div}I^{fin} + S^{fin}I^{add}\right] + \cdots . \tag{5.13}$$

Suppose we choose the finite part of the counterterm to vanish,[1]

$$S^{fin} = 0.$$

In this case we can see that the term proportional to ϵ^{-1} is given by

$$\frac{1}{\epsilon}\,S^{div}\,I^{fin}. \tag{5.14}$$

It has to satisfy the Ward identities since for this choice of S it is the only term proportional to ϵ^{-1} in the ϵ expansion of $S\,I$. By changing the renormalization scheme to also include finite terms in the subtraction terms, the product in Eq. (5.14) does not change, but we obtain the more general expression of Eq. (5.13). Considering the term proportional to ϵ^{-1} and keeping in mind that Eq. (5.14) respects the Ward identities we now see that

$$\frac{1}{\epsilon}\,S^{fin}\,I^{add} \tag{5.15}$$

satisfies the Ward identities separately. Since the additional divergences have to cancel in the sum of I and R it follows that $I^{add} = -R^{add}$ and

$$-\frac{1}{\epsilon}\,S^{fin}\,R^{add} \tag{5.16}$$

[1] In baryonic ChPT this would result in terms violating the power counting. So far we are only concerned with the symmetries of the theory, which are conserved for $S^{fin} = 0$. The issue of power counting is addressed below.

does not violate any symmetry constraints. Using the fact that $S\,R$ respects all symmetries and choosing the subtraction term S to be $\tilde{R}_j$ (which only contains UV divergences),

$$S = \tilde{R}_j, \quad S^{div} = H_j^{UV}, \quad S^{fin} = \tilde{R}_j^0,$$

it follows that

$$-\frac{H_j^{UV} R^{add}}{\epsilon^2} - \tilde{R}_j^0 \frac{R^{add}}{\epsilon} \tag{5.17}$$

satisfies the Ward identities and therefore also our prescription for the subtraction terms of the counterterm diagrams of Eq. (5.10) satisfies the Ward identities.

Using the above method the sum of the original expression and the renormalized counterterm integrals gives

$$\begin{aligned}
&H_1 H_2 - \tilde{R}_1 H_2 + \tilde{R}_1 R_2 - \frac{H_1^{UV} R_2^{add}}{\epsilon^2} - \tilde{R}_1^0 \frac{R_2^{add}}{\epsilon} - \tilde{R}_2 H_1 + \tilde{R}_2 R_1 - \frac{R_1^{add} H_2^{UV}}{\epsilon^2} \\
&\quad -\tilde{R}_2^0 \frac{R_1^{add}}{\epsilon} \\
&= I_1 I_2 + I_1 R_2 + I_2 R_1 + R_1 R_2 - \tilde{R}_1 I_2 - \frac{H_1^{UV} R_2^{add}}{\epsilon^2} - \tilde{R}_1^0 \frac{R_2^{add}}{\epsilon} - \tilde{R}_2 I_1 \\
&\quad -\frac{R_1^{add} H_2^{UV}}{\epsilon^2} - \tilde{R}_2^0 \frac{R_1^{add}}{\epsilon} \\
&= I_1 I_2 + I_1 (R_2 - \tilde{R}_2) + I_2 (R_1 - \tilde{R}_1) - \frac{H_1^{UV} R_2^{add} + R_1^{add} H_2^{UV}}{\epsilon^2} - \tilde{R}_1^0 \frac{R_2^{add}}{\epsilon} \\
&\quad -\tilde{R}_2^0 \frac{R_1^{add}}{\epsilon} + R_1 R_2\,.
\end{aligned} \tag{5.18}$$

The difference between R_i and $\tilde{R}_i$ is only given by the additional divergences R_i^{add}/ϵ, resulting in

$$\begin{aligned}
&\left(\tilde{I}_1 + \frac{I_1^{add}}{\epsilon}\right)\left(\tilde{I}_2 + \frac{I_2^{add}}{\epsilon}\right) + \left(\tilde{I}_1 + \frac{I_1^{add}}{\epsilon}\right)\frac{R_2^{add}}{\epsilon} + \left(\tilde{I}_2 + \frac{I_2^{add}}{\epsilon}\right)\frac{R_1^{add}}{\epsilon} \\
&\quad -\frac{H_1^{UV} R_2^{add} + R_1^{add} H_2^{UV}}{\epsilon^2} - \tilde{R}_1^0 \frac{R_2^{add}}{\epsilon} - \tilde{R}_2^0 \frac{R_1^{add}}{\epsilon} + R_1 R_2\,.
\end{aligned} \tag{5.19}$$

Using $I_i^{add} = -R_i^{add}$ we obtain

$$\tilde{I}_1 \tilde{I}_2 - \frac{I_1^{add} I_2^{add}}{\epsilon^2} - \frac{H_1^{UV} R_2^{add} + R_1^{add} H_2^{UV}}{\epsilon^2} - \tilde{R}_1^0 \frac{R_2^{add}}{\epsilon} - \tilde{R}_2^0 \frac{R_1^{add}}{\epsilon} + R_1 R_2 + \mathcal{O}(\epsilon). \tag{5.20}$$

Expanding $R_1 R_2$ in ϵ and simplifying the resulting expression gives

$$\tilde{I}_1 \tilde{I}_2 - \frac{I_1^{add} I_2^{add}}{\epsilon^2} + \frac{R_1^{add} R_2^{add}}{\epsilon^2} + \frac{H_1^{UV} H_2^{UV}}{\epsilon^2} + \frac{H_1^{UV} \tilde{R}_2^0 + \tilde{R}_1^0 H_2^{UV}}{\epsilon} + (R_1 R_2)^0 + \mathcal{O}(\epsilon), \tag{5.21}$$

where $(R_1 R_2)^0$ stands for the terms proportional to ϵ^0 in the product $R_1 R_2$. Using again $I_i^{add} = -R_i^{add}$ we see that all terms containing the additional divergences vanish,

$$= \tilde{I}_1 \tilde{I}_2 + \frac{H_1^{UV} H_2^{UV}}{\epsilon^2} + \frac{H_1^{UV} \tilde{R}_2^0 + \tilde{R}_1^0 H_2^{UV}}{\epsilon} + (R_1 R_2)^0 + \mathcal{O}(\epsilon)\,. \tag{5.22}$$

The term R_1R_2 satisfies the Ward identities, in particular each term in the ϵ expansion of R_1R_2 does so individually. This means that we can subtract the finite part of R_1R_2 by a counterterm. The terms proportional to ϵ^{-2} and ϵ^{-1} stem from the UV divergences in H_1 and H_2. These terms also satisfy the Ward identities individually and are absorbed in counterterms. As desired, the renormalized result for the product of two one-loop integrals including the counterterm integrals is then simply the product of the renormalized one-loop integrals,

$$(H_1H_2)^r = \tilde{I}_1\tilde{I}_2. \tag{5.23}$$

Besides respecting all symmetries the renormalization prescription must also result in a proper power counting for renormalized integrals. The chiral order of a product of two integrals is the sum of the individual orders. For a one-loop integral the infrared singular part $\tilde{I}$ satisfies the power counting. Therefore the result of Eq. (5.23) also satisfies power counting.

5.4 Infrared renormalization of two-loop integrals relevant to the nucleon mass calculation

In this section we describe the renormalization procedure for two-loop integrals that do not directly factorize into the product of two one-loop integrals. We follow the general method presented in Ref. [SGS 04b], but give more details. After showing how the proper renormalization of two-loop integrals and the corresponding counterterm integrals preserves the underlying symmetries, we describe a simplified formalism to arrive at the same results while greatly reducing the calculational difficulties.

5.4.1 General method

Denote a general two-loop integral contributing to the self-energy by H,

$$H = \iint \frac{d^nk_1d^nk_2}{(2\pi)^{2n}}\frac{1}{A^aB^bC^cD^dE^e}\,, \tag{5.24}$$

where

$$\begin{aligned}
A &= k_1^2 - M^2 + i0^+,\\
B &= k_2^2 - M^2 + i0^+,\\
C &= k_1^2 + 2p\cdot k_1 + i0^+,\\
D &= k_2^2 + 2p\cdot k_2 + i0^+,\\
E &= k_1^2 + 2p\cdot k_1 + 2k_1\cdot k_2 + 2p\cdot k_2 + k_2^2 + i0^+.
\end{aligned} \tag{5.25}$$

Using a dimensional counting analysis we can write H as

$$H = F_1 + F_2 + F_3 + F_4. \tag{5.26}$$

F_1 is obtained by simply expanding the integrand in M and interchanging summation and integration. For F_2 we rescale the first loop momentum k_1 by

$$k_1 \mapsto \frac{M}{m}\, k_1, \tag{5.27}$$

expand the resulting integrand in M and interchange summation and integration. F_3 is obtained analogously to F_2, only that instead of k_1 the second loop momentum k_2 is rescaled,

$$k_2 \mapsto \frac{M}{m}\, k_2. \tag{5.28}$$

Finally F_4 is defined as the result from simultaneously rescaling both loop momenta,

$$k_1 \mapsto \frac{M}{m}\, k_1, \quad k_2 \mapsto \frac{M}{m}\, k_2, \tag{5.29}$$

and expanding the integrand with subsequent interchange of summation and integration. F_1, $F_2 + F_3$, and F_4 separately satisfy the Ward identities due to different overall factors of M. This is analogous to the one-loop sector, where the infrared singular and infrared regular parts separately satisfy the Ward identities, since the infrared singular part is nonanalytic in small quantities for noninteger n, while the infrared regular term is analytic. As in the one-loop case the interchange of summation and integration generates additional divergences not present in H in each of the terms F_1, $F_2 + F_3$, and F_4. Again, these additional divergences cancel in the sum of all terms.

In addition to the two-loop integral we also need to determine the corresponding subintegrals. To identify the first subintegral we consider the k_1 integration in H,

$$H_{sub_1} = \int \frac{d^n k_1}{(2\pi)^n}\, \frac{1}{A^a C^c E^e}\,. \tag{5.30}$$

This is a one-loop integral which is renormalized using "standard" infrared renormalization. The infrared regular part R_{sub_1} of this integral is obtained by expanding the integrand in M and interchanging summation and integration. The only term in Eq. (5.30) depending on M is A. Symbolically we write

$$R_{sub_1} = \sum \int \frac{d^n k_1}{(2\pi)^n}\, \frac{1}{\underline{A}^a C^c E^e}\,, \tag{5.31}$$

where underlined expressions are understood as an expansion in M. R_{sub_1} contains additional divergences, and we define $\widetilde{R}_{sub_1}$ as R_{sub_1} without these divergences,[2]

$$\widetilde{R}_{sub_1} = R_{sub_1} - \frac{R^{add}_{sub_1}}{\epsilon}\,. \tag{5.32}$$

As in the definition of Eq. (3.27), $\widetilde{R}_{sub_1}$ again contains all terms of positive power of ϵ. Since H_{sub_1} is a standard one-loop integral, $\widetilde{R}_{sub_1}$ will satisfy the Ward identities and can be absorbed in counterterms of the Lagrangian.

[2]Note that for the integrals of interest here, the UV divergence is included in the infrared regular part R.

Using these counterterms as a vertex we obtain a counterterm integral of the form

$$H_{CT_1} = -\int \frac{d^n k_2}{(2\pi)^n}\, \widetilde{R}_{sub_1} \frac{1}{B^b D^d}\,. \tag{5.33}$$

H_{CT_1} is generated by a Lagrangian that is consistent with the considered symmetries. Therefore, H_{CT_1} satisfies the Ward identities. Inserting Eqs. (5.31) and (5.32) we rewrite H_{CT_1} as

$$H_{CT_1} = -\int \frac{d^n k_2}{(2\pi)^n} \sum \int \frac{d^n k_1}{(2\pi)^n} \frac{1}{\underline{A}^a B^b C^C D^d E^e} + \int \frac{d^n k_2}{(2\pi)^n} \frac{R^{add}_{sub_1}}{\epsilon} \frac{1}{B^b D^d}\,. \tag{5.34}$$

Equation (5.34) still needs to be renormalized. After the k_1 integration has been performed, Eq. (5.34) is a one-loop integral and standard infrared renormalization can be used. To obtain the infrared singular part I_{CT_1} we rescale $k_2 \mapsto \frac{M}{m}\, k_2$, expand in M, and interchange summation and integration. Symbolically we write

$$I_{CT_1} = -\sum \int \frac{d^n k_2}{(2\pi)^n} \sum \int \frac{d^n k_1}{(2\pi)^n} \frac{1}{\underline{A}^a \underline{\underline{B}}^b C^C \underline{\underline{D}}^d \underline{\underline{E}}^e} + \sum \int \frac{d^n k_2}{(2\pi)^n}\, \epsilon^{-1} \underline{\underline{R^{add}_{sub_1}}}\, \frac{1}{\underline{\underline{B}}^b \underline{\underline{D}}^d}\,, \tag{5.35}$$

where double-underlined quantities are first rescaled and then expanded. Note that $R^{add}_{sub_1}$ can also depend on k_2 through the denominator E in Eq. (5.30). Since I_{CT_1} is obtained from a one-loop integral that satisfies the Ward identities through the standard infrared renormalization process, it will itself satisfy the Ward identities. The infrared renormalized expression for the counterterm integral,

$$\widetilde{I}_{CT_1} = I_{CT_1} - \frac{I^{add}_{CT_1}}{\epsilon}\,, \tag{5.36}$$

then also satisfies the Ward identities. Note that $I^{add}_{CT_1}$ itself contains terms proportional to $\frac{1}{\epsilon}$, since it stems from the one-loop counterterm for the subintegral, but we choose not to include any terms proportional to positive powers of ϵ. This means that $\epsilon^{-1} I^{add}_{CT_1}$ only contains terms proportional to ϵ^{-2} and ϵ^{-1}. The expression for $\widetilde{I}_{CT_1}$ therefore does not contain any divergent terms stemming from additional divergences.

We now show how $\widetilde{I}_{CT_1}$ is related to the term F_3 of Eq. (5.26). As explained above, F_3 is obtained by rescaling k_2, expanding the resulting integrand and interchanging summation and integration. In the above notation this would correspond to

$$F_3 = \sum \iint \frac{d^n k_1 d^n k_2}{(2\pi)^{2n}} \frac{1}{\underline{A}^a \underline{\underline{B}}^b C^C \underline{\underline{D}}^d \underline{\underline{E}}^e}\,. \tag{5.37}$$

Comparing with the first term in Eq. (5.35) we see that the integrands in both cases are expanded in the same way. Therefore, when adding the counterterm diagram $\widetilde{I}_{CT_1}$ to H it cancels parts of F_3. The difference between $\widetilde{I}_{CT_1}$ and F_3 is that in F_3 the terms stemming from the additional divergences $R^{add}_{sub_1}$ (including *finite* terms) as well as the additional divergences $I^{add}_{CT_1}/\epsilon$ that are proportional to ϵ^{-2} and ϵ^{-1} are not subtracted. As pointed out above, the original integral H only contains UV divergences, therefore the additional divergences cancel in the sum $F_1+F_2+F_3+F_4$. The terms remaining in the sum $\widetilde{I}_{CT_1}+F_3$ are the finite contributions stemming from the additional divergences in R_{sub_1}. Since in F_3 the variable k_2 is rescaled before expanding while the k_1 variable remains unchanged, F_3 can be considered as a sum of products of infrared singular and infrared regular terms, which we symbolically write as

$$F_3 = \sum R_1 I_2\,. \tag{5.38}$$

In this notation the remaining finite terms are $\sum R_1^{add} I_2^{\epsilon}$, where $\epsilon^{-1} R_1^{add}$ is the additional divergence of R_1 and I_2^{ϵ} is the part of I_2 proportional to ϵ.

The second subdiagram can be calculated analogously, and is related to the term F_2 in Eq. (5.26).

Taking the above considerations into account we obtain for the sum of the original integral H and the corresponding counterterm integrals

$$\begin{aligned}
H + \widetilde{I}_{CT_1} + \widetilde{I}_{CT_2} &= F_1 + F_2 + F_3 + F_4 + \widetilde{I}_{CT_1} + \widetilde{I}_{CT_2} \\
&= \widetilde{F}_1 + \widetilde{F}_4 + \sum R_1^{add} I_2^{\epsilon} + \sum R_2^{add} I_1^{\epsilon} \\
&= \widetilde{F}_1 + \widetilde{F}_4 - \sum I_1^{add} I_2^{\epsilon} - \sum I_2^{add} I_1^{\epsilon}\,,
\end{aligned} \tag{5.39}$$

where $\widetilde{F}_i$ indicates that the additional divergences are excluded.

The expression in Eq. (5.39) satisfies the Ward identities since each term in the sum on the left side of the first line does so individually. F_1 separately satisfies the Ward identities, in particular this is the case for each term in its ϵ expansion. This means that we can subtract the finite part of $\widetilde{F}_1$ by an overall counterterm without violating the symmetries. Since the remaining UV divergences also satisfy the Ward identities, absorbing them in an overall counterterm does not violate the symmetries. The result for the renormalized two-loop diagram is then

$$H^r = \widetilde{F}_4 - \sum I_1^{add} I_2^{\epsilon} - \sum I_2^{add} I_1^{\epsilon}\,. \tag{5.40}$$

Since all subtractions preserve the symmetries H^r will satisfy the Ward identities.

So far we have subtracted pole parts in the epsilon expansion. Following [BL 99] we choose to absorb the combination

$$\lambda = \frac{1}{(4\pi)^2}\left[\frac{1}{n-4} - \frac{1}{2}\left(\log(4\pi) + \Gamma'(1) + 1\right)\right] \tag{5.41}$$

instead, which is achieved by simply replacing the t'Hooft parameter μ by

$$\mu \to \frac{\mu}{(4\pi)^{1/2}}\, e^{\frac{\gamma_E - 1}{2}}\,, \tag{5.42}$$

where $\gamma_E = -\Gamma'(1)$ (see also App. D).

F_4 is obtained by rescaling both k_1 and k_2 and satisfies the power counting rules. Since the terms I_i result from the rescaling of k_i, the product $I_1 I_2$ has the same analytic structure in M as F_4, and therefore satisfies the power counting. This means that also the renormalized integral $H^r = \widetilde{F}_4 - \sum I_1^{add} I_2^{\epsilon} - \sum I_2^{add} I_1^{\epsilon}$ obeys the power counting.

5.4.2 Simplified method

In the previous subsection we have established the concept of infrared renormalization of two-loop integrals. The procedure outlined above is quite involved when applied to actual calculations of physical processes. Therefore, we now describe a simpler method of obtaining the renormalized expression H^r which, however, is only applicable to integrals with a *single* small scale. This is the case for the calculation of the nucleon mass, whereas e.g. the nucleon form factors contain the momentum transfer as an additional small quantity.

Instead of calculating the subintegrals of the original integral H, consider just the terms in F_4. F_4 itself is a sum of two-loop integrals. Each two-loop integral contains one-loop subintegrals, i.e. only one loop integration is performed while the other one is kept fixed. These subintegrals contain divergences, resulting in divergent as well as finite contributions when the second loop integration is performed. In addition to the subintegral contributions, F_4 contains finite parts and additional divergences originating in the interchange of summation and integration when generating F_4. We can symbolically write F_4 as

$$F_4 = \bar{F}_4 + \frac{\bar{F}_4^{add,2}}{\epsilon^2} + \frac{\bar{F}_4^{add,1}}{\epsilon} + \frac{F_4^{Sub_1,div}}{\epsilon}\, F_4^{k_2} + \frac{F_4^{Sub_2,div}}{\epsilon}\, F_4^{k_1}\,. \tag{5.43}$$

Here, the finite parts of F_4 are denoted by $\bar{F}_4$ to distinguish them from $\widetilde{F}_4$ in Eq. (5.39). The bar notation is also used for the divergent terms $\bar{F}_4^{add,2}$ and $\bar{F}_4^{add,1}$ to show that these are not the complete divergent expressions for F_4, but only the additional divergences of order ϵ^{-2} and ϵ^{-1}, respectively. The terms $\epsilon^{-1}F_4^{Sub_i,div}$ denote the divergences of the subintegral with respect to the integration over k_i, while $F_4^{k_j}$ stands for the remaining second integration of the counterterm integral. Note that the divergent part of the first loop integration over k_i in general depends on the second loop momentum k_j. This dependance is included in the expression $F_4^{k_j}$.

We now show how the different parts in Eq. (5.43) are related to expressions in F_2 and F_3 and then describe the simplified renormalization method. F_4 is obtained from the original integral H by rescaling k_1 and k_2, expanding the resulting integrand in M and interchanging summation and integration. For the denominators of Eq. (5.25) the rescaling results in

$$\begin{aligned}
k_1^2 - M^2 + i0^+ \quad &\mapsto \quad \left(\frac{M}{m}\right)^2 (k_1^2 - m^2 + i0^+),\\
k_2^2 - M^2 + i0^+ \quad &\mapsto \quad \left(\frac{M}{m}\right)^2 (k_2^2 - m^2 + i0^+),\\
k_1^2 + 2p\cdot k_1 + i0^+ \quad &\mapsto \quad \left(\frac{M}{m}\right)\left(\frac{M}{m}\, k_1^2 + 2p\cdot k_1 + i0^+\right),\\
k_2^2 + 2p\cdot k_2 + i0^+ \quad &\mapsto \quad \left(\frac{M}{m}\right)\left(\frac{M}{m}\, k_2^2 + 2p\cdot k_2 + i0^+\right),\\
k_1^2 + 2p\cdot k_1 + 2k_1\cdot k_2 + 2p\cdot k_2 + k_2^2 + i0^+ \quad &\mapsto\\
\left(\frac{M}{m}\right)\left(\frac{M}{m}\, k_1^2 + 2p\cdot k_1 + 2\frac{M}{m}\, k_1\cdot k_2 + 2p\cdot k_2 + \frac{M}{m}\, k_2^2 + i0^+\right)&.
\end{aligned}$$

After the interchange of summation and integration one can perform the substitution $k_i \mapsto \frac{m}{M} k_i$ to bring the denominators $k_1^2 - m^2 + i0^+$ and $k_2^2 - m^2 + i0^+$ back into the form A and B, respectively. The result can be interpreted as obtained from the original integral by leaving A and B unchanged and expanding C in k_1^2, D in k_2^2, and E in $k_1^2 + 2k_1 \cdot k_2 + k_2^2$, respectively. Symbolically

$$F_4 \sim \sum \iint \frac{d^n k_1 d^n k_2}{(2\pi)^{2n}} \frac{1}{[k_1^2 - M^2 + i0^+]^a [k_2^2 - M^2 + i0^+]^b [\underline{k_1}^2 + 2p \cdot k_1 + i0^+]^c}$$
$$\times \frac{1}{[\underline{k_2}^2 + 2p \cdot k_2 + i0^+]^d [\underline{k_1}^2 + 2p \cdot k_1 + \underline{2k_1 \cdot k_2} + 2p \cdot k_2 + \underline{k_2}^2 + i0^+]^e}, \tag{5.44}$$

where we have used the underlined notation to mark terms that we have expanded in.

The divergent parts of the k_1 subintegral stem from the integration region $k_1 \to \infty$. They can be generated by further expanding each term in F_4 in *inverse* powers of k_1. This corresponds to an expansion in *positive* powers of M for the first denominator and in *positive* powers of $2p \cdot k_2$ in the resulting last propagator,

$$\frac{F_4^{Sub_1,div}}{\epsilon} F_4^{k_2} \sim \sum \iint \frac{d^n k_2 d^n k_1}{(2\pi)^{2n}} \frac{1}{[k_1^2 - \underline{M}^2 + i0^+]^a [k_2^2 - M^2 + i0^+]^b}$$
$$\times \frac{1}{[\underline{k_1}^2 + 2p \cdot k_1 + i0^+]^c [\underline{k_2}^2 + 2p \cdot k_2 + i0^+]^d}$$
$$\times \frac{1}{[\underline{k_1}^2 + 2p \cdot k_1 + \underline{2k_1 \cdot k_2} + \underline{2p \cdot k_2} + \underline{k_2}^2 + i0^+]^e}. \tag{5.45}$$

We see that the expression for $F_4^{k_2}$ is of the form

$$F_4^{k_2} \sim \sum \int \frac{d^n k_2}{(2\pi)^n} \frac{f_{\mu\nu\lambda\ldots} k_2^\mu k_2^\nu k_2^\lambda \cdots}{[k_2^2 - M^2 + i0^+]^b [2p \cdot k_2 + i0^+]^{d+i_1}}, \tag{5.46}$$

where $f_{\mu\nu\lambda\ldots}$ denotes the coefficients that result from the expansion in Eq. (5.45).

Next we show that $F_4^{k_2}$ is related to terms in F_3. F_3 is generated from the original integral H by rescaling k_2, expanding the resulting integrand and interchanging summation and integration. After the substitution $k_2 \mapsto \frac{m}{M} k_2$ and using the above notation we write

$$F_3 \sim \sum \iint \frac{d^n k_1 d^n k_2}{(2\pi)^{2n}} \frac{1}{[k_1^2 - \underline{M}^2 + i0^+]^a [k_2^2 - M^2 + i0^+]^b [k_1^2 + 2p \cdot k_1 + i0^+]^c}$$
$$\times \frac{1}{[\underline{k_2}^2 + 2p \cdot k_2 + i0^+]^d [k_1^2 + 2p \cdot k_1 + \underline{2k_1 \cdot k_2} + \underline{2p \cdot k_2} + \underline{k_2}^2 + i0^+]^e}$$
$$\sim \sum \iint \frac{d^n k_1 d^n k_2}{(2\pi)^{2n}} \frac{[k_2^2]^{j_4} [2k_1 \cdot k_2]^{j_5}}{[k_1^2 + i0^+]^{a+j_1} [k_1^2 + 2p \cdot k_1 + i0^+]^{c+e+j_2} [k_2^2 - M^2 + i0^+]^b}$$
$$\times \frac{1}{[2p \cdot k_2 + i0^+]^{d+j_3}}. \tag{5.47}$$

We see that F_3 is the sum of products of one-loop (tensorial) integrals. As explained above these products of one-loop integrals are in fact products of infrared singular and infrared regular parts of integrals (see Eq. (5.38)),

$$F_3 = \sum R_1 I_2 \,,$$

and the expressions for I_2 are given by

$$I_2 \sim \sum \int \frac{d^n k_2}{(2\pi)^n} \frac{k_2^\alpha k_2^\beta k_2^\gamma \cdots}{[k_2^2 - M^2 + i0^+]^b [2p \cdot k_2 + i0^+]^{d+i_2}} \,. \tag{5.48}$$

Considering the k_2 integrals of Eqs. (5.45) and (5.47) one sees that one has expanded in the same quantities. While the ordering of the expansions as well as the interchanges of summation and integration are different, the two expansions are equivalent. Therefore, comparing Eqs. (5.46) and (5.48), one finds that for each term in $F_4^{k_2}$ there is a corresponding term in I_2, or symbolically

$$F_4^{k_2} = I_2 \,. \tag{5.49}$$

An analogous analysis for the second subintegral gives

$$F_4^{k_1} = I_1 \,. \tag{5.50}$$

As a next step we show that the divergences of the F_4 subintegrals are related to the additional divergences of the integrals R_i in F_2 and F_3. From Eq. (5.44) we see that the k_1 subintegral is given by integrals of the type

$$\begin{aligned} F_4^{Sub_1} &\sim \sum \int \frac{d^n k_1}{(2\pi)^n} \frac{1}{[k_1^2 - M^2 + i0^+]^a [\underline{k_1}^2 + 2p \cdot k_1 + i0^+]^c} \\ &\quad \times \frac{1}{[\underline{k_1}^2 + 2p \cdot k_1 + \underline{2k_1 \cdot k_2} + \underline{2p \cdot k_2} + \underline{k_2}^2 + i0^+]^e} \\ &\sim \sum \int \frac{d^n k_1}{(2\pi)^n} \frac{k_1^\mu k_1^\nu \cdots}{[k_1^2 - M^2 + i0^+]^a [2p \cdot k_1 + i0^+]^{c+e+l_2}} \,. \end{aligned} \tag{5.51}$$

The infrared regular integrals R_1 in Eq. (5.47) read

$$R_1 \sim \sum \int \frac{d^n k_1}{(2\pi)^n} \frac{k_1^\mu k_1^\nu \cdots}{[k_1^2 + i0^+]^{a+m_1} [k_1^2 + 2p \cdot k_1 + i0^+]^{c+e+m_2}} \,. \tag{5.52}$$

$F_4^{Sub_1}$ and R_1 can be interpreted as the infrared singular and infrared regular parts of the auxiliary integrals

$$h \sim \sum \int \frac{d^n k_1}{(2\pi)^n} \frac{k_1^\mu k_1^\nu \cdots}{[k_1^2 - M^2 + i0^+]^\alpha [k_1^2 + 2p \cdot k_1 + i0^+]^\beta [k_1^2 + 2p \cdot k_1 + 2Mp \cdot k_2 + i0^+]^\gamma} \,, \tag{5.53}$$

respectively. Note the extra factor of M in the last denominator necessary for this identification. Since h is a "standard" one-loop integral that is only UV divergent, the additional divergences in its IR regular part R_1 must cancel exactly with the divergences in its IR singular part $F_4^{Sub_1,div}$. Therefore,

$$\frac{F_4^{Sub_1,div}}{\epsilon} = -\frac{R_1^{add}}{\epsilon}\,, \tag{5.54}$$

and, using $R_1^{add} = -I_1^{add}$, it also follows that

$$\frac{F_4^{Sub_1,div}}{\epsilon} = \frac{I_1^{add}}{\epsilon}\,. \tag{5.55}$$

Analogously

$$\frac{F_4^{Sub_2,div}}{\epsilon} = -\frac{R_2^{add}}{\epsilon} = \frac{I_2^{add}}{\epsilon}\,. \tag{5.56}$$

Having established the relationship between the terms in F_4 and the terms in F_2 and F_3 we now describe the renormalization procedure. Our method consists of treating each two-loop integral contributing to F_4 as an independent integral. We then renormalize each two-loop integral in the $\widetilde{\mathrm{MS}}$ scheme, i.e. we

- determine the divergences in the subintegrals,
- use the divergences as vertices in one-loop counterterm integrals that are added to F_4,
- perform an additional overall subtraction by absorbing all remaining divergences in counterterms,
- replace $\tilde{\mu} = \frac{\mu}{(4\pi)^{1/2}}\, e^{\frac{\gamma_E - 1}{2}}$ and set $\mu = m$.

The divergences in the subintegrals are given by $\epsilon^{-1} F_4^{Sub_i,div}$. The one-loop counterterm integrals using these divergences read

$$-\frac{F_4^{Sub_1,div}}{\epsilon}\, F_4^{k_2} - \frac{F_4^{Sub_2,div}}{\epsilon}\, F_4^{k_1}\,. \tag{5.57}$$

According to Eqs. (5.49), (5.50), (5.55), and (5.56) this can be written as

$$-\frac{I_2^{add}}{\epsilon}\, I_1 - \frac{I_1^{add}}{\epsilon}\, I_2\,. \tag{5.58}$$

When added to F_4 we obtain

$$F_4 - \frac{I_2^{add}}{\epsilon}\, I_1 - \frac{I_1^{add}}{\epsilon}\, I_2\,. \tag{5.59}$$

Using the notation of Subsec. 5.4.1, we write F_4 as the sum of the additional divergences and a remainder $\widetilde{F}_4$,

$$F_4 = \frac{F_4^{add,2}}{\epsilon^2} + \frac{F_4^{add,1}}{\epsilon} + \widetilde{F}_4\,. \tag{5.60}$$

Note that the divergent terms $F_4^{add,i}$ are not the divergent expressions $\bar{F}_4^{add,i}$ of Eq. (5.43). Performing the ϵ expansion for the integrals I_i,

$$I_i = \epsilon^{-1} I_i^{add} + I_i^0 + \epsilon I_i^\epsilon \,,$$

the sum of F_4 and the counterterm integrals is given by

$$\frac{F_4^{add,2}}{\epsilon^2} + \frac{F_4^{add,1}}{\epsilon} - 2\frac{I_2^{add} I_1^{add}}{\epsilon^2} - \frac{I_1^{add}}{\epsilon} I_2^0 - \frac{I_2^{add}}{\epsilon} I_1^0 + \widetilde{F}_4 - I_1^{add} I_2^\epsilon - I_2^{add} I_1^\epsilon \,. \tag{5.61}$$

We now show that the remaining divergences are analytical in M^2 and can therefore be absorbed by counterterms. Recall that the sum of all additional divergences has to vanish, since they are not present in the original integral,

$$0 = \frac{F_1^{add,2}}{\epsilon^2} + \frac{F_1^{add,1}}{\epsilon} + \frac{F_2^{add,2}}{\epsilon^2} + \frac{F_2^{add,1}}{\epsilon} + \frac{F_3^{add,2}}{\epsilon^2} + \frac{F_3^{add,1}}{\epsilon} + \frac{F_4^{add,2}}{\epsilon^2} + \frac{F_4^{add,1}}{\epsilon} \,. \tag{5.62}$$

As shown above F_2 and F_3 are the sums of products of one-loop integrals, so Eq. (5.62) can be rewritten as

$$\begin{aligned} 0 \;=\; & \frac{F_1^{add,2}}{\epsilon^2} + \frac{F_1^{add,1}}{\epsilon} + \frac{I_1^{add} R_2^{add}}{\epsilon^2} + \frac{I_1^{add}}{\epsilon} R_2^0 + I_1^0 \frac{R_2^{add}}{\epsilon} + \frac{I_2^{add} R_1^{add}}{\epsilon^2} + \frac{I_2^{add}}{\epsilon} R_1^0 \\ & + I_2^0 \frac{R_1^{add}}{\epsilon} + \frac{F_4^{add,2}}{\epsilon^2} + \frac{F_4^{add,1}}{\epsilon} \,. \end{aligned} \tag{5.63}$$

Making use of $I_i^{add} = -R_i^{add}$ the sum of all additional divergences takes the form

$$\begin{aligned} 0 \;=\; & \frac{F_1^{add,2}}{\epsilon^2} + \frac{F_1^{add,1}}{\epsilon} - \frac{R_1^{add}}{\epsilon} R_2^0 - \frac{R_2^{add}}{\epsilon} R_1^0 \\ & -2\frac{I_1^{add} I_2^{add}}{\epsilon^2} - \frac{I_1^{add}}{\epsilon} I_2^0 - \frac{I_2^{add}}{\epsilon} I_1^0 + \frac{F_4^{add,2}}{\epsilon^2} + \frac{F_4^{add,1}}{\epsilon} \,. \end{aligned} \tag{5.64}$$

All terms in F_1 for the two-loop integral as well as the infrared regular terms in one-loop integrals are analytic in M^2. Therefore the first line in Eq. (5.64) is analytic in M^2. Since the sum of all terms vanishes the second line also has to be analytic. This second line, however, comprises exactly the remaining divergences in Eq. (5.61), which are therefore analytic in M^2 and can be subtracted. After these divergences have been absorbed in counterterms, the resulting expression for the renormalized contribution of F_4 reads

$$F_4^r = \widetilde{F}_4 - \sum I_1^{add} I_2^\epsilon - \sum I_2^{add} I_1^\epsilon \,, \tag{5.65}$$

where we have explicitly shown the sums again. Comparing with Eq. (5.40) we see that our result exactly reproduces the expression for the renormalized original integral H^r.

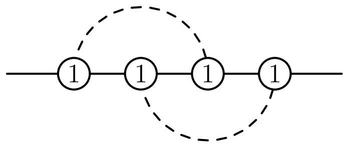

Figure 5.2: Two-loop diagram contributing to the nucleon self-energy.

5.4.3 ϵ-dependent factors

For actual calculations it is often convenient to reduce appearing tensorial integrals to scalar integrals before performing the dimensional counting analysis as well as the renormalization. The reduction of the tensorial integrals can result in ϵ-dependent factors multiplying the scalar integrals. These change the form of the result of Eq. (5.40) since additional finite terms can appear. Let the ϵ-dependent factor be given by

$$\phi(\epsilon) = \phi^0 + \epsilon\phi^1 + \epsilon^2\phi^2 + \cdots . \tag{5.66}$$

Consider performing the k_1 integration first. Suppose that from the result one can extract an ϵ-dependent factor $\varphi_1(\epsilon)$, and the subsequently performed k_2 integration leads to another ϵ-dependent factor, $\varphi_2(\epsilon)$, with

$$\phi(\epsilon) = \varphi_1(\epsilon) \cdot \varphi_2(\epsilon). \tag{5.67}$$

One can also perform the k_2 integration first, which leads to a different factor $\tilde{\varphi}_2(\epsilon)$, followed by the k_1 integration resulting in a factor $\tilde{\varphi}_1(\epsilon)$ with

$$\phi(\epsilon) = \tilde{\varphi}_2(\epsilon) \cdot \tilde{\varphi}_1(\epsilon)\,. \tag{5.68}$$

The terms $\varphi_1(\epsilon) = \varphi_1^0 + \epsilon\varphi_1^1 + \epsilon^2\varphi_1^2 + \cdots$ and $\tilde{\varphi}_2(\epsilon) = \tilde{\varphi}_2^0 + \epsilon\tilde{\varphi}_2^1 + \epsilon^2\tilde{\varphi}_2^2 + \cdots$ can then directly be taken into account when determining the divergent contributions from subintegrals. The result $H^{r,\phi}$ for the renormalized integral $\phi(\epsilon)H$ reads

$$H^{r,\phi} = \widetilde{F}_4^{\phi} - \varphi_1^0 I_1^{add}\left(\varphi_2^2 I_2^{add} + \varphi_2^1 I_2^0 + \varphi_2^0 I_2^{\epsilon}\right) - \tilde{\varphi}_2^0 I_2^{add}\left(\tilde{\varphi}_1^2 I_1^{add} + \tilde{\varphi}_1^1 I_1^0 + \tilde{\varphi}_1^0 I_1^{\epsilon}\right)\,, \tag{5.69}$$

where $\widetilde{F}_4^{\phi}$ denotes the finite terms in $\phi(\epsilon)\,F_4$, and I_i^0, φ_1^0 and $\tilde{\varphi}_2^0$ are the ϵ-independent terms in I_i, φ_1 and $\tilde{\varphi}_2$, respectively. Our simplified method still holds provided the ϵ-dependent factors are taken into account.

As an example consider the diagram of Fig. 5.2. Ignoring constant factors, one can show that in a calculation up to order $\mathcal{O}(q^6)$ the nucleon mass only receives contributions from

$$\gamma_\mu(\not{p} - m)\gamma_\alpha(\not{p} + m)\gamma_\nu(\not{p} - m)\gamma_\beta \iint \frac{d^{n+2}k_1\, d^{n+2}k_2}{(2\pi)^{2n+4}} \frac{g^{\alpha\beta}g^{\mu\nu}}{ABCDE}, \tag{5.70}$$

where the denominators are given in Eq. (5.25). One would also obtain the contribution of Eq. (5.70) if one considered a diagram with fictitious particles as shown

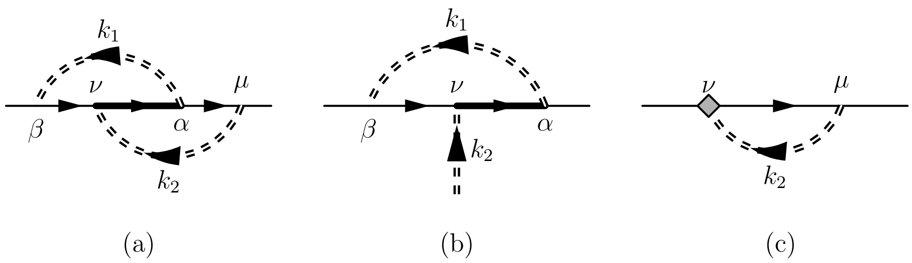

Figure 5.3: Two-loop diagram and diagrams corresponding to k_1 and subsequent k_2 integrations. The diamond-shaped vertex corresponds to the result of the k_1 integration.

in Fig. 5.3 (a), with Feynman rules given by

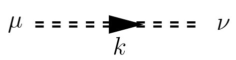

$$\frac{g^{\mu\nu}}{k^2 - M^2 + i0^+},$$

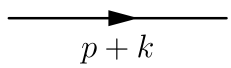

$$\frac{\not{p} - m}{k^2 + 2p \cdot k + i0^+},$$

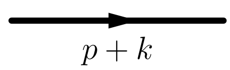

$$\frac{\not{p} + m}{k^2 + 2p \cdot k + i0^+},$$

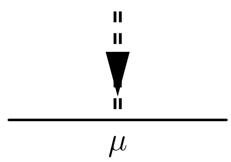

$$\gamma_\mu,$$

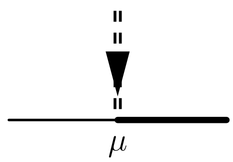

$$\gamma_\mu.$$

The subintegral corresponding to performing the k_1 integration first is shown in Fig. 5.3 (b). With the Feynman rules above it is proportional to

$$(n-3)\left(4m^2\gamma_\nu - 4mp_\nu\right), \tag{5.71}$$

so that we can identify $\varphi_1(\epsilon) = n - 3 = 1 + 2\epsilon$. The subsequent k_2 integration corresponds to the diagram of Fig. 5.3 (c), where the diamond-shaped vertex is given by the result of the k_1 integration. One finds that the term proportional to p_ν only contributes to higher orders and can be ignored. The remaining expression is proportional to

$$(n-3)\gamma_\mu(\not{p} - m)\gamma_\nu g^{\mu\nu} = -2m(n-3)(n-1), \tag{5.72}$$

and therefore $\varphi_2(\epsilon) = n - 1 = 3 + 2\epsilon$. On the other hand, considering the k_2 integration first leads to an analogous analysis with the results $\tilde{\varphi}_2(\epsilon) = n - 3 = 1 + 2\epsilon = \varphi_1(\epsilon)$ and $\tilde{\varphi}_1(\epsilon) = n - 1 = 3 + 2\epsilon = \varphi_2(\epsilon)$.

In the cases where one *cannot* identify the individual contributions to $\phi(\epsilon)$ from the integrations of k_1 and k_2, respectively (this happens for example for tensor integrals of the type $k_1^\mu k_2^\nu$), one has to perform the dimensional counting analysis before reducing the tensor integrals.

Chapter 6

Nucleon mass to order $\mathcal{O}(q^6)$

In this chapter we calculate the nucleon mass up to order $\mathcal{O}(q^6)$ using the reformulated infrared renormalization. Besides the evaluation of contact and one-loop diagrams this includes the analysis of all two-loop diagrams containing pion and nucleon lines that can be constructed up to this order. To the best of our knowledge this is the first complete two-loop calculation in manifestly Lorentz-invariant BChPT.

6.1 Nucleon propagator

A one-particle state in the spectrum of a Hamiltonian has the (physical) mass m_N if $p^2 = m_N^2$ for this one-particle state. The corresponding full propagator S_N has a simple pole at $p^2 = m_N^2$. In terms of the bare mass m_0 appearing as a parameter in the free Lagrangian $\mathcal{L}_0$ the full propagator of a spin-1/2 particle can be written as

$$S_N(\not{p}) = \frac{1}{\not{p} - m_0 - \Sigma(\not{p}, m_0) + i0^+}, \tag{6.1}$$

where $i\Sigma(\not{p}, m_0)$ is the sum of all one-particle irreducible self-energy diagrams. The physical mass is determined by the solution to the equation

$$S_N^{-1}\big|_{\not{p}=m_N} = [\not{p} - m_0 - \Sigma(\not{p}, m_0)]\big|_{\not{p}=m_N} = 0. \tag{6.2}$$

The self-energy receives contributions from contact terms as well as from loop diagrams,

$$\Sigma(\not{p}, m_0) = \Sigma_c + \Sigma_{loop}(\not{p}, m_0). \tag{6.3}$$

With the form of the BChPT Lagrangian given in Chapter 2, Σ_c for the nucleon is independent of $\not{p}$. Inserting Eq. (6.3) into Eq. (6.2) one finds

$$[\not{p} - m_0 - \Sigma_c - \Sigma_{loop}(\not{p}, m_0)]\big|_{\not{p}=m_N} = 0. \tag{6.4}$$

In a loop expansion Eq. (6.4) has the perturbative solution

$$m_N = m_0 + \Sigma_c + \mathcal{O}(\hbar). \tag{6.5}$$

In the above the bare propagator which is used in the calculation of the self-energy diagrams has been chosen to be

$$S_N^0(\not{p}) = \frac{1}{\not{p} - m_0 + i0^+} \,. \tag{6.6}$$

However, one can also choose this propagator to be

$$\tilde{S}_N^0(\not{p}) = \frac{1}{\not{p} - m_0 - \Sigma_c + i0^+} \,. \tag{6.7}$$

This corresponds to including in the free Lagrangian those bilinear terms which generate the contact term diagrams in the self-energy contribution. The advantage of this choice is that all self-energy diagrams with contact interaction insertions in the propagator are summed up automatically. With this choice of the propagator the self-energy is now given by the sum of *loop* diagrams only, i. e.

$$\Sigma(\not{p}, m_0) \to \widetilde{\Sigma}_{loop}(\not{p}, \tilde{m}) \,, \tag{6.8}$$

where

$$\tilde{m} = m_0 + \Sigma_c \,. \tag{6.9}$$

As an additional benefit, when working to two-loop accuracy, one can set $\not{p} = \tilde{m}$ in the expression of two-loop diagrams, since corrections are at least of order $\mathcal{O}(\hbar^3)$. To obtain m_N one has to solve the equation

$$\tilde{S}_N^{-1}(m_N) = [\not{p} - \tilde{m} - \widetilde{\Sigma}_{loop}(\not{p}, \tilde{m})]\Big|_{\not{p}=m_N} = 0 \,. \tag{6.10}$$

Inserting the loop expansion for $\widetilde{\Sigma}_{loop}(\not{p}, \tilde{m})$,

$$\widetilde{\Sigma}_{loop}(\not{p}, \tilde{m}) = \hbar \widetilde{\Sigma}^{(1)}_{loop}(\not{p}, \tilde{m}) + \hbar^2 \widetilde{\Sigma}^{(2)}_{loop}(\not{p}, \tilde{m}) + \cdots \,, \tag{6.11}$$

using the ansatz

$$m_N = \tilde{m} + \hbar \delta m_1 + \hbar^2 \delta m_2 + \cdots \,, \tag{6.12}$$

and expanding around $\tilde{m}$ we obtain up to the two-loop level

$$\begin{aligned} 0 &= \tilde{m} + \hbar\delta m_1 + \hbar^2 \delta m_2 - \tilde{m} - \hbar \widetilde{\Sigma}^{(1)}_{loop}(\tilde{m} + \hbar\delta m_1, \tilde{m}) - \hbar^2 \widetilde{\Sigma}^{(2)}_{loop}(\tilde{m}, \tilde{m}) \\ &= \hbar \left[\delta m_1 - \widetilde{\Sigma}^{(1)}_{loop}(\tilde{m}, \tilde{m})\right] + \hbar^2 \left[\delta m_2 - \delta m_1\, \widetilde{\Sigma}^{(1)\prime}_{loop}(\tilde{m}, \tilde{m}) - \widetilde{\Sigma}^{(2)}_{loop}(\tilde{m}, \tilde{m})\right] . \end{aligned} \tag{6.13}$$

The solutions for δm_1 and δm_2 are given by

$$\delta m_1 = \widetilde{\Sigma}^{(1)}_{loop}(\tilde{m}, \tilde{m}), \tag{6.14}$$

$$\delta m_2 = \widetilde{\Sigma}^{(1)}_{loop}(\tilde{m}, \tilde{m}) \widetilde{\Sigma}^{(1)\prime}_{loop}(\tilde{m}, \tilde{m}) + \widetilde{\Sigma}^{(2)}_{loop}(\tilde{m}, \tilde{m}) \,. \tag{6.15}$$

To obtain the nucleon mass up to chiral order $\mathcal{O}(q^6)$ one needs to determine Σ_c, δm_1, and δm_2 up to that order.

In principle, the nucleon propagator is a 2×2 matrix in isospin space. For arbitrary values of the up and down quark masses the propagator is a diagonal matrix; since, however, in this work the isospin-symmetric case $m_u = m_d$ is considered, the masses of proton and neutron are identical and the propagator is proportional to the unit matrix.

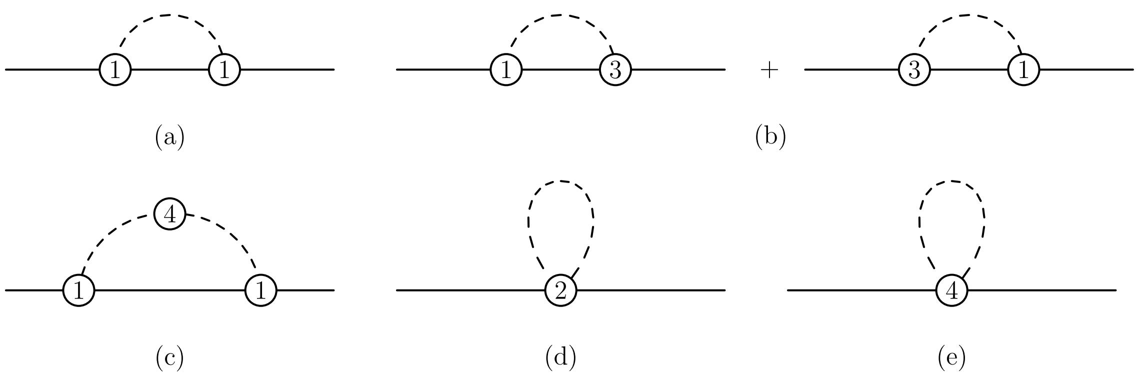

Figure 6.1: One-loop diagrams contributing to the nucleon self-energy up to order $\mathcal{O}(q^6)$.

6.2 Contact terms

The contributions to the nucleon mass from contact interactions are given by

$$\begin{aligned}\Sigma_c &= -4c_1M^2 - (16e_{38} + 2e_{115} + 2e_{116})M^4 + \hat{g}_1 M^6 \\ &= -4c_1M^2 - \hat{e}_1M^4 + \hat{g}_1M^6\,,\end{aligned} \tag{6.16}$$

where we use the notation $\hat{e}_1 = 16e_{38} + 2e_{115} + 2e_{116}$ and $\hat{g}_1$ denotes a linear combination of LECs from the Lagrangian at order $\mathcal{O}(q^6)$ (see Subsection 2.4.3). As discussed above we replace the mass in the chiral limit m by

$$m_4 = m - 4c_1M^2 - \hat{e}_1M^4 \tag{6.17}$$

in the expression for loop integrals. This ensures that all diagrams with contact interaction insertions in the nucleon propagator are automatically taken into account.

6.3 One-loop contributions

The one-loop diagrams contributing to the nucleon mass up to order $\mathcal{O}(q^6)$ are shown in Fig. (6.1). Diagrams (a) and (d) are of order $\mathcal{O}(q^3)$ and $\mathcal{O}(q^4)$, respectively, and already contribute in a one-loop calculation. Diagrams (b) and (c) are of order $\mathcal{O}(q^5)$, while the power counting gives $D = 6$ for diagram (e).

Using dimensional regularization the unrenormalized results for the one-loop diagrams up to order $\mathcal{O}(q^6)$ read

$$\begin{aligned}\Sigma_{1(a)} &= -\frac{3\mathrm{g}_A^2}{4F^2}\left[(\not p + m)I_N + (\not p + m)M^2 I_{\pi N}(p^2) + (p^2 - m^2)\not p I_{\pi N}^{(p)}(p^2)\right], \\ \Sigma_{1(b)} &= -\frac{3\mathrm{g}_A}{F^2}(2d_{16} - d_{18})M^2\left[(\not p + m)I_N + (\not p + m)M^2 I_{\pi N}(p^2)\right. \\ &\quad \left.+(p^2 - m^2)\not p I_{\pi N}^{(p)}(p^2)\right],\end{aligned}$$

$$
\begin{aligned}
\Sigma_{1(c)} &= -\frac{3\mathrm{g}_A^2}{F^4}\, mM^4 \left[(l_3 - l_4) I_{\pi N}(p^2) + l_3 M^2 I_{\pi\pi N}(0)\right], \\
\Sigma_{1(d)} &= \frac{3}{F^2}\left[(2c_1 - c_3) M^2 I_\pi - c_2 \frac{p^2}{m^2}\, I_\pi^{(00)}\right], \\
\Sigma_{1(e)} &= -\frac{12}{F^2}\left\{\left[2(e_{14}+e_{19}) - e_{36} + 4e_{38}\right] I_\pi + \left[e_{15} + 2e_{20}\right] \frac{p^2}{m^2} M^2 I_\pi^{(00)}\right. \\
&\quad \left. - 2e_{16} \frac{p^4}{m^4}\, I_\pi^{(0000)}\right\}.
\end{aligned}
\tag{6.18}
$$

The integrals $I_\pi, I_{\pi N}(p^2), \ldots$ are given in App. B. The infrared renormalized expressions, denoted by a superscript r, up to order M^6 are given by

$$
\begin{aligned}
\Sigma_{1(a)}^r &= -\frac{3\mathrm{g}_A^2}{32\pi F^2}\, M^3 - \frac{3\mathrm{g}_A^2}{64\pi^2 F^2 m}\left[2\ln\frac{M}{\mu} + 1\right] M^4 \\
&\quad + \frac{3\mathrm{g}_A^2}{1024\pi^3 F^4 m^2}\left[4\pi^2 F^2 + 3\mathrm{g}_A^2 m^2 + 9\mathrm{g}_A^2 m^2 \ln\frac{M}{\mu}\right] M^5 \\
&\quad - \frac{\mathrm{g}_A^2}{2048\pi^4 F^4 m^3}\Bigg[27\pi^2 \mathrm{g}_A^2 m^2 + 384\pi^2 c_1 F^2 m - 16\pi^2 F^2 - 9m^2(\mathrm{g}_A^2 - c_2 m) \\
&\quad + 3m\left[-15\mathrm{g}_A^2 m + 16c_1(3m^2 + 16\pi^2 F^2) + 3m^2(c_2 - 8c_3)\right] \ln\frac{M}{\mu} \\
&\quad - 54m^2\left(\mathrm{g}_A^2 - 8c_1 m + c_2 m + 4c_3 m\right) \ln^2\frac{M}{\mu}\Bigg] M^6, \\
\Sigma_{1(b)}^r &= -\frac{3\mathrm{g}_A}{8\pi F^2}\,(2d_{16} - d_{18})\, M^5 - \frac{3\mathrm{g}_A}{16\pi^2 F^2 m}\,(2d_{16} - d_{18})\left[2\ln\frac{M}{\mu} + 1\right] M^6, \\
\Sigma_{1(c)}^r &= -\frac{3\mathrm{g}_A^2}{32\pi F^4}\,(3l_3 - 2l_4) M^5 - \frac{3\mathrm{g}_A^2}{32\pi^2 F^4 m}\left[3l_3 - l_4 + 2(2l_3 - l_4)\ln\frac{M}{\mu}\right] M^6, \\
\Sigma_{1(d)}^r &= \frac{3}{128\pi^2 F^2}\left[c_2 + \ln\frac{M}{\mu}\,(32c_1 - 4c_2 - 16c_3)\right] M^4 + \frac{3c_1 c_2}{16\pi^2 F^2 m}\left[4\ln\frac{M}{\mu} - 1\right] M^6, \\
\Sigma_{1(e)}^r &= \frac{M^6}{96\pi^2 F^2}\,\left[18(e_{15} + e_{20} + e_{35}) + 5e_{16}\right] \\
&\quad - \frac{M^6}{8\pi^2 F^2}\ln\frac{M}{\mu}\left[24(e_{14} + e_{19}) + 6(e_{15} + e_{20} + e_{35}) + e_{16} - 12e_{36} - 48e_{38}\right].
\end{aligned}
\tag{6.19}
$$

Various combinations of fourth-order baryonic LECs appear through the vertex in diagram (e). To simplify the notation we use

$$
\begin{aligned}
\hat{e}_1 &= 16e_{38} + 2e_{115} + 2e_{116}, \\
\hat{e}_2 &= 2e_{14} + 2e_{19} - e_{36} - 4e_{38}, \\
\hat{e}_3 &= e_{15} + e_{20} + e_{35}
\end{aligned}
\tag{6.20}
$$

for these combinations.

6.4 Two-loop contributions

The two-loop diagrams relevant for a calculation of the nucleon self-energy up to order $\mathcal{O}(q^6)$ are shown in Fig. 6.2. According to the power counting there are further diagrams at the given order. An example would be diagram 6.2 (c) with one first-order vertex replaced by a second-order one. As a result of our calculation we find that these diagrams give vanishing contributions to the nucleon mass up to the order we are considering.

We again employ dimensional regularization. The unrenormalized expressions for the diagrams of Fig. 6.2 up to order $\mathcal{O}(q^6)$ can be reduced to

$$
\begin{aligned}
\Sigma_{2(a)} &= -\frac{6\mathrm{g}_A^4}{F^4}\,\pi^2 m^3 (n-1)(n-3) J_2(1,1,1,1,1|n+2)\,,\\
\Sigma_{2(b)} &= \frac{9\mathrm{g}_A^4}{F^4}\, m\pi^2 (n-1)\left\{2m^2 J_2(1,1,1,0,2|n+2) - M^2 J_2(1,2,1,0,1|n+2)\right.\\
&\quad - 4m^2M^2\left[J_2(1,2,2,0,1|n+2) + J_2(1,1,2,0,2|n+2)\right]\\
&\quad \left.-32\pi^2 m^2\left[2J_2(1,2,1,0,3|n+4) + J_2(1,2,2,0,2|n+4)\right]\right\}\,,\\
\Sigma_{2(c)} &= \frac{1}{2}\frac{3}{F^4}\, m\left\{\frac{1}{2}\, J_2(1,1,0,0,0|n) - M^2 J_2(1,1,0,0,1|n) - J_2(1,0,0,0,1|n)\right.\\
&\quad \left. + 8\pi^2(n-1)J_2(1,1,0,0,2|n+2) - 16\pi^2(M^2-2m^2)J_2(1,2,0,0,2|n+2)\right\}\,,\\
\Sigma_{2(d)} &= \frac{24\mathrm{g}_A^2}{F^4}\,\left[32\pi^2 m^3(n-1)\left[2J_2(1,2,1,0,3|n+4) + J_2(1,2,2,0,2|n+4)\right]\right.\\
&\quad \left. +\pi^2 m M^2\left[(n-1)J_2(1,2,1,0,1|n+2) + J_2(1,2,0,0,2|n+2)\right]\right]\,,\\
\Sigma_{2(e)} &= -\frac{48\mathrm{g}_A^2}{F^4}\,\pi^2 m^2(n-1)\left\{c_3\left[J_2(1,1,0,0,2|n+2) - 64\pi^2 m^2 J_2(2,1,1,0,3|n+4)\right]\right.\\
&\quad + c_4\left[2J_2(1,1,0,0,2|n+2) - 2M^2 J_2(1,2,1,0,1|n+2)\right.\\
&\quad \left.\left. -64\pi^2 m^2 J_2(2,1,1,0,3|n+4)\right]\right\}\,,\\
\Sigma_{2(f)} &= \frac{3\mathrm{g}_A^2}{2F^4}\, m M^4 J_{\pi N}(1,1|n) J_{\pi N}(1,1|n)\,,\\
\Sigma_{2(g)} &= \frac{24\mathrm{g}_A^2}{F^4}\,\pi^2 m^2 (n-1)\left[(n-2)c_4 - c_3\right] J_{\pi N}(1,1|n+2) J_{\pi N}(1,1|n+2)\,,\\
\Sigma_{2(h)} &= \frac{18\mathrm{g}_A^2}{F^4}\,\pi m^2 M^2 (n-1)\left[\frac{c_2}{n} + c_3 - 2c_1\right] J_{\pi N}(1,0|n) J_{\pi N}(1,2|n+2)\\
&= -\frac{72\mathrm{g}_A^2}{F^4}\,\pi^2 m^2 M^2 (n-1)\left[\frac{c_2}{n} + c_3 - 2c_1\right] J_{\pi N}(2,0|n+2) J_{\pi N}(1,2|n+2)\,,\\
\Sigma_{2(i)} &= -\frac{\mathrm{g}_A^2}{F^4}\, m M^2 J_{\pi N}(1,0|n) J_{\pi N}(1,1|n)\,,\\
\Sigma_{2(j)} &= \frac{1}{8}\frac{4M^2}{F^4}\,\left[5c_1 - 4\frac{c_2}{n} - 4c_3\right] J_{\pi N}(1,0|n) J_{\pi N}(1,0|n)\,,\\
\Sigma_{2(k)} &= \frac{1}{4}\frac{2}{F^4}\,\left\{3\left[\frac{c_2}{n} + c_3 - 2c_1\right] M^4 J_{\pi N}(1,0|n) J_{\pi N}(2,0|n)\right.\\
&\quad \left. + \left[7\frac{c_2}{n} + 7c_3 - 8c_1\right] M^2 J_{\pi N}(1,0|n) J_{\pi N}(1,0|n)\right\}\,,
\end{aligned}
$$

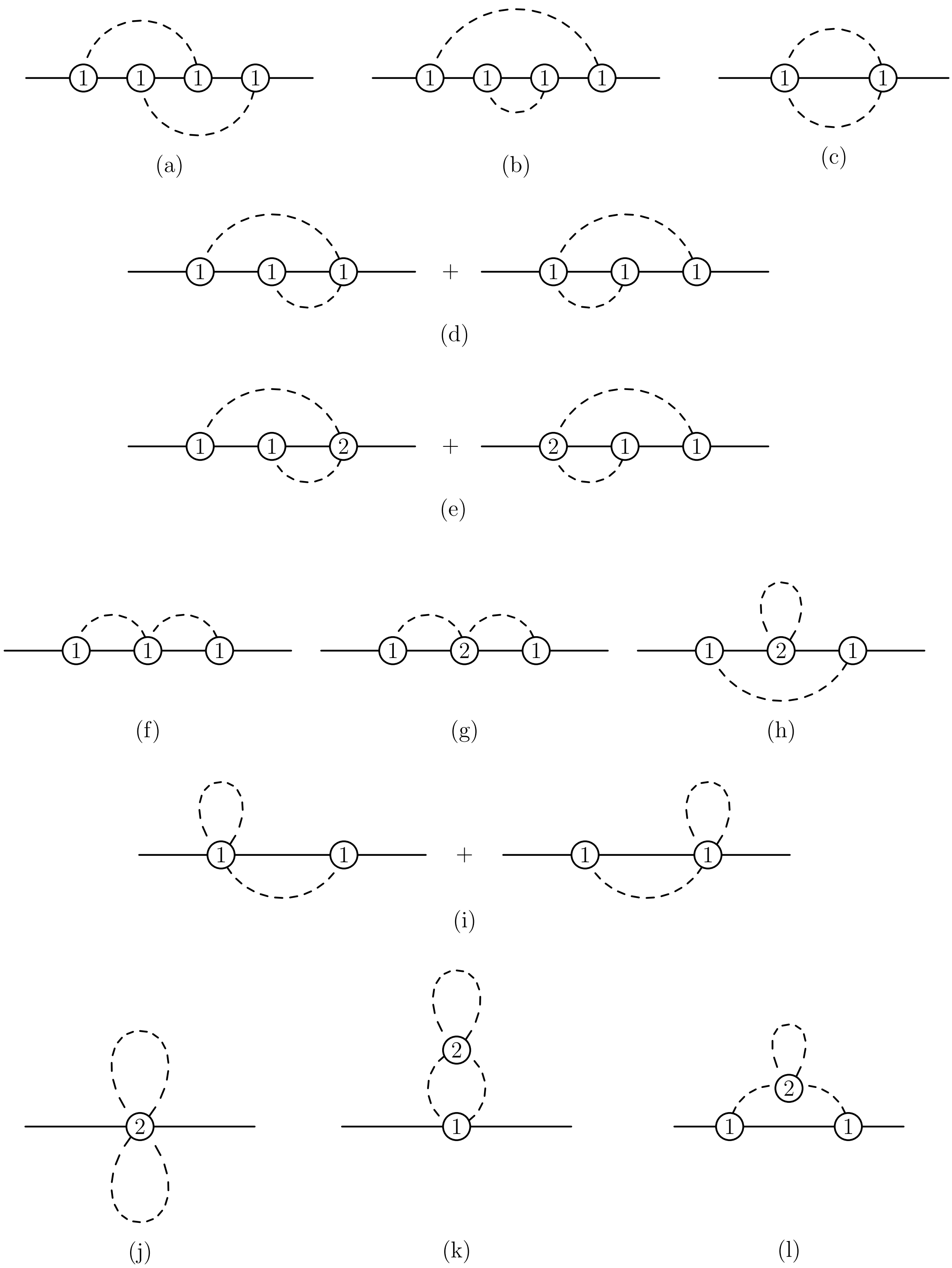

Figure 6.2: Two-loop diagrams contributing to the nucleon self-energy up to order $\mathcal{O}(q^6)$.

$$\Sigma_{2(l)} = \frac{g_A^2}{4F^4} m J_{\pi N}(1,0|n) \left[4J_{\pi N}(0,1|n) + 7M^2 J_{\pi N}(1,1|n) + 3M^4 J_{\pi N}(2,1|n)\right] . \tag{6.21}$$

The integrals $J_{\pi N}(a,b|n)$ and $J_2(a,b,c,d,e|n)$ are defined in App. B. Here we have expressed tensor integrals in terms of scalar integrals in higher dimensions where convenient (see App. B and also Ref. [Tar 96]).

After performing the infrared renormalization as described in Chapter 5 the contributions to the nucleon self-energy up to order $\mathcal{O}(q^6)$ read

$$\begin{aligned}
\Sigma^r_{2(a)} &= -\frac{g_A^4}{512\pi^3 F^4}\left[3M^5\left(1+\ln\frac{M}{\mu}\right) - \frac{M^6}{48\pi m}\left(5+36\pi^2+48\ln\frac{M}{\mu}\right)\right], \\
\Sigma^r_{2(b)} &= \frac{g_A^4}{F^4}\left[\frac{9}{1024\pi^3}M^5\left(1+3\ln\frac{M}{\mu}\right) - \frac{27}{4096\pi^4 m}M^6\left(1+6\ln\frac{M}{\mu}+4\ln^2\frac{M}{\mu}\right)\right], \\
\Sigma^r_{2(c)} &= \frac{M^6}{2048\pi^4 F^4 m}, \\
\Sigma^r_{2(d)} &= -\frac{g_A^2}{1536\pi^4 F^4 m} M^6\left[1+9\pi^2-6\ln\frac{M}{\mu}\right], \\
\Sigma^r_{2(e)} &= \frac{g_A^2}{128\pi^2 F^4} M^6\left[c_3-2c_4\right], \\
\Sigma^r_{2(f)} &= -\frac{3g_A^2}{512\pi^2 F^4 m} M^6, \\
\Sigma^r_{2(g)} &= \frac{g_A^2}{128\pi^2 F^4}\left[c_3-2c_4\right] M^6, \\
\Sigma^r_{2(h)} &= -\frac{9g_A^2}{256\pi^4 F^4} M^6\left[(c_3-2c_1)\left(\ln\frac{M}{\mu}+3\ln^2\frac{M}{\mu}\right)+\frac{c_2}{16}\left(-1+\ln\frac{M}{\mu}\right.\right. \\
&\quad \left.\left.+12\ln^2\frac{M}{\mu}\right)\right], \\
\Sigma^r_{2(i)} &= \frac{g_A^2}{128\pi^3 F^4}\ln\frac{M}{\mu} M^5 + \frac{g_A^2}{256\pi^4 F^4 m}\left(\ln\frac{M}{\mu}+2\ln^2\frac{M}{\mu}\right) M^6, \\
\Sigma^r_{2(j)} &= -\frac{M^6}{128\pi^4 F^4}\left[(5c_1-c_2-4c_3)\ln^2\frac{M}{\mu}+\frac{c_2}{4}\ln\frac{M}{\mu}\right], \\
\Sigma^r_{2(k)} &= \frac{M^6}{512\pi^4 F^4}\left[(12c_1+c_2-6c_3)\ln\frac{M}{\mu}+2(28c_1-5c_2-20c_3)\ln^2\frac{M}{\mu}\right], \\
\Sigma^r_{2(l)} &= -\frac{17g_A^2}{1024\pi^3 F^4}\ln\frac{M}{\mu} M^5 - \frac{g_A^2}{1024\pi^4 F^4 m}\left(13\ln\frac{M}{\mu}+20\ln^2\frac{M}{\mu}\right) M^6 .
\end{aligned} \tag{6.22}$$

6.5 Results and discussion

Combining the contributions from the contact interactions with the one- and two-loop results we obtain for the nucleon mass up to order $\mathcal{O}(q^6)$

$$m_N = m + k_1 M^2 + k_2 M^3 + k_3 M^4 \ln\frac{M}{\mu} + k_4 M^4 + k_5 M^5 \ln\frac{M}{\mu} + k_6 M^5$$

$$+ k_7 M^6 \ln^2 \frac{M}{\mu} + k_8 M^6 \ln \frac{M}{\mu} + k_9 M^6 \,. \tag{6.23}$$

The coefficients k_i are given by

$$\begin{aligned}
k_1 &= -4c_1 \,, \\
k_2 &= -\frac{3\mathrm{g}_A^2}{32\pi F^2} \,, \\
k_3 &= -\frac{3}{32\pi^2 F^2 m} \left(\mathrm{g}_A^2 - 8c_1 m + c_2 m + 4c_3 m\right) \,, \\
k_4 &= -\hat{e}_1 - \frac{3}{128\pi^2 F^2 m} \left(2\mathrm{g}_A^2 - c_2 m\right) \,, \\
k_5 &= \frac{3\mathrm{g}_A^2}{1024\pi^3 F^4} \left(16\mathrm{g}_A^2 - 3\right) \,, \\
k_6 &= \frac{3\mathrm{g}_A^2}{256\pi^3 F^4} \left[\mathrm{g}_A^2 + \frac{\pi^2 F^2}{m^2} - 8\pi^2(3l_3 - 2l_4) - \frac{32\pi^2 F^2}{\mathrm{g}_A}(2d_{16} - d_{18})\right] \,, \\
k_7 &= -\frac{3}{256\pi^4 F^4 m} \left[\mathrm{g}_A^2 - 6c_1 m + c_2 m + 4c_3 m\right] \,, \\
k_8 &= -\frac{\mathrm{g}_A^4}{64\pi^4 F^4 m} - \frac{\mathrm{g}_A^2}{1024\pi^4 F^4 m^2} \left[384\pi^2 F^2 c_1 + 5m + 192\pi^2 m(2l_3 - l_4)\right] \\
&\quad - \frac{3\mathrm{g}_A}{8\pi^2 F^2 m} \left[2d_{16} - d_{18}\right] + \frac{3}{256\pi^4 F^4} \left[2c_1 - c_3\right] \\
&\quad + \frac{1}{8\pi^2 F^2 m} \left[6c_1 c_2 - 12\hat{e}_2 m - 6\hat{e}_3 m - e_{16} m\right] \,, \\
k_9 &= \hat{g}_1 - \frac{\mathrm{g}_A^4}{24576\pi^4 F^4 m} \left(49 + 288\pi^2\right) - \frac{3\mathrm{g}_A}{16\pi^2 F^2 m} (2d_{16} - d_{18}) \\
&\quad - \frac{\mathrm{g}_A^2}{1536\pi^4 F^4 m^3} \left[m^2(1 + 18\pi^2) - 12\pi^2 F^2 + 144\pi^2 m^2 (3l_3 - l_4) \right. \\
&\quad \left. + 288\pi^2 F^2 m c_1 - 24\pi^2 m^3 (c_3 - 2c_4)\right] \\
&\quad + \frac{1}{6144\pi^4 F^4 m} \left[3 - 1152\pi^2 F^2 c_1 c_2 + 1152\pi^2 F^2 m\, \hat{e}_3 + 320\pi^2 F^2 m\, e_{16}\right] \,.
\end{aligned} \tag{6.24}$$

The combinations $\hat{e}_i$ of fourth-order baryonic LECs are given in Eq. (6.20), while $\hat{g}_1$ denotes a combination of LECs from the Lagrangian at order $\mathcal{O}(q^6)$.

In general, the expressions of the coefficients in the chiral expansion of a physical quantity differ in various renormalization schemes, since analytic contributions can be absorbed by redefining LECs. However, this is not possible for the leading nonanalytic terms, which therefore have to agree in all renormalization schemes. Comparing our result with the HBChPT calculation of [MB 99], we see that the expressions for the coefficients k_2, k_3, and k_5 agree as expected. At order $\mathcal{O}(q^6)$ also the coefficient k_7 has to be the same in all renormalization schemes. Note that, while $k_6 M^5$ and $k_8 M^6 \ln \frac{M}{\mu}$ are nonanalytic in the quark masses, the algebraic form of the coefficients k_6 and k_8 are renormalization scheme *dependent*. This is due to the different treatment of one-loop diagrams. The counterterms for one-loop subdiagrams depend on the renormalization scheme and produce nonanalytic terms proportional to M^5 and $M^6 \ln \frac{M}{\mu}$ when used as vertices in counterterm diagrams. We find that our result for k_6 coincides with the HBChPT calculation of Ref. [MB 99] except for a term proportional to d_{28}, which, however, does not have a finite contribution for manifestly-Lorentz invariant renormalization schemes [FMS 98]. Therefore, at order $\mathcal{O}(q^5)$ the chiral expansion of the IR renormalized result reproduces the HBChPT result.

The numerical contributions from higher-order terms cannot be calculated so far, since most expressions in Eq. (6.24) contain LECs which are not reliably known in IR renormalization. In order to get an estimate of these contributions we consider several terms for which the LECs have previously been determined. The coefficient k_5 is free of higher-order LECs and is given in terms of the axial-vector coupling constant g_A and the pion decay constant F. While the values for both g_A and F should be taken in the chiral limit, we evaluate k_5 using the physical values $g_A = 1.2695(29)$ [Yao+ 06] and $F_\pi = 92.42(26)$ MeV. Setting $\mu = m_N$, $m_N = (m_p + m_n)/2 = 938.92$ MeV, and $M = M_{\pi^+} = 139.57$ MeV we obtain $k_5 M^5 \ln(M/m_N) = -3.8$ MeV. This amounts to approximately 25% of the leading nonanalytic contribution at one-loop order, $k_2 M^3$. The mesonic LECs appearing in k_6 can be found in Ref. [GL 84] and are given by $l_3 = 1.4 \times 10^{-3}$ and $l_4 = 3.7 \times 10^{-3}$ at the scale $\mu = m_N$. The parameter d_{18} can be related to the Goldberger-Treiman discrepancy [BL 01] and is given by $d_{18} = -0.80\,\mathrm{GeV}^{-2}$. The LEC d_{16}, however, is not as reliably determined. In order to estimate the magnitude of the contribution stemming from k_6 we use the central value from the reaction $\pi N \to \pi\pi N$, $d_{16} = -1.93\,\mathrm{GeV}^{-2}$ [FBM 00, Bea 04]. It should be noted that the calculation of Ref. [FBM 00] was performed in HBChPT, and employing the obtained value for d_{16} in an infrared renormalized expression therefore only gives an estimate of the size of the corresponding term. The resulting contribution is $k_6 M^5 = 3.7$ MeV and cancels large parts of the nonanalytic term $k_5 M^5 \ln(M/m_N)$. In Ref. [MB 06] the parameter d_{16} has been determined by a fit to lattice data. At the scale $\mu = m_N$ it is given by $d_{16} = 4.11$ GeV^{-2}, which does not agree with the result from the reaction $\pi N \to \pi\pi N$. With this value of d_{16} we find $k_6 M^5 = -7.6$ MeV. The LECs appearing in k_7 have been determined in Ref. [BL 01], and we obtain $k_7 M^6 \ln^2(M/m_N) = 0.3$ MeV.

The terms k_8 and k_9 contain LECs from the fourth order Lagrangian $\mathcal{L}_{\pi N}^{(4)}$ which have not been determined. We try to get a very rough estimate of the size of these contributions by assuming that all these LECs as well as $\hat{g}_1$ are of natural size, that means $e_i \sim 1\,\mathrm{GeV}^{-3}$ and $\hat{g}_1 \sim 1\,\mathrm{GeV}^{-5}$. We choose the d_{16} value from $\pi N \to \pi\pi N$ and use the above values for the other LECs. Setting all appearing $e_i = 0\,\mathrm{GeV}^{-3}$ gives a contribution $k_8 M^6 \ln(M/m_N) \approx 10^{-2}$ MeV. The choice $e_i = 5\,\mathrm{GeV}^{-3}$ results in $k_8 M^6 \ln(M/m_N) \approx 0.7\,\mathrm{MeV}$, while $e_i = -5\,\mathrm{GeV}^{-3}$ gives $k_8 M^6 \ln(M/m_N) \approx -0.7\,\mathrm{MeV}$. A similar analysis for the term $k_9 M^6$ gives $k_9 M^6 \approx -2.8\,\mathrm{MeV}$ for all $e_i = 0\,\mathrm{GeV}^{-3}$ and $\hat{g}_1 = 0\,\mathrm{GeV}^{-5}$, while setting $e_i = 5\,\mathrm{GeV}^{-3}$, $\hat{g}_1 = 5\,\mathrm{GeV}^{-5}$ and $e_i = -5\,\mathrm{GeV}^{-3}$, $\hat{g}_1 = -5\,\mathrm{GeV}^{-5}$ results in $k_9 M^6 \approx -2.5\,\mathrm{MeV}$ and $k_9 M^6 \approx -3.1\,\mathrm{MeV}$, respectively. One should note, however, that the numbers obtained here are only very rough estimates. Choosing $e_{14} = e_{15} = 5\,\mathrm{GeV}^{-3}$ and $e_{16} = e_{19} = e_{20} = e_{35} = e_{36} = e_{38} = 1\,\mathrm{GeV}^{-3}$, $\hat{g}_1 = 1\,\mathrm{GeV}^{-5}$ leads to large cancelations between terms, resulting in a complete contribution at order $\mathcal{O}(M^6)$ of about 0.3 MeV. As a check we also use the value of d_{16} as obtained in Ref. [MB 06], which results in contributions

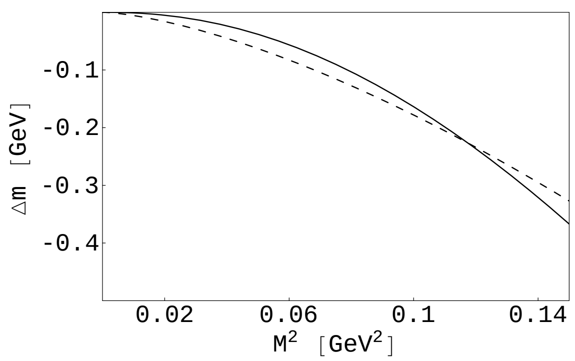

Figure 6.3: Pion mass dependence of the term $k_5 M^5 \ln(M/m_N)$ (solid line) for $M < 400\,\mathrm{MeV}$. For comparison also the term $k_2 M^3$ (dashed line) is shown.

from k_8 that are about a factor 10 larger, while the dependence of k_9 on d_{16} is much less pronounced. Clearly a more reliable determination of the higher-order LECs is desirable.

Chiral expansions like Eq. (6.23) play an important role in the extrapolation of lattice QCD results to physical quark masses, and the nucleon mass is an example that has been studied in detail (see, e.g., Refs. [PHW 04, BHM 04, LTY 04, Pro+ 06, MB 06]). In Ref. [PHW 04] such an extrapolation was performed for the nucleon mass up to order $\mathcal{O}(q^4)$, while Ref. [MB 06] includes an analysis of the fifth-order terms. It was shown, as had also been argued in Ref. [Bea 04], that the terms at order $\mathcal{O}(q^5)$ play an important role in the chiral extrapolation. As an illustration we consider the leading nonanalytic term at this order, $k_5 M^5 \ln(M/m_N)$. Its dependence on the pion mass is shown in Fig. 6.3 for pion masses below 400 MeV, which is considered a region where chiral extrapolations are valid (see, e.g., Refs. [Mei 06, DGS 06]). We see that already at $M \approx 360\,\mathrm{MeV}$ the term $k_5 M^5 \ln(M/m_N)$ becomes as large as the leading nonanalytic term at one-loop order, $k_2 M^3$, indicating the importance of the fifth-order terms at unphysical pion masses. Since the contribution at order $\mathcal{O}(M^6)$ depends on a number of unknown LECs, we do not attempt to perform a chiral extrapolation up to this order here, but restrict the discussion on the pion mass dependence of the term $k_7 M^6 \ln^2(M/m_N)$. Figure 6.4 shows this dependence for pion masses below 400 MeV. No errors are given for the LECs c_1, c_2, and c_3 in Ref. [BL 01]. For an estimate we have assumed the relative errors of these LECs and of $\mathtt{g}_A$ to be 20%, and the corresponding error for $k_7 M^6 \ln^2(M/m_N)$ is shown in Fig. 6.4. For comparison we also show the nonanalytic term at fourth order, $k_3 M^4 \ln(M/m_N)$. As expected, and in contrast to the fifth-order term, the two-loop term $k_7 M^6 \ln^2(M/m_N)$ is smaller than the one-loop contribution $k_3 M^4 \ln(M/m_N)$ in the considered pion mass region. Note that the relative difference in the pion mass dependence between $k_5 M^5 \ln(M/m_N)$ and $k_2 M^3$, as well as $k_7 M^6 \ln^2(M/m_N)$ and $k_3 M^4 \ln(M/m_N)$ is proportional to a factor $M^2 \ln(M/m_N)$, and that on an absolute scale the differences in the two cases are comparable. We also show the pion mass dependence of the terms $k_7 M^6 \ln^2(M/m_N)$ and $k_3 M^4 \ln(M/m_N)$ up to $M \approx 700\,\mathrm{MeV}$, which, however, is beyond the domain that is considered suitable for

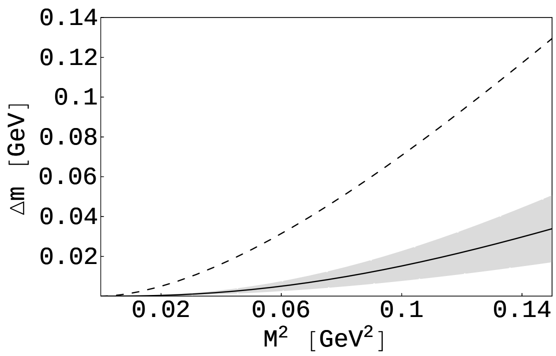

Figure 6.4: Pion mass dependence of the term $k_7 M^6 \ln^2(M/m_N)$ (solid line) for $M < 400\,\mathrm{MeV}$. The shaded band corresponds to relative errors of 20% in the LECs. For comparison also the term $k_3 M^4 \ln(M/m_N)$ (dashed line) is shown.

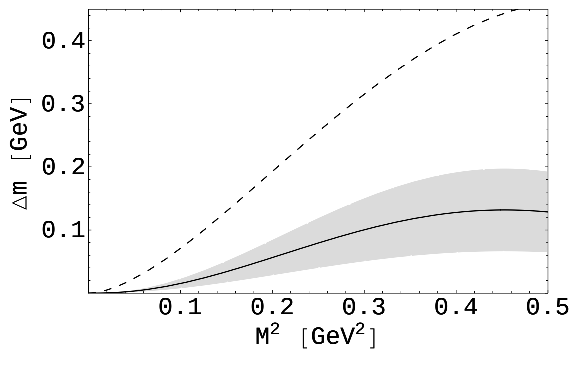

Figure 6.5: Pion mass dependence of the term $k_7 M^6 \ln^2(M/m_N)$ (solid line) for $M < 700\,\mathrm{MeV}$. The shaded band corresponds to relative errors of 20% in the LECs. For comparison also the term $k_3 M^4 \ln(M/m_N)$ (dashed line) is shown.

the application of Eq. (6.23). Again the sixth-order term remains much smaller than the fourth-order one, also at higher pion masses. Since here only one of the terms at order $\mathcal{O}(q^6)$ is considered, and the contribution of the analytic term proportional to M^6 can be considerably larger than $k_7 M^6 \ln^2(M/m_N)$ depending on the values of the unknown LECs, the above considerations are not reliable predictions for the behavior of the complete two-loop contributions at unphysical quark masses.

6.6 Nucleon σ term

The Feynman-Hellmann theorem [Hel 33, Fey 39] relates the nucleon mass to the value of the nucleon scalar form factor at zero momentum transfer, the so-called σ term (see, e.g., [Rey 74, Pag 75]),

$$\sigma(q^2 = 0) = M^2 \frac{\partial m_N}{\partial M^2}\,. \tag{6.25}$$

Applying the Feynman-Hellmann theorem to Eq. (6.23), the chiral expansion of $\sigma(0)$ is given by

$$\begin{aligned}\sigma(0) = {}& k_1 M^2 + \frac{3}{2}\,k_2 M^3 + 2k_3 M^4 \ln\frac{M}{\mu} + \left(\frac{k_3}{2} + 2k_4\right) M^4 + \frac{5}{2}\,k_5 M^5 \ln\frac{M}{\mu} \\ & + \frac{1}{2}\,(k_5 + 5k_6) M^5 + 3k_7 M^6 \ln^2\frac{M}{\mu} + (k_7 + 3k_8) M^6 \ln\frac{M}{\mu} + \left(\frac{k_8}{2} + 3k_9\right) M^6.\end{aligned} \tag{6.26}$$

The first four terms have already been determined in Ref. [BL 99]. To estimate the contributions of the terms of order $\mathcal{O}(M^5)$ we use the same values for the LECs as above, in particular the value of d_{16} as extracted from the reaction $\pi N \to \pi\pi N$. The combined contributions at order order $\mathcal{O}(M^5)$ are

$$\frac{5}{2}\,k_5 M^5 \ln\frac{M}{\mu} + \frac{1}{2}\,(k_5 + 5k_6) M^5 \approx 0.1\,\mathrm{MeV}. \tag{6.27}$$

Given the dependence of the order $\mathcal{O}(M^6)$ nucleon mass contribution on the specific values of the LECs e_i, we do not attempt to evaluate the terms at order $\mathcal{O}(M^6)$ in Eq. (6.26).

Chapter 7

Conclusions

In this thesis we have performed calculations in manifestly Lorentz-invariant baryon chiral perturbation theory beyond order $\mathcal{O}(q^4)$. With a suitable renormalization scheme ChPT exhibits a close connection between the chiral and the loop counting. In infrared renormalization as used in this work, calculations up to chiral order $\mathcal{O}(q^4)$ correspond to tree and one-loop diagrams, while at chiral order $\mathcal{O}(q^5)$ and $\mathcal{O}(q^6)$ also two-loop diagrams have to be taken into account. We have used two approaches to calculate contributions beyond order $\mathcal{O}(q^4)$.

The first method consists of including additional particles as explicit degrees of freedom in the effective theory. In the standard formulation of ChPT resonance contributions are included in the values of the low-energy coupling constants. By keeping additional particles as explicit degrees of freedom one can resum some of the contributions that are of higher-order in a strict chiral expansion. Based on phenomenological observations one chooses those additional degrees of freedom that are expected to give the most dominant contributions. Infrared renormalization in its reformulated version then allows for the consistent treatment of diagrams with these particles as internal lines in addition to pions and nucleons. Once the choice of particles to include has been made there exists a power counting that determines which diagrams to consider up to a certain order and which allows for systematic corrections. As an application we have calculated the axial, induced pseudoscalar, and pion-nucleon form factors in BChPT up to order $\mathcal{O}(q^4)$ with and without the inclusion of the axial-vector meson $a_1(1260)$ in Chapter 4. From a calculation up to and including $\mathcal{O}(q^4)$ without the a_1 meson the axial form factor G_A is described by $G_A(q^2) = g_A + \frac{1}{6}\, g_A \,\langle r_A^2\rangle\, q^2 + \frac{\mathrm{g}_A^3}{4F^2} H(q^2)$, where the loop contributions $H(q^2)$ are found to be negligible. ChPT can neither predict the axial-vector coupling constant g_A nor the mean-square axial radius $\langle r_A^2\rangle$. Instead, empirical information on these quantities is used to absorb the relevant LECs d_{16} and d_{22} in g_A and $\langle r_A^2\rangle$. As in the case of the electromagnetic form factors, the BChPT result for $G_A(q^2)$ up to order $\mathcal{O}(q^4)$ does not produce sufficient curvature to describe the available data beyond very small values of q^2. While a comparison to data is possible for the case of the axial form factor $G_A(q^2)$, the experimental situation of the induced pseudoscalar form factor G_P is less clear and mainly limited to the value of the induced pseudoscalar coupling g_P. In BChPT $G_P(q^2)$ is dominated by a pion-pole contribution and is completely fixed from $\mathcal{O}(q^{-2})$ up to and including $\mathcal{O}(q)$, once the LEC d_{18} has been expressed in terms of the Goldberger-Treiman discrepancy. Using $g_{\pi N} = 13.21$ for the pion-nucleon coupling constant, we obtain for the induced pseudoscalar coupling $g_P = 8.29^{+0.24}_{-0.13} \pm 0.52$. The first error is due to the error of the empirical quantities entering the expression for g_P and the second error represents our estimate for the truncation in the chiral expansion. Our result is smaller than the average experimental results, but still within the range of 1-1.5 standard deviations. Also, the experimental situation on the determination of g_P is not entirely clear. The pion-nucleon form factor is entirely determined in terms of the axial and induced pseudoscalar form factors. Assuming this pion-nucleon form factor to be proportional to the axial form factor leads to a restriction for G_P which is not supported by the most general structure of ChPT.

As a next step we have included the a_1 meson as an explicit degree of freedom. While the Lagrangian for the coupling to pions and external fields was already given in Ref. [Eck+ 89], we have constructed the relevant Lagrangian for the coupling to the nucleon. At order $\mathcal{O}(q^0)$ only one term appears, while there is no term allowed by the symmetries at order $\mathcal{O}(q^1)$. With these Lagrangians we find three additional diagrams relevant to the axial and induced pseudoscalar form factors up to order $\mathcal{O}(q^4)$. Two of these are loop diagrams without any internal pion lines, which vanish in infrared renormalization. Therefore only one tree diagram contributes up to this order, and effectively only one additional coupling constant appears. With a fit of this coupling constant to the available data the axial form factor $G_A(q^2)$ is described well up to momentum transfers $-q^2 = 0.4\,\mathrm{GeV}^2$. The inclusion of the a_1 meson has only a very small effect on the induced pseudoscalar form factor $G_P(q^2)$, which is still dominated by the pion-pole contribution. We also find that the axial-vector meson in our calculation does not contribute to the pion-nucleon form factor.

The method of resumming higher-order contributions by the inclusion of additional degrees of freedom has to be viewed as a phenomenological approach. In a strict chiral expansion the results with and without the additional particles completely agree up to a given order. Having determined the coupling constant of the axial-vector meson by a fit to the data, the question arises if the obtained value also leads to a good description of further physical quantities. However, these would most likely require the calculation of a larger number of diagrams with possibly more unknown constants. In this thesis the inclusion of additional degrees of freedom has been used as a method to resum some higher-order contributions to physical quantities. The applied power counting is only valid in the low-energy region in which also standard BChPT is applicable. It would be of great interest to obtain a consistent power counting that also holds at energies of about the ρ meson mass. In that case the inclusion of the ρ meson should extend the range of applicability of the EFT to higher energies.

The second method for calculations beyond order $\mathcal{O}(q^4)$ consists of a systematic analysis of higher-order contributions in the standard formulation of BChPT, which includes the evaluation and renormalization of two-loop diagrams. In Chapter 5 we showed how the infrared renormalization can be performed at the two-loop level such that renormalized expressions fulfill the relevant Ward identities. The proper renormalization of subintegrals and the inclusion of terms proportional to ϵ in counterterms play a crucial role. As a next step we presented a simplified method of how to renormalize the two-loop integrals relevant to the nucleon mass. This method relies on a dimensional counting analysis. Instead of complete integrals one only has to consider those terms obtained from rescaling both integration variables. These F_4 terms are themselves two-loop integrals that one renormalizes using the $\widetilde{\text{MS}}$ prescription. The results agree with the infrared renormalized expressions of the original integrals. This method simplifies the calculations considerably, especially since the renormalization of multi-loop integrals using the $\widetilde{\text{MS}}$ scheme is significantly easier than infrared renormalization.

As an application we calculated the nucleon mass up to and including order $\mathcal{O}(q^6)$ in Chapter 6. This is the first complete two-loop calculation in manifestly Lorentz-invariant baryon chiral perturbation theory. We find that a number of diagrams that appear up to order $\mathcal{O}(q^6)$ only start to contribute at higher orders beyond the accuracy considered here. Figure 6.2 shows the two-loop diagrams that are relevant to our analysis. The result of our calculation is the chiral expansion of the nucleon mass up to order $\mathcal{O}(q^6)$. At order $\mathcal{O}(q^5)$ our results agree with the ones obtained in the heavy-baryon formulation of ChPT [MB 99], while no previous results at order $\mathcal{O}(q^6)$ exist. Due to the lack of reliable values for some of the low-energy constants appearing in the obtained results we can only estimate the contributions from higher-order terms. As expected the chiral expansion of the nucleon mass seems to converge well. The combined contributions at order $\mathcal{O}(q^5)$ amount to less than 1 MeV. The nonanalytic terms at order $\mathcal{O}(q^6)$ are also estimated to be smaller than 1 MeV each. The analytic contribution depends on the values of unknown LECs, and can amount to a few MeV for natural values of these constants. However, there also exists a combination of natural values for which the complete contribution at order $\mathcal{O}(q^6)$ is less than 1 MeV. Since the chiral expansion of the nucleon mass might be useful for future extrapolations of lattice QCD results, we have also considered the pion mass dependence of the leading nonanalytic term at order $\mathcal{O}(q^6)$ compared to the nonanalytic contribution proportional to M^4. As expected the M^6 term remains much smaller up to pion masses of about 700 MeV, which, however, is already beyond the region of applicability of ChPT. In the future we plan to perform such an extrapolation with the currently available lattice QCD results for the nucleon mass. The results for the nucleon mass were used to estimate higher-order contributions to the nucleon σ term via the Feynman-Hellmann theorem. Due to the dependence of the order $\mathcal{O}(q^6)$ terms on the values of the unknown LECs we only determined the contributions to the nucleon σ term at order $\mathcal{O}(q^5)$. We find these higher-order terms to be approximately 0.1 MeV.

The analysis at order $\mathcal{O}(q^4)$ already shows a good convergence behavior for the chiral expansion of the nucleon mass. There are other quantities though for which this is not the case. One example is the nucleon axial-vector coupling g_A. Since it does not depend on any small scale besides the pion mass it would be possible to apply the simplified renormalization procedure introduced in Chapter 5 in a future two-loop calculation. Other quantities to consider are the anomalous magnetic moments of the proton and neutron. While a calculation of form factors or scattering cross sections would in principle also be possible, the introduction of additional small scales like a momentum transfer complicates the analysis a lot. Also the lack of reliable values for the LECs at order $\mathcal{O}(q^4)$ presents a problem for further calculations at the two-loop level. Some of these parameters, however, will be directly available from lattice QCD calculations in the future [Wit 07].

Appendix A

Feynman rules

We list the Feynman rules needed for the calculations in this thesis as derived from the Lagrangians in Chapter 2. For simplicity we give expressions that appear for special combinations of incoming and outgoing momenta and isospin indices in some cases. All momenta of the axial source are assumed to be incoming.

A.1 Propagators

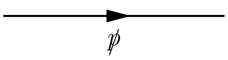

$$\frac{i}{\not{p} - m + i0^+}$$

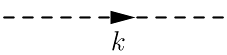

$$\frac{i}{k^2 - M^2 + i0^+}$$

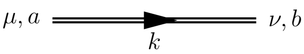

$$-i\left(g_{\mu\nu} - \frac{k_\mu k_\nu}{M_{a_1}^2}\right)\frac{1}{k^2 - M_{a_1}^2 + i0^+}\,\delta_{ab}$$

A.2 Vertices

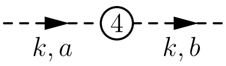

$$-2i\,\frac{M^2}{F^2}\left[l_3 M^2 - l_4(k^2 - M^2)\right]\delta_{ab}$$

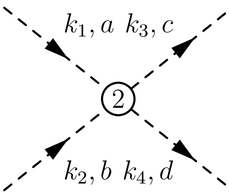

$$\begin{aligned}\frac{i}{3F^2}\Big\{&\delta_{ab}\delta_{cd}\left[3(k_1+k_2)^2 - k_1^2 - k_2^2 - k_3^2 - k_4^2 + M^2\right]\\ &+ \delta_{ac}\delta_{bd}\left[3(k_1-k_3)^2 - k_1^2 - k_2^2 - k_3^2 - k_4^2 + M^2\right]\\ &+ \delta_{ad}\delta_{bc}\left[3(k_1-k_4)^2 - k_1^2 - k_2^2 - k_3^2 - k_4^2 + M^2\right]\Big\}\end{aligned}$$

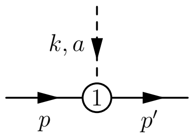

$$-\frac{g_A}{2F}\not{k}\gamma_5\tau_a$$

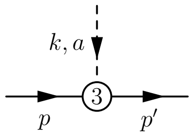

$$-\frac{1}{F}(2d_{16}-d_{18})M^2\not{k}\gamma_5\tau_a$$

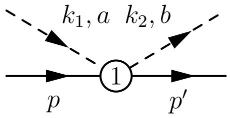

$$\frac{1}{4F^2}(\not{k}_1+\not{k}_2)\epsilon_{abc}\tau_c$$

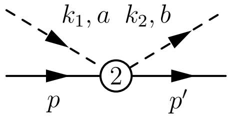

$$-4ic_1\frac{M^2}{F^2}\,\delta_{ab}+i\frac{c_2}{m^2F^2}(p\cdot k_1 p\cdot k_2+p'\cdot k_1 p'\cdot k_2)\delta_{ab} \\ +2i\frac{c_3}{F^2}k_1\cdot k_2\delta_{ab}-i\frac{c_4}{F^2}\,k_1^\mu k_2^\nu\sigma_{\mu\nu}\epsilon_{abc}\tau_c$$

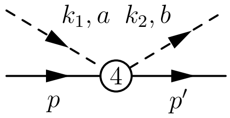

$$\frac{i}{F^2}\,\delta_{ab}\Big\{16e_{14}(k_1\cdot k_2)^2+8\frac{e_{15}}{m^2}\,k_1\cdot k_2\,[(p\cdot k_1)(p\cdot k_2) \\ +(p'\cdot k_1)(p'\cdot k_2)]+8\frac{e_{16}}{m^2}\,\big[(p\cdot k_1)^2(p\cdot k_2)^2 \\ +(p'\cdot k_1)^2(p'\cdot k_2)^2\big]+16e_{19}M^2k_1\cdot k_2 \\ +8\frac{e_{20}}{m^2}\,M^2\,[(p\cdot k_1)(p\cdot k_2)+(p'\cdot k_1)(p'\cdot k_2)] \\ +4e_{22}M^2(k_2-k_1)^2+4\frac{e_{35}}{m^2}\,M^2\,\big[(p\cdot k_1)^2 \\ +(p\cdot k_2)^2+(p'\cdot k_1)^2+(p'\cdot k_2)^2\big] \\ -8e_{36}M^2k_1\cdot k_2-32e_{38}M^4\Big\}$$

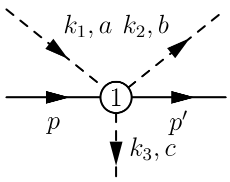

$$\frac{g_A}{12F^3}\,\Big\{\not{k}_1\gamma_5(2\delta_{bc}\tau_a-\delta_{ac}\tau_b-\delta_{ab}\tau_c)-\not{k}_2\gamma_5(2\delta_{ac}\tau_b \\ -\delta_{ab}\tau_c-\delta_{bc}\tau_a)-\not{k}_3\gamma_5(2\delta_{ab}\tau_c-\delta_{ac}\tau_b-\delta_{bc}\tau_a)\Big\}$$

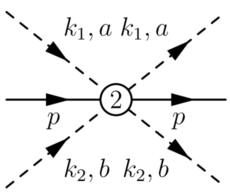

$$20ic_1\frac{M^2}{F^4}-8i\frac{c_2}{m^2F^4}[(p\cdot k_1)^2+(p\cdot k_2)^2] \\ -8i\frac{c_3}{F^4}(k_1^2+k_2^2)$$

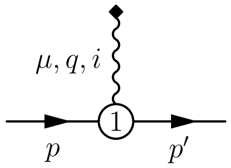

$$i\mathrm{g}_A\gamma_\mu\gamma_5\frac{\tau_i}{2}$$

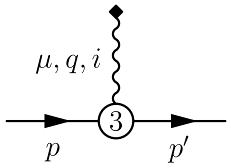

$$i(4M^2d_{16} - q^2d_{22})\gamma_\mu\gamma_5\frac{\tau_i}{2} + id_{22}\not{q}q_\mu\gamma_5\frac{\tau_i}{2}$$

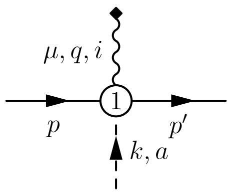

$$-\frac{i}{F}\,\epsilon_{iab}\gamma_\mu\frac{\tau_b}{2}$$

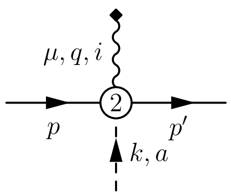

$$-2\frac{c_3}{F}k_\mu\delta_{ia} + \frac{2}{F}\left(c_4\,\sigma_{\mu\nu}k^\nu + c_6\sigma_{\mu\nu}q^\nu\right)\epsilon_{iab}\frac{\tau_b}{2}$$

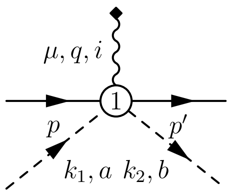

$$i\frac{\mathrm{g}_A}{2F^2}\,\gamma_\mu\gamma_5\left(\delta_{ia}\frac{\tau_b}{2} + \delta_{ib}\frac{\tau_a}{2} - 2\delta_{ab}\frac{\tau_i}{2}\right)$$

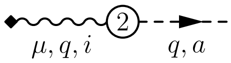

$$q_\mu F\delta_{ia}$$

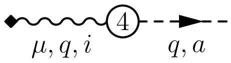

$$2l_4\frac{M^2}{F}\,q_\mu\delta_{ia}$$

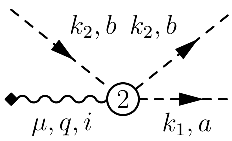

$$-\frac{8}{3F}\,q_\mu\delta_{ia}$$

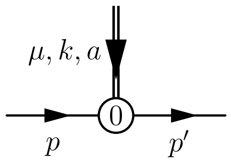

$$ig_{a_1}\gamma_\mu\gamma_5\tau_a$$

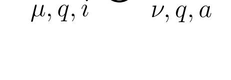

$$-4if_A(q^2g_{\mu\nu} - q_\mu q_\nu)\delta_{ia}$$

Appendix B

Definition of integrals

B.1 Integrals at the one-loop level

We define the one-loop integrals appearing in the results of the nucleon form factors in Chapter 4, as well as in the one-loop contributions to the nucleon mass in Chapter 6. We employ the notation

$$P^\mu = p_i^\mu + p_f^\mu, \quad q^\mu = p_f^\mu - p_i^\mu.$$

Using dimensional regularization [HV 72] the loop integrals with one or two internal lines are defined as

$$\begin{aligned}
I_\pi &= i \int \frac{d^n k}{(2\pi)^n} \frac{1}{k^2 - M^2 + i0^+}, \\
g^{\mu\nu} I_\pi^{(00)} &= i \int \frac{d^n k}{(2\pi)^n} \frac{k^\mu k^\nu}{k^2 - M^2 + i0^+}, \\
(g^{\mu\nu} g^{\rho\sigma} + g^{\mu\rho} g^{\nu\sigma} + g^{\mu\sigma} g^{\nu\rho}) I_\pi^{(0000)} &= i \int \frac{d^n k}{(2\pi)^n} \frac{k^\mu k^\nu k^\rho k^\sigma}{k^2 - M^2 + i0^+}, \\
I_N &= i \int \frac{d^n k}{(2\pi)^n} \frac{1}{k^2 - m^2 + i0^+}, \\
I_{NN}(q^2) &= i \int \frac{d^n k}{(2\pi)^n} \frac{1}{[k^2 - m^2 + i0^+][(k+q)^2 - m^2 + i0^+]}, \\
I_{\pi N}(p^2) &= i \int \frac{d^n k}{(2\pi)^n} \frac{1}{[k^2 - M^2 + i0^+][(k+p)^2 - m^2 + i0^+]}, \\
p^\mu I_{\pi N}^{(p)}(p^2) &= i \int \frac{d^n k}{(2\pi)^n} \frac{k^\mu}{[k^2 - M^2 + i0^+][(k+p)^2 - m^2 + i0^+]}, \\
g^{\mu\nu} I_{\pi N}^{(00)}(p^2) + p^\mu p^\nu I_{\pi N}^{(pp)}(p^2) &= i \int \frac{d^n k}{(2\pi)^n} \frac{k^\mu k^\nu}{[k^2 - M^2 + i0^+][(k+p)^2 - m^2 + i0^+]}.
\end{aligned}$$

For integrals with three internal lines we assume on-shell kinematics, $p_f^2 = p_i^2 = m_N^2$,

$$\begin{aligned}
&I_{\pi\pi N}(q^2) \\
&\quad = i \int \frac{d^n k}{(2\pi)^n} \frac{1}{[k^2 - M^2 + i0^+][(k+q)^2 - M^2 + i0^+][(k+p_i)^2 - m^2 + i0^+]},
\end{aligned}$$

$$
\begin{aligned}
&I_{\pi NN}(q^2) \\
&\quad = i\int \frac{d^n k}{(2\pi)^n} \frac{1}{[k^2-M^2+i0^+][(k+p_i)^2-m^2+i0^+][(k+p_f)^2-m^2+i0^+]}, \\
&P^\mu I^{(P)}_{\pi NN}(q^2) \\
&\quad = i\int \frac{d^n k}{(2\pi)^n} \frac{k^\mu}{[k^2-M^2+i0^+][(k+p_i)^2-m^2+i0^+][(k+p_f)^2-m^2+i0^+]}, \\
&g^{\mu\nu} I^{(00)}_{\pi NN}(q^2) + P^\mu P^\nu I^{(PP)}_{\pi NN}(q^2) + q^\mu q^\nu I^{(qq)}_{\pi NN}(q^2) \\
&\quad = i\int \frac{d^n k}{(2\pi)^n} \frac{k^\mu k^\nu}{[k^2-M^2+i0^+][(k+p_i)^2-m^2+i0^+][(k+p_f)^2-m^2+i0^+]}.
\end{aligned}
$$

The tensorial loop integrals can be reduced to scalar ones [PV 79] and we obtain

$$
\begin{aligned}
I^{(00)}_\pi &= \frac{M^2}{n} I_\pi, \\
I^{(0000)}_\pi &= \frac{M^4}{n(n+2)}\, I_\pi, \\
I^{(p)}_{\pi N}(p^2) &= \frac{1}{2p^2}\left[I_\pi - I_N - (p^2-m^2+M^2) I_{\pi N}(p^2)\right], \\
I^{(00)}_{\pi N}(p^2) &= \frac{1}{2(n-1)}\left[I_N + 2M^2 I_{\pi N}(p^2) + \frac{(p^2-m^2+M^2)}{p^2} I^{(p)}_{\pi N}(p^2)\right], \\
I^{(P)}_{\pi NN}(q^2) &= \frac{1}{4m_N^2-q^2}\left[I_{\pi N}(m_N^2) - I_{NN}(q^2) - M^2 I_{\pi NN}(q^2)\right], \\
I^{(00)}_{\pi NN}(q^2) &= \frac{1}{n-2}\left\{\left[I_{\pi NN}(q^2) + I^{(P)}_{\pi NN}(q^2)\right] M^2 + \frac{1}{2} I_{NN}(q^2)\right\}, \\
I^{(PP)}_{\pi NN}(q^2) &= \frac{1}{(n-2)(4m_N^2-q^2)}\left\{\left[(n-1) I^{(P)}_{\pi NN}(q^2) + I_{\pi NN}(q^2)\right] M^2\right. \\
&\quad \left. -\frac{n-2}{2} I^{(p)}_{\pi N}(m_N^2) - \frac{n-3}{2} I_{NN}(q^2)\right\}, \\
I^{(qq)}_{\pi NN}(q^2) &= -\frac{1}{(n-2)q^2}\left\{\left[I^{(P)}_{\pi NN}(q^2) + I_{\pi NN}(q^2)\right] M^2 + \frac{n-2}{2} I^{(p)}_{\pi N}(m_N^2) + \frac{1}{2} I_{NN}(q^2)\right\}.
\end{aligned}
$$

Defining

$$
\bar{\lambda} = \frac{m^{n-4}}{16\pi^2}\left\{\frac{1}{n-4} - \frac{1}{2}\left[\ln(4\pi) - \gamma_E + 1\right]\right\},
$$

where $\gamma_E = \Gamma'(1)$ is Euler's constant, and

$$
\Omega = \frac{p^2-m^2-M^2}{2mM},
$$

the scalar loop integrals are given by [Fuc+ 03a]

$$
\begin{aligned}
I_\pi &= 2M^2\bar{\lambda} + \frac{M^2}{8\pi^2}\ln\left(\frac{M}{m}\right), \\
I_N &= 2m^2\bar{\lambda}, \\
I_{\pi\pi}(q^2) &= 2\bar{\lambda} + \frac{1}{16\pi^2}\left[1 + 2\ln\left(\frac{M}{m}\right) + J^{(0)}\left(\frac{q^2}{M^2}\right)\right], \\
I_{NN}(q^2) &= 2\bar{\lambda} + \frac{1}{16\pi^2}\left[1 + J^{(0)}\left(\frac{q^2}{m^2}\right)\right] \\
I_{\pi N}(p^2) &= 2\bar{\lambda} + \frac{1}{16\pi^2}\left[-1 + \frac{p^2 - m^2 + M^2}{p^2}\ln\left(\frac{M}{m}\right) + \frac{2mM}{p^2}F(\Omega)\right],
\end{aligned}
$$

where

$$
\begin{aligned}
J^{(0)}(x) &= \int_0^1 dz \ln[1 + x(z^2 - z) - i0^+] \\
&= \begin{cases} -2 - \sigma\ln\left(\frac{\sigma-1}{\sigma+1}\right), & x < 0, \\ -2 + 2\sqrt{\frac{4}{x} - 1}\,\mathrm{arccot}\left(\sqrt{\frac{4}{x} - 1}\right), & 0 \le x < 4, \\ -2 - \sigma\ln\left(\frac{1-\sigma}{1+\sigma}\right) - i\pi\sigma, & 4 < x, \end{cases}
\end{aligned}
$$

with

$$
\sigma(x) = \sqrt{1 - \frac{4}{x}}, \quad x \notin [0, 4],
$$

and

$$
F(\Omega) = \begin{cases} \sqrt{\Omega^2 - 1}\ln\left(-\Omega - \sqrt{\Omega^2 - 1}\right), & \Omega \le -1, \\ \sqrt{1 - \Omega^2}\arccos(-\Omega), & -1 \le \Omega \le 1, \\ \sqrt{\Omega^2 - 1}\ln\left(\Omega + \sqrt{\Omega^2 - 1}\right) - i\pi\sqrt{\Omega^2 - 1}, & 1 \le \Omega. \end{cases}
$$

Integrals with three propagators are analyzed numerically using a Schwinger parametrization.

For purely mesonic integrals only the terms proportional to $\bar{\lambda}$ have to be subtracted. To determine the infrared regular parts R of the scalar loop integrals, we use the reformulated version of infrared regularization described in Chapter 3. On-shell-kinematics are assumed for the subtraction terms. Note that we also list divergent terms, as they might give finite contributions in the expressions for tensor integrals when multiplied by terms depending on $\epsilon = (n-4)/2$,

$$
\begin{aligned}
R_N &= I_N, \\
R_{NN} &= I_{NN}, \\
R_{\pi N} &= \bar{\lambda}\left[2 - \frac{M^2}{m^2}(1 - 8c_1 m) + \frac{3g_A^2 M^3}{16\pi F^2 m}\right] - \frac{1}{16\pi^2} - \frac{M^2}{32\pi^2 m^2}(3 + 8c_1 m) \\
&\quad - \frac{3g_A^2 M^3}{512\pi^3 F^2 m} + \mathcal{O}(q^4),
\end{aligned}
$$

$$
R_{\pi NN} = \frac{\bar{\lambda}}{m^2}\left[1 + \frac{q^2}{6m^2} + 8c_1\frac{M^2}{m} + \frac{3g_A^2 M^3}{16\pi F^2 m}\right] + \frac{1}{32\pi^2 m^2} - \frac{M^2}{32\pi^2 m^4}(1 - 16c_1 m)
+ \frac{3g_A^2 M^3}{256\pi^3 F^2 m^3} + \mathcal{O}(q^4).
$$

B.2 Integrals at the two-loop level

In addition to the integrals in the previous section, the calculation of the nucleon mass at the two-loop level requires further integrals. We define the one-loop integral

$$
J_{\pi N}(a,b|n) = \int \frac{d^n k}{(2\pi)^n} \frac{1}{[k^2 - M^2 + i0^+]^a [k^2 + 2p\cdot k + i0^+]^b}.
$$

Note that we have not included a factor i in the definition, since the one-loop integrals $J_{\pi N}(a,b|n)$ always appear in the product $J_{\pi N}(a_1,b_1|n_1)J_{\pi N}(a_2,b_2|n_2)$.

The two-loop integrals $J_2(a,b,c,d,e|n)$ are defined as

$$
J_2(a,b,c,d,e|n) = \iint \frac{d^n k_1 d^n k_2}{(2\pi)^{2n}} \frac{1}{A^a B^b C^c D^d E^e},
$$

where

$$
\begin{aligned}
A &= k_1^2 - M^2 + i0^+, \\
B &= k_2^2 - M^2 + i0^+, \\
C &= k_1^2 + 2p\cdot k_1 + i0^+, \\
D &= k_2^2 + 2p\cdot k_2 + i0^+, \\
E &= k_1^2 + 2p\cdot k_1 + 2k_1\cdot k_2 + 2p\cdot k_2 + k_2^2 + i0^+.
\end{aligned}
$$

The product of two one-loop integrals with the same space-time dimension n can then be written as

$$
J_{\pi N}(a_1,b_1|n)J_{\pi N}(a_2,b_2|n) = J_2(a_1,a_2,b_1,b_2,0|n).
$$

We do not attempt to evaluate the integrals $J_2(a,b,c,d,e|n)$ here. Instead the expressions for the renormalized integrals relevant to the nucleon mass including the corresponding counterterm contributions are given in App. D.

Tensorial integrals have been reduced to scalar ones in the same dimension using methods similar to the one-loop integrals, or the following relations to scalar integrals in higher dimensions have been used:

$$
\begin{aligned}
J_2^{\mu,}(a,b,c,d,e|n) &= \iint \frac{d^n k_1 d^n k_2}{(2\pi)^{2n}} \frac{k_1^\mu}{A^a B^b C^c D^d E^e} \\
&= -16\pi^2 p^\mu \Big[b\,c\,J_2(a,b+1,c+1,d,e|n+2) + c\,d\,J_2(a,b,c+1,d+1,e|n+2) \\
&\quad + c\,e\,J_2(a,b,c+1,d,e+1|n+2) + b\,e\,J_2(a,b+1,c,d,e+1|n+2)\Big],
\end{aligned}
$$

$$
\begin{aligned}
& J_2^{\mu\nu,}(a,b,c,d,e|n) \\
&= \iint \frac{d^n k_1 d^n k_2}{(2\pi)^{2n}} \frac{k_1^\mu k_1^\nu}{A^a B^b C^c D^d E^e} \\
&= \frac{(4\pi)^2}{2} g^{\mu\nu} \left[b\, J_2(a,b+1,c,d,e|n+2) + d\, J_2(a,b,c,d+1,e|n+2) \right. \\
&\quad \left. + e\, J_2(a,b,c,d,e+1|n+2) \right] + \mathcal{O}(p), \\
& J_2^{\mu\nu\lambda,}(a,b,c,d,e|n) = \iint \frac{d^n k_1 d^n k_2}{(2\pi)^{2n}} \frac{k_1^\mu k_1^\nu k_1^\lambda}{A^a B^b C^c D^d E^e} \\
&= -\frac{(4\pi)^4}{2} \left[g^{\mu\nu} p^\lambda + g^{\mu\lambda} p^\nu + g^{\nu\lambda} p^\mu \right] \left[b\,(b+1)\, c\, J_2(a,b+2,c+1,d,e|n+4) \right. \\
&\quad \left. + b\,(b+1)\, e\, J_2(a,b+2,c,d,e+1|n+4) \right] + \mathcal{O}(p^3), \\
& J_2^{\mu,\nu}(a,b,c,d,e|n) = \iint \frac{d^n k_1 d^n k_2}{(2\pi)^{2n}} \frac{k_1^\mu k_2^\nu}{A^a B^b C^c D^d E^e} \\
&= -\frac{(4\pi)^2}{2} g^{\mu\nu}\, e\, J_2(a,b,c,d,e+1|n+2) + \mathcal{O}(p), \\
& J_2^{\mu,\alpha\beta}(a,b,c,d,e|n) = \iint \frac{d^n k_1 d^n k_2}{(2\pi)^{2n}} \frac{k_1^\mu k_2^\alpha k_2^\beta}{A^a B^b C^c D^d E^e} \\
&= -\frac{(4\pi)^2}{2} g^{\alpha\beta} p^\mu \left[c\, J_2(a,b,c+1,d,e|n+2) + e\, J_2(a,b,c,d,e+1|n+2) \right] \\
&\quad + \frac{(4\pi)^4}{2} \left[g^{\alpha\beta} p^\mu + g^{\mu\alpha} p^\beta + g^{\mu\beta} p^\alpha \right] \left[a\, e\,(e+1)\, J_2(a+1,b,c,d,e+2|n+4) \right. \\
&\quad + a\, d\, e\, J_2(a+1,b,c,d+1,e+1|n+4) \\
&\quad + c\, d\, e\, J_2(a,b,c+1,d+1,e+1|n+4) \\
&\quad \left. + d\, e\,(e+1)\, J_2(a,b,c,d+1,e+2|n+4) \right] + \mathcal{O}(p^3), \\
& J_2^{\alpha\beta,\mu\nu}(a,b,c,d,e|n) = \iint \frac{d^n k_1 d^n k_2}{(2\pi)^{2n}} \frac{k_1^\alpha k_1^\beta k_2^\mu k_2^\nu}{A^a B^b C^c D^d E^e} \\
&= \frac{(4\pi)^4}{4} \left[g^{\alpha\beta} g^{\mu\nu} + g^{\alpha\mu} g^{\beta\nu} + g^{\alpha\nu} g^{\beta\mu} \right] e\,(e+1)\, J_2(a,b,c,d,e+2|n+4) \\
&\quad + \frac{(4\pi)^2}{4} g^{\alpha\beta} g^{\mu\nu} J_2(a,b,c,d,e|n+2) + \mathcal{O}(p).
\end{aligned}
$$

Here, $\mathcal{O}(p)$ stands for terms proportional to p^ρ, where ρ denotes the Lorentz index corresponding to the integral under consideration. These terms appear in combination with expressions like $(\not{p}-m)\gamma_\rho(\not{p}+m)$, resulting in higher-order contributions to the nucleon mass that are not considered. As an example we show how to obtain the first of the previous relations. One uses a Schwinger parametrization to rewrite the scalar integral as

$$
J_2(a,b,c,d,e|n) = \frac{1}{(2\pi)^{2n}} \int \prod_{i=1}^{5} dx_i \frac{i^{-\alpha_i}}{\Gamma[\alpha_i]} x_i^{\alpha_i - 1} \iint d^n k_1 d^n k_2\, e^{f(x_j,k_1,k_2,p,M)}, \quad \text{(B.1)}
$$

where $\alpha_1 = a, \ldots, \alpha_5 = e$ and $f(x_j, k_1, k_2, p, M)$ is a function of the Schwinger parameters, the loop momenta, the external nucleon momentum and the pion mass.

Subsequently performing the integrations over the two loop momenta, using

$$\int d^n k\, e^{iAk^2-2iB\cdot k} = i^{1-n/2}\pi^{n/2}A^{-n/2}e^{-iB^2/A}, \tag{B.2}$$

leads to

$$J_2(a,b,c,d,e|n) = \frac{i^{2-n}\pi^n}{(2\pi)^{2n}}\int\prod dx_i\frac{i^{-\alpha_i}}{\Gamma[\alpha_i]}\,x_i^{\alpha_i-1}A_1^{-n/2}A_2^{-n/2}e^{g(x_j,p,M)}, \tag{B.3}$$

where A_1 and A_2 are functions of the Schwinger parameters and $g(x_j,p,M)$ is a function of the Schwinger parameters, the external momentum and the pion mass. In order to relate the vector integral to scalar integrals one performs similar steps, writing

$$J_2^{\mu,}(a,b,c,d,e|n) = \frac{1}{(2\pi)^{2n}}\int\prod dx_i\frac{i^{-\alpha_i}}{\Gamma[\alpha_i]}\,x_i^{\alpha_i-1}\iint d^nk_1d^nk_2\,k_1^{\mu}e^{f(x_j,k_1,k_2,p,M)}. \tag{B.4}$$

The integration over loop momenta can again be performed, using

$$\int d^n k\, k^\mu e^{iAk^2-2iB\cdot k} = i^{1-n/2}\pi^{n/2}B^\mu A^{-(n+2)/2}e^{-iB^2/A}, \tag{B.5}$$

which can be obtained by differentiating Eq. (B.2) with respect to B^μ. The result reads

$$\begin{aligned}J_2^{\mu,}(a,b,c,d,e|n) = p^\mu\frac{i^{2-n}\pi^n}{(2\pi)^{2n}}\int\prod dx_i\frac{i^{-\alpha_i}}{\Gamma[\alpha_i]}\,x_i^{\alpha_i-1}(-x_2x_3-x_2x_5-x_3x_4-x_3x_5)\\ A_1^{-(n+2)/2}A_2^{-(n+2)/2}e^{g(x_j,p,M)}.\end{aligned} \tag{B.6}$$

The function $g(x_j,p,M)$ and the A_i are the same as the ones appearing in Eq. (B.3). Including the appropriate factors of $2i\pi$ one can therefore write Eq. (B.6) as the sum of scalar integrals in $n{+}2$ dimensions with different coefficients α_i. All other relations can be obtained analogously.

Appendix C

Dimensional counting analysis

Analytic expressions for two-loop integrals, especially when two mass scales such as the pion mass M and the nucleon mass in the chiral limit m appear in the same integral, can be extremely difficult to obtain. Since we are interested in the chiral expansion of the considered integrals in the present work, we do not have to find a closed-form solution to the appearing integrals, but can use a method called dimensional counting analysis [GJT 94] for the evaluation of integrals. A closely related way of calculating loop integrals is the so-called "strategy of regions" [Smi 02]. Here we present an illustration of dimensional counting for one- and two-loop integrals.

C.1 One-loop integrals

The advantage of dimensional counting analysis for one-loop integrals lies in its applicability to dimensionally regulated integrals containing several different masses. Consider integrals with two different mass scales, M and m, where $M < m$, and a possible external momentum p with $p^2 \approx m^2$. Dimensional counting provides a method to reproduce the expansion of the integral for small values of M at fixed $p^2 - m^2$. To that end one rescales the loop momentum $k \mapsto M^{\alpha_i}\tilde{k}$, where α_i is a non-negative real number. After extracting an overall factor of M one expands the integrand in positive powers of M and interchanges summation and integration. The sum of all possible rescalings with subsequent expansions with nontrivial coefficients then reproduces the expansion of the result of the original integral.

To be specific, consider the integral

$$I_{\pi N}(p^2) = \frac{i}{(2\pi)^n} \int \frac{d^n k}{(k^2 - M^2 + i0^+)[(k+p)^2 - m^2 + i0^+]}. \tag{C.1}$$

It can be evaluated analytically and the result is given in App. B. After rescaling one obtains

$$I_{\pi N}(p^2) \mapsto \frac{i}{(2\pi)^n} \int \frac{M^{n\alpha_i} d^n \tilde{k}}{[\tilde{k}^2 M^{2\alpha_i} - M^2 + i0^+][\tilde{k}^2 M^{2\alpha_i} + 2p\cdot\tilde{k}M^{\alpha_i} + p^2 - m^2 + i0^+]}. \tag{C.2}$$

No overall factor of M can be extracted from the second propagator, which is therefore expanded in positive powers of M. As a result the integration variable $\tilde{k}$ only appears in positive powers in the expanded expression of this propagator. If $0 < \alpha_i < 1$ one can extract the factor $M^{-2\alpha_i}$ from the first propagator, which takes the form

$$\frac{1}{\tilde{k}^2 - M^{2-2\alpha_i} + i0^+} \,. \tag{C.3}$$

Expanding in positive powers of M and interchanging summation and integration one obtains integrals of the type

$$\int d^n\tilde{k} \frac{1}{(\tilde{k}^2 + i0^+)^j} \,. \tag{C.4}$$

Combined with the expansion of the second propagator the resulting coefficients in the expansion in M are integrals of the type

$$\int d^n\tilde{k} \frac{\tilde{k}^m}{(\tilde{k}^2 + i0^+)^j} \,, \tag{C.5}$$

which vanish in dimensional regularization. For the case $1 < \alpha_i$ the first propagator in Eq. (C.2) can be rewritten as

$$\frac{1}{M^2} \, \frac{1}{(\tilde{k}^2 M^{2\alpha_i - 2} - 1 + i0^+)} \,. \tag{C.6}$$

Expanding in M and combining with the expansion of the second propagator one obtains integrals of the type

$$\int d^n\tilde{k} \, \tilde{k}^j \,, \tag{C.7}$$

which, again, vanish in dimensional regularization. The only contributions to $I_{\pi N}(p^2)$ can therefore stem from $\alpha_i = 0$ and $\alpha_i = 1$. For $\alpha_i = 0$ one obtains

$$I^{(0)}_{\pi N}(p^2) = \frac{i}{(2\pi)^n} \sum_{i=0}^{\infty} \left(M^2\right)^i \int \frac{d^n k}{[k^2 + i0^+]^{1+i}[(k+p)^2 - m^2 + i0^+]} \,, \tag{C.8}$$

while the expression for $\alpha_i = 1$ reads

$$I^{(1)}_{\pi N}(p^2) = \frac{i}{(2\pi)^n} \sum_{i=0}^{\infty} (-1)^i \frac{M^{n-2+i}}{(p^2 - m^2)^{1+i}} \int \frac{d^n\tilde{k}(\tilde{k}^2 M + 2p \cdot \tilde{k})^i}{[\tilde{k}^2 - 1 + i0^+]} . \tag{C.9}$$

The expansion of $I_{\pi N}(p^2)$ is then given by

$$I_{\pi N}(p^2) = I^{(0)}_{\pi N}(p^2) + I^{(1)}_{\pi N}(p^2), \tag{C.10}$$

which correctly reproduces the result of App. B.

C.2 Two-loop integrals

While one of the advantages of the dimensional counting method lies in its applicability to integrals containing several mass scales, a difficulty arises for the calculation of the nucleon mass. Since integrals have to be evaluated on-mass-shell, the two small scales M and $p^2 - m^2$ are not independent of each other and are comparable in size. Therefore an expansion in $\frac{M}{p^2-m^2}$ does not converge. By the choice of the nucleon propagator mass to include all contact interaction contributions (see Chapter 6), the terms $p^2 - m^2$ in the propagator can be neglected in two-loop integrals since they are of higher order in the loop expansion. The two-loop integrals contributing to the nucleon mass are therefore reduced to integrals with only one small mass scale, for which an expansion in M can be obtained.

For the extension of the dimensional counting method to two-loop integrals $J_2(a, b, c, d, e|n)$,

$$
\begin{aligned}
J_2(a,b,c,d,e|n) &= \iint \frac{d^n k_1 d^n k_2}{(2\pi)^{2n}} \frac{1}{[k_1^2 - M^2 + i0^+]^a [k_2^2 - M^2 + i0^+]^b} \\
&\times \frac{1}{[k_1^2 + 2p\cdot k_1 + i0^+]^c [k_2^2 + 2p\cdot k_2 + i0^+]^d [(k_1+k_2)^2 + 2p\cdot k_1 + 2p\cdot k_2 + i0^+]^e}\,,
\end{aligned}
\tag{C.11}
$$

one has to consider all possible combinations of rescaling the integration variables $k_1 \mapsto M^{\alpha_i}\tilde{k}_1$, $k_2 \mapsto M^{\beta_i}\tilde{k}_2$. The expansion of the two-loop integral is then given by

$$
J_2(a,b,c,d,e|n) = \sum_{\alpha_i,\beta_i} M^{\varphi(\alpha_i,\beta_i)} f_{\alpha_i,\beta_i}(p^2, m^2, M, n), \tag{C.12}
$$

where $\varphi(\alpha_i, \beta_i)$ is the overall power of M extracted for each rescaling and the functions $f_{\alpha_i,\beta_i}(p^2, m^2, M, n)$ are the expressions for the integrated expansions. Following the discussion of the one-loop sector one sees that the only combinations (α_i, β_i) that give non-vanishing contributions are $(0, 0)$, $(1, 0)$, $(0, 1)$ and $(1, 1)$. The corresponding contributions are denoted by F_1, F_2, F_3 and F_4, respectively, so that a two-loop integral is given by

$$
J_2(a,b,c,d,e|n) = F_1 + F_2 + F_3 + F_4. \tag{C.13}
$$

From a technical point of view it is convenient to consider the rescaling $k_1 \mapsto (M/m)^{\alpha_i}\tilde{k}_1$, $k_2 \mapsto (M/m)^{\beta_i}\tilde{k}_2$, since then the integration variables $\tilde{k}$ have dimension of momenta. This also facilitates the evaluation of certain loop integrals appearing in the calculation of the nucleon mass.

As an example consider the integral $J_2(1, 1, 1, 1, 1|n)$. For $(0, 0)$ the resulting integrals read

$$
\begin{aligned}
F_1 = J_2^{(0,0)}(1,1,1,1,1|n) &= \sum_{i,j} M^{2i+2j} \iint \frac{d^n k_1 d^n k_2}{(2\pi)^{2n}} \frac{1}{[k_1^2 + i0^+]^{1+i} [k_2^2 + i0^+]^{1+j}} \\
&\times \frac{1}{[k_1^2 + 2p\cdot k_1 + i0^+][k_2^2 + 2p\cdot k_2 + i0^+][(k_1+k_2)^2 + 2p\cdot k_1 + 2p\cdot k_2 + i0^+]}\,.
\end{aligned}
\tag{C.14}
$$

While still a two-loop integral that does not directly factorize into the product of one-loop integrals, the vanishing of the mass scale M simplifies the evaluation of the integral. The rescaling of only k_1 leads to

$$F_2 = J_2^{(1,0)}(1,1,1,1,1|n) = \sum_{i,j,l}(-1)^{j+l}M^{n-3+2i+j+l}m^{3-n-j-l}\iint\frac{d^n\tilde{k}_1 d^n k_2}{(2\pi)^{2n}}$$
$$\times\frac{(\tilde{k}_1^2)^j(\frac{M}{m}\tilde{k}_1^2+2p\cdot\tilde{k}_1+2\tilde{k}_1\cdot k_2)^l}{[\tilde{k}_1^2-m^2+i0^+][k_2^2+i0^+]^{1+i}[2p\cdot\tilde{k}_1+i0^+]^{1+i}[k_2^2+2p\cdot k_2+i0^+]^{2+l}}, \tag{C.15}$$

while the expression for F_3 can be obtained by substituting $\tilde{k}_1 \mapsto \tilde{k}_2$ and $k_2 \mapsto k_1$ in Eq. (C.15). One sees that the integrals of Eq. (C.15) can be reduced to the product of tensorial one-loop integrals, which is a considerable simplification compared to the original integral. The last contribution stems from $\alpha_i = 1$, $\beta_i = 1$ and reads

$$F_4 = J_2^{(1,1)}(1,1,1,1,1|n) =$$
$$\sum_{i,j,l}(-1)^{i+j+l}\left(\frac{M}{m}\right)^{2n-7+i+j+l}\iint\frac{d^n\tilde{k}_1 d^n\tilde{k}_2}{(2\pi)^{2n}}\frac{1}{[\tilde{k}_1^2-m^2+i0^+][\tilde{k}_2^2-m^2+i0^+]}$$
$$\times\frac{(\tilde{k}_1^2)^i(\tilde{k}_2^2)^j(\tilde{k}_1^2+2\tilde{k}_1\cdot\tilde{k}_2+\tilde{k}_2^2)^l}{[2p\cdot\tilde{k}_1+i0^+]^{1+i}[2p\cdot\tilde{k}_2+i0^+]^{1+j}[2p\cdot\tilde{k}_1+2p\cdot\tilde{k}_2+i0^+]^{1+l}}, \tag{C.16}$$

where the integration can be reduced to the evaluation of a set of basis integrals (see App. D). The sum of all four contributions reproduces the M expansion of the integral $J_2(1,1,1,1,1|n)$,

$$\begin{aligned} J_2(1,1,1,1,1|n) &= J_2^{(0,0)}(1,1,1,1,1|n) + J_2^{(1,0)}(1,1,1,1,1|n) + J_2^{(0,1)}(1,1,1,1,1|n) \\ &\quad + J_2^{(1,1)}(1,1,1,1,1|n). \end{aligned} \tag{C.17}$$

Appendix D

Evaluation of two-loop integrals

As seen in Chapter 5 the calculation of the two-loop integrals relevant to the nucleon mass reduces to the evaluation of the F_4 part of the respective integrals. The F_4 parts are sums of tensor integrals, which can be reduced to scalar integrals [PV 79] of the form

$$J_2^{(1,1)}(a,b,c,d,e|n) = \iint \frac{d^nk_1 d^nk_2}{(2\pi)^{2n}} \frac{1}{[k_1^2-m^2+i0^+]^a[k_2^2-m^2+i0^+]^b[2p\cdot k_1+i0^+]^c} \times \frac{1}{[2p\cdot k_2+i0^+]^d[2p\cdot k_1+2p\cdot k_2+i0^+]^e}\,, \tag{D.1}$$

where the superscript $(1,1)$ indicates that these integrals have been obtained after rescaling both integration variables (see App. C) and a,b,c,d,e are integers. Depending on the values of the exponents c, d, and e, one can evaluate $J_2^{(1,1)}(a,b,c,d,e|n)$ with the help of several basic integrals.

D.1 $e = 0$

If the exponent e vanishes, the integral can be written as the product of one-loop integrals,

$$J_2^{(1,1)}(a,b,c,d,0|n) = J_1^{(1)}(a,c|n)J_1^{(1)}(b,d|n), \tag{D.2}$$

where

$$\begin{aligned} J_1^{(1)}(a,b|n) &= \int \frac{d^nk}{(2\pi)^n}\frac{1}{[k^2-m^2+i0^+]^a[2p\cdot k+i0^+]^b} \\ &= \frac{i^{1-2a-2b}}{2^b(4\pi)^{n/2}}\frac{\Gamma[\frac{1}{2}]\Gamma[a+\frac{b}{2}-\frac{n}{2}]}{\Gamma[a]\Gamma[\frac{b+1}{2}]}(m^2)^{n/2-a-b/2}(p^2)^{-b/2}\,. \end{aligned} \tag{D.3}$$

D.2 $c = d = 0, e \neq 0$

If $c = d = 0$, the expression for the integral $J_2(a, b, 0, 0, e|n)$ reads

$$\begin{aligned} & J_2^{(1,1)}(a, b, 0, 0, e|n) \\ & = \iint \frac{d^n k_1 d^n k_2}{(2\pi)^{2n}} \frac{1}{[k_1^2 - m^2 + i0^+]^a [k_2^2 - m^2 + i0^+]^b [2p \cdot k_1 + 2p \cdot k_2 + i0^+]^e} \\ & = \frac{i^{2-2a-2b-2e}}{2(4\pi)^n} (m^2)^{n-a-b-e/2} (p^2)^{-e/2} \frac{\Gamma[a + \frac{e}{2} - \frac{n}{2}]\Gamma[b + \frac{e}{2} - \frac{n}{2}]\Gamma[a + b + \frac{e}{2} - n]\Gamma[\frac{e}{2}]}{\Gamma[a]\Gamma[b]\Gamma[e]\Gamma[a + b + e - n]}. \end{aligned} \tag{D.4}$$

D.3 $d = 0,\ c \neq 0,\ e \neq 0$ and $c = 0,\ d \neq 0,\ e \neq 0$

For vanishing d with non-vanishing c and e we consider the integral $J_2^{(1,1)}(a, b, c, 0, e|n)$ for $p^2 = m^2$,

$$\begin{aligned} J_2^{(1,1)}(a, b, c, d, e|n) = & \iint \frac{d^n k_1 d^n k_2}{(2\pi)^{2n}} \frac{1}{[k_1^2 - m^2 + i0^+]^a [k_2^2 - m^2 + i0^+]^b [2p \cdot k_1 + i0^+]^c} \\ & \times \left. \frac{1}{[2p \cdot k_2 + i0^+]^d [2p \cdot k_1 + 2p \cdot k_2 + i0^+]^e} \right|_{p^2 = m_N^2} . \end{aligned} \tag{D.5}$$

Note that the mass terms m in the first two propagators stem from the rescaling of the loop momenta, while we have to consider $p^2 = m_N^2$ when evaluating the nucleon mass. In the calculations performed in this work the difference between $p^2 = m^2$ and $p^2 = m_N^2$ in these integrals is of higher order.

The result for $J_2^{(1,1)}(a, b, c, 0, e|n)$ is given by the sum

$$J_2^{(1,1)}(a, b, c, 0, e|n) = \sum_{l=0}^{c-1} \binom{c-1}{l} (-1)^l Z_{(c+l-2)/2}(a, b, c, 0, e|n), \tag{D.6}$$

where

$$\begin{aligned} Z_\alpha(a, b, c, 0, e|n) = & \frac{i^{2-2a-2b-2c-2e}}{(4\pi)^n} m^{2n-2a-2b-2c-2e} \frac{\Gamma[\alpha + 1]}{\Gamma[\alpha + 2]} \\ & \times \frac{\Gamma[a + \frac{c}{2} + \frac{e}{2} - \frac{n}{2}]\Gamma[b + \frac{c}{2} + \frac{e}{2} - \frac{n}{2}]\Gamma[\frac{c}{2} + \frac{e}{2}]\Gamma[a + b + \frac{c}{2} + \frac{e}{2} - n]}{\Gamma[a]\Gamma[b]\Gamma[c]\Gamma[e]\Gamma[a + b + c + e - n]} \\ & \times {}_3F_2 \left(\left. \begin{matrix} 1, c/2 + e/2, a + c/2 + e/2 - n/2 \\ \alpha + 2, a + b + c + e - n \end{matrix} \right| 1 \right) \end{aligned} \tag{D.7}$$

and ${}_3F_2 \left(\left. \begin{smallmatrix} a,b,c \\ d,e \end{smallmatrix} \right| z \right)$ is a hypergeometric function (see Appendix E). The case $c = 0$, $d \neq 0$, $e \neq 0$ is obtained by replacing c with d and interchanging a and b in Eq. (D.7).

D.4 $c \neq 0,\ d \neq 0,\ e \neq 0$

For the case that none of the exponents c, d, e vanishes, it is convenient to perform an expansion into partial fractions,

$$\begin{aligned}
&\frac{1}{[2p\cdot k_2 + i0^+][2p\cdot k_1 + 2p\cdot k_2 + i0^+]} \\
&\quad = \frac{1}{[2p\cdot k_1 + i0^+][2p\cdot k_2 + i0^+]} - \frac{1}{[2p\cdot k_1 + i0^+][2p\cdot k_1 + 2p\cdot k_2 + i0^+]}\,,
\end{aligned} \tag{D.8}$$

until one obtains a sum of integrals of the form $J_2^{(1,1)}(a,b,\tilde{c},0,\tilde{e})$ and $J_2^{(1,1)}(a,b,\tilde{c},\tilde{d},0)$, which are evaluated as described above.

D.5 Subtraction terms

In addition to the integrals given above the evaluation of the subintegrals for the F_4 terms requires the integrals

$$J_1^{(1,1)}(a,b;\omega|n) = \int \frac{d^n k}{(2\pi)^n} \frac{1}{[k^2 - m^2 + i0^+]^a [2p\cdot k + \omega + i0^+]^b}\,, \tag{D.9}$$

where $\omega = 2p\cdot q$ with q the second loop momentum. The integral $J_1^{1,1}(a,b;\omega|n)$ is given by the sum

$$\begin{aligned}
&J_1^{(1,1)}(a,b;\omega|n) \\
&\quad = \frac{i^{1-2a-2b} m^{n-2a-2b}}{(4\pi)^{n/2}} \sum_{l=0}^{\infty} \frac{\Gamma[\frac{b}{2}+\frac{l}{2}]\Gamma[a+\frac{b}{2}-\frac{n}{2}+\frac{l}{2}]}{2\Gamma[a]\Gamma[b]\Gamma[l+1]} \left(\frac{\omega}{m^2}\right)^l \left(\frac{m^2}{p^2}\right)^{b/2+l/2}.
\end{aligned} \tag{D.10}$$

The sum contains an infinite number of terms. However, when performing the second loop integration over q in the considered counterterm integrals, increasing orders of $\omega = 2p\cdot q$ contribute to increasing chiral orders. Therefore only a finite number of terms in Eq. (D.10) is needed in the calculation of the nucleon mass.

D.6 Results for $J_2^{(1,1)}(a,b,c,d,e|n)$ and counterterm integrals

The results for the $J_2^{(1,1)}$ parts of the two-loop integrals contributing to the nucleon mass evaluated on-mass-shell are given by

$$\begin{aligned}
&\tilde{\mu}^{8-2n} J_2^{(1,1)}(1,1,0,0,1|n) \\
&\quad = -\frac{1}{\epsilon^2}\frac{3M^4}{1024\pi^4 m^2} - \frac{1}{\epsilon}\frac{M^4}{1024\pi^4 m^2}\left[1 + 12\ln\frac{M}{\mu}\right] - \frac{M^4}{2048\pi^4 m^2}\left[\pi^2 + 10\right.
\end{aligned}$$

$$+8\ln\frac{M}{\mu}+48\ln^2\frac{M}{\mu}\Bigg],$$

$$\tilde{\mu}^{8-2n}J_2^{(1,1)}(1,1,0,0,2|n+2)$$
$$=\frac{1}{\epsilon^2}\frac{M^6}{24576\pi^6m^2}-\frac{1}{\epsilon}\frac{M^6}{36864\pi^6m^2}\left[1-6\ln\frac{M}{\mu}\right]+\frac{M^6}{442368\pi^6m^2}\Bigg[3\pi^2$$
$$+26-48\ln\frac{M}{\mu}+144\ln^2\frac{M}{\mu}\Bigg],$$

$$\tilde{\mu}^{8-2n}J_2^{(1,1)}(1,2,0,0,2|n+2)$$
$$=\frac{1}{\epsilon^2}\frac{M^4}{16384\pi^6m^2}+\frac{1}{\epsilon}\frac{M^4}{4096\pi^6m^2}\ln\frac{M}{\mu}+\frac{M^4}{98304\pi^6m^2}\left[\pi^2+6+48\ln^2\frac{M}{\mu}\right],$$

$$\tilde{\mu}^{8-2n}J_2^{(1,1)}(1,1,1,0,2|n+2)$$
$$=-\frac{1}{\epsilon^2}\frac{M^6}{98304\pi^6m^4}+\frac{1}{\epsilon}\left\{\frac{M^5}{12288\pi^5m^3}+\frac{M^6}{147456\pi^6m^4}\left[1-6\ln\frac{M}{\mu}\right]\right\}$$
$$+\frac{M^5}{36864\pi^5m^3}\left[6\ln(2)-5+12\ln\frac{M}{\mu}\right]-\frac{M^6}{1769472\pi^6m^4}\Bigg[75\pi^2+26$$
$$-48\ln\frac{M}{\mu}+144\ln^2\frac{M}{\mu}\Bigg],$$

$$\tilde{\mu}^{8-2n}J_2^{(1,1)}(1,1,2,0,2|n+2)$$
$$=-\frac{1}{\epsilon^2}\frac{5M^4}{98304\pi^6m^4}-\frac{1}{\epsilon}\frac{M^4}{147456\pi^6m^4}\left[1+30\ln\frac{M}{\mu}\right]-\frac{M^4}{1769472\pi^6m^4}\Bigg[87\pi^2$$
$$+82+48\ln\frac{M}{\mu}-720\ln^2\frac{M}{\mu}\Bigg],$$

$$\tilde{\mu}^{8-2n}J_2^{(1,1)}(1,2,1,0,1|n+2)$$
$$=\frac{1}{\epsilon^2}\frac{M^4}{49152\pi^6m^2}-\frac{1}{\epsilon}\frac{M^4}{73728\pi^6m^2}\left[1-6\ln\frac{M}{\mu}\right]-\frac{M^4}{884736\pi^6m^2}\Bigg[69\pi^2-26$$
$$+48\ln\frac{M}{\mu}-144\ln^2\frac{M}{\mu}\Bigg],$$

$$\tilde{\mu}^{8-2n}J_2^{(1,1)}(1,2,2,0,1|n+2)$$
$$=\frac{1}{\epsilon^2}\frac{11M^4}{98304\pi^6m^4}-\frac{1}{\epsilon}\left[\frac{M^3}{12288\pi^5m^3}-\frac{M^4}{73728\pi^6m^4}\left(5+33\ln\frac{M}{\mu}\right)\right]$$
$$+\frac{M^3}{18432\pi^5m^3}\left[1-\ln 8-6\ln\frac{M}{\mu}\right]+\frac{M^4}{1769472\pi^6m^4}\Bigg[190+105\pi^2$$
$$+480\ln\frac{M}{\mu}+1584\ln^2\frac{M}{\mu}\Bigg],$$

$$2\tilde{\mu}^{8-2n}J_2^{(1,1)}(1,2,1,0,3|n+4)+\tilde{\mu}^{8-2n}J_2^{(1,1)}(12202|n+4)$$
$$=-\frac{1}{\epsilon^2}\frac{M^6}{786432\pi^8m^4}+\frac{1}{\epsilon}\frac{M^6}{1179648\pi^8m^4}\left[1-6\ln\frac{M}{\mu}\right]-\frac{M^6}{14155776\pi^8m^4}\Bigg[3\pi^2$$

$$+26-48\ln\frac{M}{\mu}+144\ln^2\frac{M}{\mu}\Bigg],$$

$$\tilde{\mu}^{8-2n}J_2^{(1,1)}(2,1,1,0,3|n+4)$$
$$=\frac{1}{\epsilon^2}\frac{M^6}{1572864\pi^8m^4}-\frac{1}{\epsilon}\frac{M^6}{2359296}\left[1-6\ln\frac{M}{\mu}\right]+\frac{M^6}{28311552\pi^8m^4}\Bigg[27\pi^2$$
$$+26-48\ln\frac{M}{\mu}+144\ln^2\frac{M}{\mu}\Bigg],$$

$$\tilde{\mu}^{8-2n}J_2^{(1,1)}(1,1,1,1,1|n+2)$$
$$=\frac{1}{\epsilon}\frac{M^5}{6144\pi^5m^3}-\frac{M^5}{18432\pi^5m^3}\left[6\ln(2)-5+12\ln\frac{M}{\mu}\right]-\frac{M^6}{12288\pi^4m^4},$$

where $\tilde{\mu}$ is the 't Hooft parameter [Hoo 73] and we have used $\tilde{\mu}=\frac{\mu}{(4\pi)^{1/2}}e^{\frac{\gamma_E-1}{2}}$. The $\widetilde{\mathrm{MS}}$ scheme of ChPT corresponds to absorbing the quantity $\bar{\lambda}$ defined in App. B and setting $\tilde{\mu}=m$. This is equivalent to subtracting all terms proportional to ϵ^{-1} and setting $\mu=m$. The parameter μ only appears in the logarithm $\ln(M/\mu)$, and replacing μ with $\tilde{\mu}$ leads to

$$\ln\frac{M}{\mu}=\ln\frac{M}{\tilde{\mu}}-\ln\left[(4\pi)^{1/2}e^{\frac{1-\gamma_E}{2}}\right]=\ln\frac{M}{\tilde{\mu}}-\frac{1}{2}\left[\ln(4\pi)-\gamma_E+1\right],$$

where the second term on the right-hand side are just the finite contributions of $\bar{\lambda}$.

The corresponding counterterm integrals $J_{CT_1}^{(1,1)}(a,b,c,d,e)$ and $J_{CT_2}^{(1,1)}(a,b,c,d,e)$ are given by

$$\tilde{\mu}^{8-2n}J_{CT_1}^{(1,1)}(1,1,0,0,1|n)$$
$$=-\frac{1}{\epsilon^2}\frac{3M^4}{1024\pi^4m^2}-\frac{1}{\epsilon}\frac{M^4}{2048\pi^4m^2}\left[1+12\ln\frac{M}{\mu}\right]-\frac{M^4}{4096\pi^4m^2}\Bigg[\pi^2+5+4\ln\frac{M}{\mu}$$
$$+24\ln^2\frac{M}{\mu}\Bigg]$$
$$=\tilde{\mu}^{8-2n}J_{CT_2}^{(1,1)}(1,1,0,0,1|n),$$

$$\tilde{\mu}^{8-2n}J_{CT_1}^{(1,1)}(1,1,0,0,2|n+2)$$
$$=\frac{1}{\epsilon^2}\frac{M^6}{24576\pi^6m^2}-\frac{1}{\epsilon}\frac{M^6}{73728\pi^6m^2}\left[1-6\ln\frac{M}{\mu}\right]+\frac{M^6}{884736\pi^6m^2}\Bigg[3\pi^2+22$$
$$-24\ln\frac{M}{\mu}+72\ln^2\frac{M}{\mu}\Bigg]$$
$$=\tilde{\mu}^{8-2n}J_{CT_2}^{(1,1)}(1,1,0,0,2|n+2),$$

$$\tilde{\mu}^{8-2n}J_{CT_1}^{(1,1)}(1,2,0,0,2|n+2)$$
$$=\frac{1}{\epsilon^2}\frac{M^4}{16384\pi^6m^2}+\frac{1}{\epsilon}\frac{M^4}{32768\pi^6m^2}\left[1+4\ln\frac{M}{\mu}\right]+\frac{M^4}{196608\pi^6m^2}\Bigg[\pi^2+3+12\ln\frac{M}{\mu}$$
$$+24\ln^2\frac{M}{\mu}\Bigg],$$

$$
\begin{aligned}
&\tilde{\mu}^{8-2n} J^{(1,1)}_{CT_2}(1,2,0,0,2|n+2) \\
&\quad = \frac{1}{\epsilon^2}\frac{M^4}{16384\pi^6 m^2} - \frac{1}{\epsilon}\frac{M^4}{32768\pi^6 m^2}\left[1 - 4\ln\frac{M}{\mu}\right] + \frac{M^4}{196608\pi^6 m^2}\left[\pi^2 + 9 - 12\ln\frac{M}{\mu}\right. \\
&\qquad \left. +24\ln^2\frac{M}{\mu}\right], \\
&\tilde{\mu}^{8-2n} J^{(1,1)}_{CT_1}(1,1,1,0,2|n+2) \\
&\quad = \frac{1}{\epsilon^2}\frac{M^6}{32768\pi^6 m^4} - \frac{1}{\epsilon}\frac{M^6}{589824\pi^6 m^4}\left[11 - 36\ln\frac{M}{\mu}\right] + \frac{M^6}{3538944\pi^6 m^4}\left[9\pi^2 + 91\right. \\
&\qquad \left. -132\ln\frac{M}{\mu} + 216\ln^2\frac{M}{\mu}\right], \\
&\tilde{\mu}^{8-2n} J^{(1,1)}_{CT_2}(1,1,1,0,2|n+2) \\
&\quad = -\frac{1}{\epsilon^2}\frac{5M^6}{98304\pi^6 m^4} + \frac{1}{\epsilon}\left[\frac{M^5}{12288\pi^5 m^3} + \frac{M^6}{589824\pi^6 m^4}\left(31 - 60\ln\frac{M}{\mu}\right)\right] \\
&\qquad - \frac{M^5}{36864\pi^5 m^3}\left[5 - 6\ln 2 - 6\ln^2\frac{M}{\mu}\right] - \frac{M^6}{3538944\pi^6 m^4}\left[15\pi^2 + 179 - 372\ln\frac{M}{\mu}\right. \\
&\qquad \left. +360\ln^2\frac{M}{\mu}\right], \\
&\tilde{\mu}^{8-2n} J^{(1,1)}_{CT_1}(1,2,1,0,1|n+2) \\
&\quad = \frac{1}{\epsilon^2}\frac{5M^4}{49152\pi^6 m^2} + \frac{1}{\epsilon}\frac{M^4}{98304\pi^6 m^2}\left[1 + 20\ln\frac{M}{\mu}\right] + \frac{M^4}{589824\pi^6 m^2}\left[5\pi^2 + 27\right. \\
&\qquad \left. +12\ln\frac{M}{\mu} + 120\ln^2\frac{M}{\mu}\right], \\
&\tilde{\mu}^{8-2n} J^{(1,1)}_{CT_2}(1,2,1,0,1|n+2) \\
&\quad = -\frac{1}{\epsilon^2}\frac{M^4}{16384\pi^6 m^2} + \frac{1}{\epsilon}\frac{M^4}{32768\pi^6 m^2}\left[1 - 4\ln\frac{M}{\mu}\right] - \frac{M^4}{196608\pi^6 m^2}\left[\pi^2 + 9\right. \\
&\qquad \left. -12\ln\frac{M}{\mu} + 24\ln^2\frac{M}{\mu}\right], \\
&\tilde{\mu}^{8-2n} J^{(1,1)}_{CT_1}(1,2,2,0,1|n+2) \\
&\quad = \frac{1}{\epsilon^2}\frac{7M^4}{98304\pi^6 m^4} + \frac{1}{\epsilon}\frac{M^4}{196608\pi^6 m^4}\left[1 + 28\ln\frac{M}{\mu}\right] + \frac{M^4}{1179648\pi^6 m^4}\left[7\pi^2 + 39\right. \\
&\qquad \left. +12\ln\frac{M}{\mu} + 168\ln^2\frac{M}{\mu}\right], \\
&\tilde{\mu}^{8-2n} J^{(1,1)}_{CT_2}(1,2,2,0,1|n+2) \\
&\quad = \frac{1}{\epsilon^2}\frac{5M^4}{32768\pi^6 m^4} - \frac{1}{\epsilon}\left[\frac{M^3}{12288\pi^5 m^3} + \frac{M^4}{1179648\pi^6 m^4}\left(54 - 360\ln\frac{M}{\mu}\right)\right] \\
&\qquad + \frac{M^3}{36864\pi^5 m^3}\left[5 - 6\ln 2 + 6\ln\frac{M}{\mu}\right] + \frac{M^4}{393216\pi^6 m^4}\left[5\pi^2 + 39 - 36\ln\frac{M}{\mu}\right.
\end{aligned}
$$

$$
\begin{aligned}
&\quad +120\ln^2\frac{M}{\mu}\Bigg],\\
&2\tilde{\mu}^{8-2n}J^{(1,1)}_{CT_1}(1,2,1,0,3|n+4)+\tilde{\mu}^{8-2n}J^{(1,1)}_{CT_1}(12202|n+4)\\
&\quad=-\frac{1}{\epsilon^2}\frac{M^6}{786432\pi^8m^4}+\frac{1}{\epsilon}\frac{M^6}{196608\pi^8m^4}\left[1-6\ln\frac{M}{\mu}\right]-\frac{M^6}{28311552\pi^8m^4}\Bigg[3\pi^2+22\\
&\qquad-24\ln\frac{M}{\mu}+72\ln^2\frac{M}{\mu}\Bigg]\\
&\quad=2\tilde{\mu}^{8-2n}J^{(1,1)}_{CT_2}(1,2,1,0,3|n+4)+\tilde{\mu}^{8-2n}J^{(1,1)}_{CT_2}(12202|n+4),\\
&\tilde{\mu}^{8-2n}J^{(1,1)}_{CT_1}(2,1,1,0,3|n+4)\\
&\quad=-\frac{1}{\epsilon^2}\frac{M^6}{4718592\pi^8m^4}+\frac{1}{\epsilon}\frac{M^6}{28311552\pi^8m^4}\left[5-12\ln\frac{M}{\mu}\right]-\frac{M^6}{169869312\pi^8m^4}\Bigg[3\pi^2\\
&\qquad+37-60\ln\frac{M}{\mu}+72\ln^2\frac{M}{\mu}\Bigg],\\
&\tilde{\mu}^{8-2n}J^{(1,1)}_{CT_2}(2,1,1,0,3|n+4)\\
&\quad=\frac{1}{\epsilon^2}\frac{7M^6}{4718592\pi^8m^4}-\frac{1}{\epsilon}\frac{M^6}{28311552\pi^8m^4}\left[17-84\ln\frac{M}{\mu}\right]+\frac{M^6}{169869312\pi^8m^4}\Bigg[21\pi^2\\
&\qquad+169-204\ln\frac{M}{\mu}+504\ln^2\frac{M}{\mu}\Bigg],\\
&\tilde{\mu}^{8-2n}J^{(1,1)}_{CT_1}(1,1,1,1,1|n+2)\\
&\quad=\frac{1}{\epsilon^2}\left[\frac{M^5}{12288\pi^5m^3}+\frac{M^6}{36864\pi^6m^4}\right]-\frac{1}{\epsilon}\frac{M^6}{884736\pi^6m^4}\left[11-48\ln\frac{M}{\mu}\right]\\
&\quad-\frac{M^5}{36864\pi^5m^3}\left[5-6\ln(2)-6\ln\frac{M}{\mu}\right]\\
&\quad=\tilde{\mu}^{8-2n}J^{(1,1)}_{CT_2}(1,1,1,1,1|n+2).
\end{aligned}
$$

The results for the products of one-loop integrals read

$$
\begin{aligned}
&\tilde{\mu}^{8-2n}J_2^{(1,1)}(1,1,0,0,0|n)\\
&\quad=-\frac{1}{\epsilon^2}\frac{M^4}{256\pi^4}-\frac{1}{\epsilon}\frac{M^4}{64\pi^4}\ln\frac{M}{\mu}-\frac{M^4}{1536\pi^4}\left[\pi^2+6+48\ln^2\frac{M}{\mu}\right],\\
&\tilde{\mu}^{8-2n}J_2^{(1,1)}(1,2,0,0,0|n)\\
&\quad=-\frac{1}{\epsilon^2}\frac{M^2}{256\pi^4}-\frac{1}{\epsilon}\frac{M^2}{256\pi^4}\left[1+\ln\frac{M}{\mu}\right]-\frac{M^2}{1536\pi^4}\left[\pi^2+6+24\ln\frac{M}{\mu}+48\ln^2\frac{M}{\mu}\right],\\
&\tilde{\mu}^{8-2n}J_2^{(1,1)}(1,1,1,0,0|n)\\
&\quad=-\frac{1}{\epsilon^2}\frac{M^4}{512\pi^4m^2}-\frac{1}{\epsilon}\left[\frac{M^3}{256\pi^3m}+\frac{M^4}{512\pi^4m^2}\left(1+4\ln\frac{M}{\mu}\right)\right]+\frac{M^3}{256\pi^3m}\Bigg[1-2\ln(2)\\
&\qquad-4\ln\frac{M}{\mu}\Bigg]-\frac{M^4}{3072\pi^4m^2}\left[\pi^2+6+24\ln\frac{M}{\mu}+48\ln^2\frac{M}{\mu}\right],
\end{aligned}
$$

$$
\begin{aligned}
&\tilde{\mu}^{8-2n} J_2^{(1,1)}(1,2,0,1,0|n) \\
&\quad = -\frac{1}{\epsilon^2}\,\frac{M^2}{512\pi^4 m^2} - \frac{1}{\epsilon}\,\left[\frac{M}{512\pi^3 m} + \frac{M^2}{256\pi^4 m^2}\left(1+2\ln\frac{M}{\mu}\right)\right] - \frac{M}{512\pi^3 m}\,[1+2\ln(2) \\
&\qquad +4\ln\frac{M}{\mu}\Big] - \frac{M^2}{3072\pi^4 m^2}\,\left[\pi^2+12+48\ln\frac{M}{\mu}+48\ln^2\frac{M}{\mu}\right], \\
&\tilde{\mu}^{8-2n} J_2^{(1,1)}(2,1,0,2,0|n+2) \\
&\quad = \frac{1}{\epsilon^2}\,\frac{M^4}{8192\pi^6 m^2} + \frac{1}{\epsilon}\,\frac{M^4}{2048\pi^6 m^2}\ln\frac{M}{\mu} + \frac{M^4}{49152\pi^6 m^2}\,\left[\pi^2+6+48\ln^2\frac{M}{\mu}\right], \\
&\tilde{\mu}^{8-2n} J_2^{(1,1)}(1,1,1,1,0|n) \\
&\quad = -\frac{M^2}{256\pi^2 m^2}, \\
&\tilde{\mu}^{8-2n} J_2^{(1,1)}(1,1,1,1,0|n+2) \\
&\quad = -\frac{M^6}{9216\pi^4 m^2}.
\end{aligned}
$$

The integral $J_2^{(1,1)}(1,0,0,0,1|n)$ can be written as $J_2^{(1,1)}(1,0,0,1,0|n)$ by the substitution $k_2 \mapsto k_2 + k_1$, and

$$
J_2^{(1,1)}(1,0,0,1,0|n) = J_1^{(1)}(1,0|n) J_1^{(1)}(0,1|n) = 0,
$$

since the infrared singular part $J_1^{(1)}(01|n)$ of $J_1(01|n) = -iI_N$ vanishes.

The counterterm integrals corresponding to the products of one-loop integrals read

$$
\begin{aligned}
&\tilde{\mu}^{8-2n} J_{CT_1}^{(1,1)}(1,1,0,0,0|n) \\
&\quad = -\frac{1}{\epsilon^2}\frac{M^4}{256\pi^4} - \frac{1}{\epsilon}\frac{M^4}{128\pi^4}\ln\frac{M}{\mu} - \frac{M^4}{3072\pi^4}\left[\pi^2+6+24\ln^2\frac{M}{\mu}\right] \\
&\quad = \tilde{\mu}^{8-2n} J_{CT_2}^{(1,1)}(1,1,0,0,0|n), \\
&\tilde{\mu}^{8-2n} J_{CT_1}^{(1,1)}(1,2,0,0,0|n) \\
&\quad = -\frac{1}{\epsilon^2}\frac{M^2}{256\pi^4} - \frac{1}{\epsilon}\frac{M^2}{256\pi^4}\left[1+2\ln\frac{M}{\mu}\right] - \frac{M^2}{3072\pi^4}\left[\pi^2+6+24\ln\frac{M}{\mu}+24\ln^2\frac{M}{\mu}\right], \\
&\tilde{\mu}^{8-2n} J_{CT_2}^{(1,1)}(1,2,0,0,0|n) \\
&\quad = -\frac{1}{\epsilon^2}\frac{M^2}{256\pi^4} - \frac{1}{\epsilon}\frac{M^2}{128\pi^4}\ln\frac{M}{\mu} - \frac{M^2}{3072\pi^4}\left[\pi^2+6+24\ln^2\frac{M}{\mu}\right], \\
&\tilde{\mu}^{8-2n} J_{CT_1}^{(1,1)}(1,1,1,0,0|n) \\
&\quad = -\frac{1}{\epsilon^2}\frac{M^4}{512\pi^4 m^2} - \frac{1}{\epsilon}\frac{M^4}{256\pi^4 m^2}\ln\frac{M}{\mu} - \frac{M^4}{6144\pi^2 m^2}\left[\pi^2+6+24\ln^2\frac{M}{\mu}\right], \\
&\tilde{\mu}^{8-2n} J_{CT_2}^{(1,1)}(1,1,1,0,0|n) \\
&\quad = -\frac{1}{\epsilon^2}\frac{M^4}{512\pi^4 m^2} - \frac{1}{\epsilon}\left[\frac{M^3}{256\pi^3 m} + \frac{M^4}{512\pi^4 m^2}\left(1+2\ln\frac{M}{\mu}\right)\right] + \frac{M^3}{256\pi^3 m}\Big[1-2\ln(2)
\end{aligned}
$$

$$
+2\ln\frac{M}{\mu}\Bigg] - \frac{M^4}{6144\pi^2 m^2}\left[\pi^2+6+24\ln\frac{M}{\mu}+24\ln^2\frac{M}{\mu}\right],
$$

$$
\tilde{\mu}^{8-2n} J^{(1,1)}_{CT_1}(1,2,0,1,0|n)
$$

$$
= -\frac{1}{\epsilon^2}\frac{M^2}{512\pi^4 m^2} - \frac{1}{\epsilon}\left[\frac{M}{512\pi^3 m} + \frac{M^2}{256\pi^4 m^2}\left(1+\ln\frac{M}{\mu}\right)\right] - \frac{M}{512\pi^3 m}\Bigg[1+2\ln(2)
$$

$$
+2\ln\frac{M}{\mu}\Bigg] - \frac{M^2}{6144\pi^4 m^2}\left[\pi^2+18+48\ln\frac{M}{\mu}+24\ln^2\frac{M}{\mu}\right],
$$

$$
\tilde{\mu}^{8-2n} J^{(1,1)}_{CT_2}(1,2,0,1,0|n)
$$

$$
= -\frac{1}{\epsilon^2}\frac{M^2}{512\pi^4 m^2} - \frac{1}{\epsilon}\frac{M^2}{256\pi^4 m^2}\ln\frac{M}{\mu} - \frac{M^2}{6144\pi^4 m^2}\left[\pi^2+6+24\ln^2\frac{M}{\mu}\right],
$$

$$
\tilde{\mu}^{8-2n} J^{(1,1)}_{CT_1}(2,1,0,2,0|n+2)
$$

$$
= \frac{1}{\epsilon^2}\frac{M^4}{8192\pi^6 m^2} + \frac{1}{\epsilon}\frac{M^4}{4096\pi^6 m^2}\ln\frac{M}{\mu} + \frac{M^4}{98304\pi^6 m^2}\left[\pi^2+6+24\ln^2\frac{M}{\mu}\right]
$$

$$
= \tilde{\mu}^{8-2n} J^{(1,1)}_{CT_2}(2,1,0,2,0|n+2),
$$

$$
\tilde{\mu}^{8-2n} J^{(1,1)}_{CT_1}(1,1,1,1,0|n)
$$

$$
= 0
$$

$$
= \tilde{\mu}^{8-2n} J^{(1,1)}_{CT_2}(1,1,1,1,0|n),
$$

$$
\tilde{\mu}^{8-2n} J^{(1,1)}_{CT_1}(1,1,1,1,0|n+2)
$$

$$
= 0
$$

$$
= \tilde{\mu}^{8-2n} J^{(1,1)}_{CT_2}(1,1,1,1,0|n+2).
$$

Appendix E

Hypergeometric functions

The integrals of Eq. (D.5) are given in terms of generalized hypergeometric functions ${}_pF_q\left(\begin{smallmatrix} a_1,a_2,\ldots,a_p \\ b_1,\ldots,b_q \end{smallmatrix}\middle| z\right)$ (see, e.g., Ref. [GR 00]). These are defined as

$$
{}_pF_q\left(\begin{matrix} a_1, a_2, \ldots, a_p \\ b_1, \ldots, b_q \end{matrix}\middle| z\right) = \sum_{n=0}^{\infty} \frac{(a_1)_n \cdots (a_p)_n}{(b_1)_n \cdots (b_q)_n} \frac{z^n}{n!}, \tag{E.1}
$$

where $(a)_n$ denotes the Pochhammer symbol,

$$
(a)_n = \frac{\Gamma[a+n]}{\Gamma[a]} .
$$

The functions ${}_pF_q\left(\begin{smallmatrix} a_1,\ldots,a_p \\ b_1,\ldots,b_q \end{smallmatrix}\middle| z\right)$ are generalizations of

$$
{}_2F_1\left(\begin{matrix} a_1, a_2 \\ b \end{matrix}\middle| z\right) = \sum_{n=0}^{\infty} \frac{(a_1)_n (a_2)_n}{(b)_n} \frac{z^n}{n!}, \tag{E.2}
$$

which is a particular solution of the differential equation

$$
z(1-z)\frac{d^2F(z)}{dz^2} + [c - (a+b+1)z]\frac{dF(z)}{dz} - abF(z) = 0. \tag{E.3}
$$

A number of special functions can be expressed in terms of hypergeometric functions; the exponential function e^z for example is given by ${}_0F_0(|z)$. Further examples include the Bessel functions as well as the Legendre polynomials.

The following relations for hypergeometric functions are useful for the evaluation of integrals appearing in the calculation of the nucleon mass:

$$
\begin{aligned}
{}_1F_0(a|z) &= (1-z)^{-a}, && \text{(E.4)} \\
{}_2F_1\left(\begin{matrix} a, b \\ c \end{matrix}\middle| 1\right) &= \frac{\Gamma[c]\Gamma[c-a-b]}{\Gamma[c-a]\Gamma[c-b]}, && \text{(E.5)} \\
{}_3F_2\left(\begin{matrix} a, b, c \\ d, e \end{matrix}\middle| 1\right) &= \frac{\Gamma[d]\Gamma[d+e-a-b-c]}{\Gamma[d+e-a-b]\Gamma[d-c]}\, {}_3F_2\left(\begin{matrix} e-a, e-b, c \\ d+e-a-b, e \end{matrix}\middle| 1\right), && \text{(E.6)}
\end{aligned}
$$

$$
\begin{aligned}
{}_3F_2\left(\begin{matrix}a,b,c\\d,e\end{matrix}\middle|\, z\right) &= 1 + z\frac{abc}{de}\,{}_4F_3\left(\begin{matrix}1,a+1,b+1,c+1\\2,d+1,e+1\end{matrix}\middle|\, z\right), && \text{(E.7)}\\
{}_4F_3\left(\begin{matrix}a,b,c,d\\e,f,g\end{matrix}\middle|\, z\right) &= 1 + z\frac{abcd}{efg}\,{}_5F_4\left(\begin{matrix}1,a+1,b+1,c+1,d+1\\2,e+1,f+1,g+1\end{matrix}\middle|\, z\right), && \text{(E.8)}\\
{}_pF_q\left(\begin{matrix}a_1,\ldots,a_p\\b_1,\ldots,b_q\end{matrix}\middle|\, z\right) &= 1 + z\frac{a_1\cdots a_p}{b_1\cdots b_q}\,{}_{p+1}F_{q+1}\left(\begin{matrix}1,a_1+1,\ldots,a_p+1\\2,b_1+1,\ldots,b_q+1\end{matrix}\middle|\, z\right), && \text{(E.9)}
\end{aligned}
$$

$$
{}_pF_q\left(\begin{matrix}\ldots,a_{m-1},a_m,a_{m+1},\ldots\\\ldots,b_{k-1},a_m,b_{k+1},\ldots\end{matrix}\middle|\, z\right) = {}_{p-1}F_{q-1}\left(\begin{matrix}\ldots,a_{m-1},a_{m+1},\ldots\\\ldots,b_{k-1},b_{k+1},\ldots\end{matrix}\middle|\, z\right). \tag{E.10}
$$

A list of further relations can be found in [GR 00].

Relations like Eq. (E.9) are used in the calculation of the nucleon mass where the parameters a_i of a hypergeometric function depend on $\epsilon = \frac{n-4}{2}$, where n denotes the number of space-time dimensions. In these cases the functions ${}_pF_q$ cannot be evaluated directly. If, however, the coefficient of the considered hypergeometric function does not contain inverse powers of ϵ and the expansion of ${}_pF_q$ does not generate inverse powers of epsilon either, one can set $\epsilon = 0$ in the hypergeometric function. As an example consider

$$
\frac{1}{\epsilon}\,{}_3F_2\left(\begin{matrix}1,2-\epsilon,\epsilon\\2,2+\epsilon\end{matrix}\middle|\, 1\right), \tag{E.11}
$$

where we choose $z = 1$ for simplicity. Applying the relation of Eq. (E.7) leads to

$$
\frac{1}{\epsilon}\left[1 + \frac{(2-\epsilon)\epsilon}{2(2+\epsilon)}\,{}_4F_3\left(\begin{matrix}1,2,3-\epsilon,1+\epsilon\\2,3,3+\epsilon\end{matrix}\middle|\, 1\right)\right]. \tag{E.12}
$$

One sees that after expanding around $\epsilon = 0$ the coefficient of ${}_4F_3$ no longer depends on inverse powers of ϵ,

$$
\frac{1}{\epsilon} + \left(\frac{1}{2} + \mathcal{O}(\epsilon)\right){}_4F_3\left(\begin{matrix}1,2,3-\epsilon,1+\epsilon\\2,3,3+\epsilon\end{matrix}\middle|\, 1\right). \tag{E.13}
$$

Therefore one can set $\epsilon = 0$ in the hypergeometric function. Applying Eq. (E.10) the expression of Eq. (E.13) simplifies to

$$
\frac{1}{\epsilon} + \frac{1}{2}\,{}_2F_1\left(\begin{matrix}1,1\\3\end{matrix}\middle|\, 1\right) + \mathcal{O}(\epsilon), \tag{E.14}
$$

which can be evaluated using Eq. (E.5) to give

$$
\frac{1}{\epsilon} + 1 + \mathcal{O}(\epsilon). \tag{E.15}
$$

Bibliography

[AB 69] S. L. Adler and W. A. Bardeen, Phys. Rev. **182**, 1517 (1969).

[AD 68] S. L. Adler and R. F. Dashen, *Current Algebras and Applications to Particle Physics* (Benjamin, New York, 1968).

[Ada+ 06] C. Adamuscin, E. A. Kuraev, E. Tomasi-Gustafsson, and F. E. Maas, arXiv:hep-ph/0610429.

[Adl 69] S. L. Adler, Phys. Rev. **177**, 2426 (1969).

[AF 07] S. i. Ando and H. W. Fearing, Phys. Rev. D **75**, 014025 (2007).

[AG 66] S. L. Adler and F. J. Gilman, Phys. Rev. **152**, 1460 (1966).

[Alt 82] G. Altarelli, Phys. Rept. **81**, 1 (1982).

[Arn+ 06] R. A. Arndt, W. J. Briscoe, I. I. Strakovsky, and R. L. Workman, Phys. Rev. C **74**, 045205 (2006).

[Bak 06] C. A. Baker *et al.*, Phys. Rev. Lett. **97**, 131801 (2006).

[Bar 69] W. A. Bardeen, Phys. Rev. **184**, 1848 (1969).

[Bau 04] D. Baumann, PhD Thesis, Johannes Gutenberg-Universität, Mainz (2004).

[BBA 03] H. Budd, A. Bodek, and J. Arrington, arXiv:hep-ex/0308005.

[Bea 04] S. R. Beane, Nucl. Phys. **B695**, 192 (2004).

[BEM 02] V. Bernard, L. Elouadrhiri, and U.-G. Meißner, J. Phys. G **28**, R1 (2002).

[Ber+ 92] V. Bernard, N. Kaiser, J. Kambor, and U.-G. Meißner, Nucl. Phys. **B388**, 315 (1992).

[Ber+ 94] V. Bernard, N. Kaiser, T. S. H. Lee, and U.-G. Meißner, Phys. Rept. **246**, 315 (1994).

[Ber+ 98] V. Bernard, H. W. Fearing, T. R. Hemmert, and U.-G. Meißner, Nucl. Phys. **A635**, 121 (1998) [Erratum-ibid. **A642**, 563 (1998)].

[BHM 04] V. Bernard, T. R. Hemmert, and U.-G. Meißner, Nucl. Phys. **A732**, 149 (2004).

[Bij 07] J. Bijnens, Prog. Part. Nucl. Phys. **58**, 521 (2007).

[BJ 69] J. S. Bell and R. Jackiw, Nuovo Cim. A **60**, 47 (1969).

[BKM 92] V. Bernard, N. Kaiser, and U.-G. Meißner, Phys. Rev. Lett. **69**, 1877 (1992).

[BKM 94] V. Bernard, N. Kaiser, and U.-G. Meißner, Phys. Rev. D **50**, 6899 (1994).

[BKM 95] V. Bernard, N. Kaiser, and U.-G. Meißner, Int. J. Mod. Phys. E **4**, 193 (1995).

[BKM 96] V. Bernard, N. Kaiser, and U.-G. Meißner, Nucl. Phys. **A611**, 429 (1996).

[BKM 97] V. Bernard, N. Kaiser and U.-G. Meißner, Nucl. Phys. **A615**, 483 (1997).

[BL 99] T. Becher and H. Leutwyler, Eur. Phys. J. C **9**, 643 (1999).

[BL 01] T. Becher and H. Leutwyler, JHEP **0106**, 017 (2001).

[BM 06] V. Bernard and U.-G. Meißner, Phys. Lett. B **639**, 278 (2006).

[Bof+ 02] S. Boffi, L. Ya. Glozman, W. Klink, W. Plessas, M. Radici, and R. F. Wagenbrunn, Eur. Phys. J. A **14**, 17 (2002).

[Cal+ 69] C. G. . Callan, S. R. Coleman, J. Wess, and B. Zumino, Phys. Rev. **177**, 2247 (1969).

[Cho+ 93] S. Choi *et al.*, Phys. Rev. Lett. **71**, 3927 (1993).

[Cla+ 06] J. H. D. Clark *et al.*, Phys. Rev. Lett. **96**, 073401 (2006).

[Col 66] S. Coleman, J. Math. Phys. **7**, 787 (1966).

[Col 84] J. C. Collins, *Renormalization* (Cambridge University Press, Cambridge, 1984).

[CWZ 69] S. R. Coleman, J. Wess, and B. Zumino, Phys. Rev. **177**, 2239 (1969).

[DGS 06] D. Djukanovic, J. Gegelia, and S. Scherer, Eur. Phys. J. A **29**, 337 (2006).

[Eck 95] G. Ecker, Prog. Part. Nucl. Phys. **35**, 1 (1995).

[Eck+ 89] G. Ecker, J. Gasser, H. Leutwyler, A. Pich, and E. de Rafael, Phys. Lett. B **223**, 425 (1989).

[Edw+ 06] R. G. Edwards *et al.* [LHPC Collaboration], Phys. Rev. Lett. **96**, 052001 (2006).

[ELT 02] T. E. O. Ericson, B. Loiseau, and A. W. Thomas, Phys. Rev. C **66**, 014005 (2002).

[EM 96] G. Ecker and M. Mojžiš, Phys. Lett. B **365**, 312 (1996).

[ET 98] P. J. Ellis and H. Tang, Phys. Rev. C **57**, 3356 (1998).

[FBM 00] N. Fettes, V. Bernard, and U.-G. Meißner, Nucl. Phys. **A669**, 269 (2000).

[Fea+ 97] H. W. Fearing, R. Lewis, N. Mobed, and S. Scherer, Phys. Rev. D **56**, 1783 (1997).

[Fet+ 00] N. Fettes, U.-G. Meißner, M. Mojžiš, and S. Steininger, Annals Phys. **283**, 273 (2000) [Erratum-ibid. **288**, 249 (2001)].

[Fey 39] R. P. Feynman, Phys. Rev. **56**, 340 (1939).

[FGL 73] H. Fritzsch, M. Gell-Mann, and H. Leutwyler, Phys. Lett. B **47**, 365 (1973).

[FGS 04] T. Fuchs, J. Gegelia, and S. Scherer, J. Phys. G **30**, 1407 (2004).

[FMS 98] N. Fettes, U.-G. Meißner, and S. Steininger, Nucl. Phys. **A640**, 199 (1998).

[Fra 55] E. S. Fradkin, Zh. Eksp. Teor. Fiz. **29**, 258 (1955) [Sov. Phys. JETP **2**, 361 (1956)].

[Fuc+ 03a] T. Fuchs, J. Gegelia, G. Japaridze, and S. Scherer, Phys. Rev. D **68**, 056005 (2003).

[Fuc+ 03b] T. Fuchs, M. R. Schindler, J. Gegelia, and S. Scherer, Phys. Lett. B **575**, 11 (2003).

[FW 03] J. Friedrich and Th. Walcher, Eur. Phys. J. A **17**, 607 (2003).

[Gao 03] H. y. Gao, Int. J. Mod. Phys. E **12**, 1 (2003) [Erratum-ibid. E **12**, 567 (2003)].

[Gel 64] M. Gell-Mann, Physics **1**, 63 (1964).

[Geo 93] H. Georgi, Ann. Rev. Nucl. Part. Sci. **43**, 207 (1993).

[GF 04] T. Gorringe and H. W. Fearing, Rev. Mod. Phys. **76**, 31 (2004).

[GJ 99] J. Gegelia and G. Japaridze, Phys. Rev. D **60**, 114038 (1999).

[GJT 94] J. Gegelia, G. S. Japaridze, and K. S. Turashvili, Theor. Math. Phys. **101**, 1313 (1994) [Teor. Mat. Fiz. **101**, 225 (1994)].

[GJW 03] J. Gegelia, G. Japaridze, and X. Q. Wang, J. Phys. G **29**, 2303 (2003).

[GL 84] J. Gasser and H. Leutwyler, Annals Phys. **158**, 142 (1984).

[GL 85] J. Gasser and H. Leutwyler, Nucl. Phys. **B250**, 465 (1985).

[Goi+ 01] J. L. Goity, D. Lehmann, G. Prezeau, and J. Saez, Phys. Lett. B **504**, 21 (2001).

[Gol 61] J. Goldstone, Nuovo Cim. **19**, 154 (1961).

[GR 00] I. S. Gradshteyn and I. M. Ryzhik, *Table of Integrals, Series, and Products,* 6th edition (Academic Press, San Diego, 2000).

[Gra+ 06] R. Gran *et al.* [K2K Collaboration], Phys. Rev. D **74**, 052002 (2006).

[GSS 88] J. Gasser, M. E. Sainio, and A. Švarc, Nucl. Phys. **B307**, 779 (1988).

[GSW 62] J. Goldstone, A. Salam, and S. Weinberg, Phys. Rev. **127**, 965 (1962).

[GT 58a] M. L. Goldberger and S. B. Treiman, Phys. Rev. **110**, 1178 (1958).

[GT 58b] M. L. Goldberger and S. B. Treiman, Phys. Rev. **111**, 354 (1958).

[GW 73a] D. J. Gross and F. Wilczek, Phys. Rev. Lett. **30**, 1343 (1973).

[GW 73b] D. J. Gross and F. Wilczek, Phys. Rev. D **8**, 3633 (1973).

[HE 85] W. Y. P. Hwang and D. J. Ernst, Phys. Rev. D **31**, 2884 (1985).

[Hel 33] H. G. A. Hellmann, Z. Phys. **85**, 180 (1933).

[Hoo 73] G. 't Hooft, Nucl. Phys. **B61**, 455 (1973).

[HV 72] G. 't Hooft and M. J. G. Veltman, Nucl. Phys. **B44**, 189 (1972).

[HWJ 04] C. E. Hyde-Wright and K. de Jager, Ann. Rev. Nucl. Part. Sci. **54**, 217 (2004).

[JM 91] E. Jenkins and A. V. Manohar, Phys. Lett. B **255**, 558 (1991).

[Kap 95] D. B. Kaplan, arXiv:nucl-th/9506035.

[Kap 05] D. B. Kaplan, arXiv:nucl-th/0510023.

[Kha+ 05] A. A. Khan *et al.*, Nucl. Phys. Proc. Suppl. **140**, 408 (2005).

[Kho+ 04] K. Khosonthongkee, V. E. Lyubovitskij, T. Gutsche, A. Faessler, K. Pumsa-ard, S. Cheedket, and Y. Yan, J. Phys. G **30**, 793 (2004).

[KLN 06] K. S. Kuzmin, V. V. Lyubushkin, and V. A. Naumov, Acta Phys. Polon. B **37**, 2337 (2006).

[KM 99] J. Kambor and M. Mojžiš, JHEP **9904**, 031 (1999).

[KM 01] B. Kubis and U.-G. Meißner, Nucl. Phys. **A679**, 698 (2001).

[KN 06] T. Kinoshita and M. Nio, Phys. Rev. D **73**, 013003 (2006).

[Leu 94] H. Leutwyler, Annals Phys. **235**, 165 (1994).

[Lie+ 99] A. Liesenfeld *et al.* [A1 Collaboration], Phys. Lett. B **468**, 20 (1999).

[Liu+ 94] K. F. Liu, S. J. Dong, T. Draper, J. M. Wu, and W. Wilcox, Phys. Rev. D **49**, 4755 (1994).

[Liu+ 95] K. F. Liu, S. J. Dong, T. Draper, and W. Wilcox, Phys. Rev. Lett. **74**, 2172 (1995).

[LP 02] D. Lehmann and G. Prezeau, Phys. Rev. D **65**, 016001 (2002).

[LTY 04] D. B. Leinweber, A. W. Thomas, and R. D. Young, Phys. Rev. Lett. **92**, 242002 (2004).

[Man 96] A. V. Manohar, arXiv:hep-ph/9606222.

[MB 99] J. A. McGovern and M. C. Birse, Phys. Lett. B **446**, 300 (1999).

[MB 06] J. A. McGovern and M. C. Birse, Phys. Rev. D **74**, 097501 (2006).

[Mei 06] U.-G. Meißner, PoS **LAT2005**, 009 (2006).

[Mer+ 02] D. Merten, U. Loring, K. Kretzschmar, B. Metsch, and H. R. Petry, Eur. Phys. J. A **14**, 477 (2002).

[Min+ 02] K. Minamisono *et al.*, Phys. Rev. **65**, 015501 (2002).

[MP 78] W. J. Marciano and H. Pagels, Phys. Rept. **36**, 137 (1978).

[MQS 02] B. Q. Ma, D. Qing, and I. Schmidt, Phys. Rev. C **66**, 048201 (2002).

[Nam 60] Y. Nambu, Phys. Rev. Lett. **4**, 380 (1960).

[NS 62] Y. Nambu and E. Shrauner, Phys. Rev. **128**, 862 (1962).

[Oht+ 03] S. Ohta [RBC Collaboration], Nucl. Phys. Proc. Suppl. **119**, 389 (2003).

[Pag 69] H. Pagels, Phys. Rev. **179**, 1337 (1969).

[Pag 75] H. Pagels, Phys. Rept. **16**, 219 (1975).

[PHW 04] M. Procura, T. R. Hemmert, and W. Weise, Phys. Rev. D **69**, 034505 (2004).

[Pic 98] A. Pich, arXiv:hep-ph/9806303.

[Pol 73] H. D. Politzer, Phys. Rev. Lett. **30**, 1346 (1973).

[Pol 92] J. Polchinski, arXiv:hep-th/9210046.

[Pro+ 06] M. Procura, B. U. Musch, T. Wollenweber, T. R. Hemmert, and W. Weise, Phys. Rev. D **73**, 114510 (2006).

[PV 79] G. Passarino and M. J. G. Veltman, Nucl. Phys. **B160**, 151 (1979).

[Rey 74] E. Reya, Rev. Mod. Phys. **46**, 545 (1974).

[Rot 05] H. J. Rothe, World Sci. Lect. Notes Phys. **74**, 1 (2005).

[Sas+ 03] S. Sasaki, K. Orginos, S. Ohta, and T. Blum [the RIKEN-BNL-Columbia-KEK Collaboration], Phys. Rev. D **68**, 054509 (2003).

[Sch+ 01] H. C. Schröder *et al.*, Eur. Phys. J. C **21**, 473 (2001).

[Sch 03] S. Scherer, in *Advances in Nuclear Physics, Vol. 27*, edited by J. W. Negele and E. W. Vogt (Kluwer Academic/Plenum Publishers, New York, 2003).

[Sch+ 06] M. R. Schindler, D. Djukanovic, J. Gegelia, and S. Scherer, arXiv:hep-ph/0612164.

[Sch+ 07] M. R. Schindler, T. Fuchs, J. Gegelia, and S. Scherer, Phys. Rev. C **75**, 025202 (2007).

[SGS 04a] M. R. Schindler, J. Gegelia, and S. Scherer, Phys. Lett. B **586**, 258 (2004).

[SGS 04b] M. R. Schindler, J. Gegelia, and S. Scherer, Nucl. Phys. **B682**, 367 (2004).

[SGS 05] M. R. Schindler, J. Gegelia, and S. Scherer, Eur. Phys. J. A **26**, 1 (2005).

[Sil+ 05] A. Silva, H. C. Kim, D. Urbano, and K. Goeke, Phys. Rev. D **72**, 094011 (2005).

[Smi 02] V. A. Smirnov, Springer Tracts Mod. Phys. **177**, 1 (2002).

[STS 93] V. G. J. Stoks, R. Timmermans, and J. J. de Swart, Phys. Rev. C **47**, 512 (1993).

[SYT 67] A. Sato, Y. Yokoo, and J. Takahashi, Prog. Theor. Phys. **37**, 716 (1967).

[Tak 57] Y. Takahashi, Nuovo Cim. **6**, 371 (1957).

[Tar 96] O. V. Tarasov, Phys. Rev. D **54**, 6479 (1996).

[TW 83] R. Tegen and W. Weise, Z. Phys. A **314**, 357 (1983).

[VW 84] C. Vafa and E. Witten, Nucl. Phys. **B234**, 173 (1984).

[War 50] J. C. Ward, Phys. Rev. **78**, 182 (1950).

[Wei 58] S. Weinberg, Phys. Rev. **112**, 1375 (1958).

[Wei 73] S. Weinberg, Phys. Rev. Lett. **31**, 494 (1973).

[Wei 79] S. Weinberg, Physica A **96**, 327 (1979).

[Wei 91] S. Weinberg, Nucl. Phys. **B363**, 3 (1991).

[Wei 97] S. Weinberg, arXiv:hep-th/9702027.

[Wil 74] K. G. Wilson, Phys. Rev. D **10**, 2445 (1974).

[Wil 00] D. H. Wilkinson, Eur. Phys. J. A **7**, 307 (2000).

[Wit 07] H. Wittig, *Nucleon Properties from Lattice QCD*, Project G1 of the Collaborative Research Centre 443.

[Yao+ 06] W. M. Yao *et al.* [Particle Data Group], J. Phys. G **33**, 1 (2006).